CAPITAL UNIVERSITY OF SCIENCE AND
TECHNOLOGY, ISLAMABAD

Heat and Mass Transfer Analysis of MHD Casson Fluid with Soret and Dufour Effect

by

Altaf Hussain

A thesis submitted in partial fulfillment for the
degree of Master of Philosphy

in the

Faculty of Computing
Department of Mathematics

2020

I dedicate this sincere effort to my beloved **parents** *and my elegant* **teachers** *whose devotions and contributions to my life are really worthless and whose deep consideration on part of my academic career,made me consolidated and inspired me as I am upto this grade now.*

CERTIFICATE OF APPROVAL

Heat and Mass Transfer Analysis of MHD Casson Fluid with Soret and Dufour Effect

by

Altaf hussain

(MMT173034)

THESIS EXAMINING COMMITTEE

S. No.	Examiner	Name	Organization
(a)	External Examiner	Dr. Muhammad Sabeel Khan	Sukkur IBA University
(b)	Internal Examiner	Dr. Abdul Rahman Kashif	CUST, Islamabad
(c)	Supervisor	Dr. Shafqat Hussain	CUST, Islamabad

Dr. Shafqat Hussain
Thesis Supervisor
May, 2020

Dr. Muhammad Sagheer
Head
Dept. of Mathematics
May, 2020

Dr. Muhammad Abdul Qadir
Dean
Faculty of Computing
May, 2020

Author's Declaration

I, **Altaf hussain** hereby state that my M.Phil thesis titled "**Heat and Mass Transfer Analysis of MHD Casson Fluid with Soret and Dufour Effect**" is my own work and has not been submitted previously by me for taking any degree from Capital University of Science and Technology, Islamabad or anywhere else in the country/abroad.

At any time if my statement is found to be incorrect even after my graduation, the University has the right to withdraw my M.Phil Degree.

(Altaf hussain)
Registration No: MMT173034

Plagiarism Undertaking

I solemnly declare that research work presented in this thesis titled "**Heat and Mass Transfer Analysis of MHD Casson Fluid with Soret and Dufour Effect**" is solely my research work with no significant contribution from any other person. Small contribution/help wherever taken has been duly acknowledged and that complete thesis has been written by me.

I understand the zero tolerance policy of the HEC and Capital University of Science and Technology towards plagiarism. Therefore, I as an author of the above titled thesis declare that no portion of my thesis has been plagiarized and any material used as reference is properly referred/cited.

I undertake that if I am found guilty of any formal plagiarism in the above titled thesis even after award of M.Phil Degree, the University reserves the right to withdraw/revoke my M.Phil degree and that HEC and the University have the right to publish my name on the HEC/University website on which names of students are placed who submitted plagiarized work.

(Altaf hussain)
Registration No: MMT173034

Acknowledgements

All praises to Almighty **Allah**, the Creator of all the creatures in the universe, who has created us in the structure of human beings as the best creature. Many thanks to Him, who created us as a muslim and blessed us with knowledge to differentiate between right and wrong. Many many thanks to Him as he blessed us with the **Holy Prophet, Hazrat Muhammad (Sallallahu Alaihay Wa'alihi wasalam)** for whom the whole universe is created. He (Sallallahu Alaihay Wa'alihi wasalam) brought us out of darkness and enlightened the way to heaven. I express my heart-felt gratitude to my supervisor **Dr. Shafqat Hussain** for his passionate interest, superb guidance and inexhaustible inspiration throughout this investigation. His textural and verbal criticism enabled me in formatting this manuscript. I would like to acknowledge CUST for providing me such a favorable environment to conduct this research. I especially deem to express my unbound thanks to **Dr. Muhammad Sagheer** for his excellent supervision merged with his affection and obligation, without him I would have not been able to commence this current research study.

(Altaf Hussain)
Registration No: MMT 173034

Abstract

The main objective of this dissertation is to focus on a numerical investigation of magnetohydrodynamics (MHD) Casson nanofluid flow over a stretching surface with convective boundary condition. Effects of inclined magnetic field, Soret and Dufour have also been incorporated. A mathematical model which governs the physical flow problem has been developed. Appropriate similarity transformations are used to convert the modeled partial differential equations (PDEs) into a system of nonlinear ordinary differential equations (ODEs). The resulting system of ordinary differential equations (ODEs) is solved numerically by using a well known shooting method implemented the computational software package MATLAB. Impact of various physical parameters on the dimensionless velocity, temperature and concentration profiles are presented and analyzed in the form of graphs. Numerical values of the skin friction coefficient, Nusselt number and Sherwood number are also and discussed.

Contents

List of Figures

List of Tables

Abbreviations

MHD	Magnetohydrodynamics
ODEs	Ordinary Differential Equations
PDEs	Partial Differential Equations
RK	Runge Kutta
IVP	Initial Value Problem
2D	Two Dimensional

Symbols

u, v	velocity components in x and y direction
k	thermal conductivity
k^*	mean absorption coefficient
σ^*	Boltzmann constant
α	thermal diffusivity
B_0	constant
ν	kinematic viscosity
τ	stress tensor
ρ	density
μ	coefficient of viscosity
g	acceleration due to gravity
V_s	specific volume
C_f	skin friction coefficient
N_u	Nusselt number
Sh	Sherwood number
L	characteristic length
λ	convective heat transfer
u_0	flow velocity
τ_w	wall shear stress
q_w	heat fluxes
q_m	mass fluxes
β	Casson fluid parameter
ρ_f	density of the base fluid

D_B	Brownian diffusion coefficient
D_T	thermophoresis diffusion coefficient
Q_0	volumetric heat generation/absorption
C_p	specific heat at constant pressure
T	fluid temperature
C	fluid concentration
k_0	chemical reaction coefficient
v_w	suction velocity
ψ	stream function
T_w	wall temperature
C_w	nanoparticle concentration
T_∞	ambient value of temperature
C_∞	ambient value of the nanoparticle fraction
$(\rho c)_f$	heat capacity of the fluid
$(\rho c)_p$	effective heat capacity of a nanoparticle
n	nonlinear stretching parameter
a, b	positive constant
U_w	stretching velocity
U_∞	free stream velocity
$B(x)$	magnetic field
δ	slip parameter
Bi	Biot number
M	magnetic parameter
D_m	mass diffusivity
C_s	concentration susceptibility
K_T	thermal-diffusion ratio
T_m	mean fluid temperature
Pr	Prandtl number
R	radiation parameter
Nb	Brownian motion parameter
Nt	thermophoresis parameter

Ec	Eckert number
Q	heat generation/absorption coefficient
Le	Lewis number
γ	chemical reaction parameter
S	suction parameter
Du	Dufour number
Sc	Schmidt number
Sr	Soret number

Chapter 1

Introduction

Fluid is a phase of matter that deforms or flows under an applied external force. Fluid exists in the form of liquids, gases or plasma [1]. It is a substance with vanishing shear modulus or, in more simple words, substance which cannot resist any applied shear force. Fluid is the basic need of every day life and because of its importance in many natural processes, scientists in different part of world are trying to explore various facts regarding the flow of fluid. Fluid dynamics is the sub-branch of fluid mechanics in which we study the fluid flow, also by analyzing the cause of flow. And how forces influence the fluid flow. It provides methods for understanding the evolutions of stars, ocean, current, tectonics plate, as well as the blood circulation [2]. Few important applications of fluid flows include wind turbines, oil pipelines, rocket engine and air-conditioning systems [3]. Archimedes was the first mathematician who formulated the Archimedes principle about the static of fluid and is considered to be the basics of fluid mechanics. The proper study of fluid mechanics start from early fifteen century. Fluid can be further classified into Newtonian or non-Newtonian fluid, depending on the relationship between two physical quantities i.e., stress and strain.

1.1 Nanofluid

The mixture of nanoparticles with dimension less than 100nm and the conventional low thermal conductivity fluid is known as nanofluid. The word nanofluid was first introduced by Choi [4] that presented a new class of fluid. Nanofluids are suspension of small sized (nano size) particles in a base fluid. Carbon nanotubes, carbides, metals, or oxides are the most commonly used nanoparticles in nanofluids. These fluids are synthesized to obtain improved thermal conductivity as compared with any base fluids. The thermal conductivity of nanofluid can be increased by using nanoparticle of gold, copper, silver etc., into the base fluid. The factor that lead to an increase in the thermal conductivity of nanofluids was studied by Buongiorno [5]. He observed that, both thermophoresis effect and the Brownian motion causes a change in thermal conductivity of the fluid. Nanofluid can also be used as a coolant in information technology and heavy vehicle industry. Overall, nanofluid acts as boon in many industrial, biomedicine and engineering fields. The nanofluid flow over a horizontal sheet in the presence of an external magnetic field using the Joul heating effect was investigated by Shahzad et al. [6]. Naramgari and Soluchana [7] analyzed the effect of thermal radiation on MHD nanofluid over a stretching surface. Abolbashari et al. [8] investigated the transfer of energy and heat in the steady laminar Casson nanofluid flow using both slip velocity and surface boundary condition. Ghadikolaei et al. [9] investigated the influence of different physical parameters such as chemical reaction, thermal radiation, suction, Joule heating, heat generation and absorption in the MHD flow of Casson nanofluid using a porous non-linear sheet. The unsteady nanofluid flow in the existence of thermal radiation using a stretching surface was analyzed by Kalidas et al. [10]. Ibrahim and Shankar [11] observed the boundary layer flow of non-Newtonian nanofluid using slip boundary condition, thermal radiation and magnetic field effect. The numerical analysis of Williamson nanofluid flow over a permeable surface along with the effect of chemical parameter in the presence of nanoparticles has been studied by Krishnamurthy et al. [12].

1.2 Magnetohydrodynamics (MHD)

Magnetohydrodynamics is that branch of mechanics which we deals with the study of conduction fluid flow in the presence of an external magnetic filed. Salt water, plasma, liquid metals and electrolytes are the common example of magneto fluid. It establishes a coupling between Maxwells equations of electromagnetism and Navier-Stoke equation for fluid dynamics. Generally, external magnetic field produces electric current in the conducting fluid as a result force is exerted on the moving fluid, that in turns influence the magnetic field itself this is the main concept behind MHD. Due to the importance of MHD, it plays a significant role in many flow phenomenon. It has wide range of applications in various fields of science such as, metallurgical science, mental working process, aerodynamics, fluid dynamics, and many others engineering disciplines for example, ceramic and biomedical engineering etc [13]. The boundary layer structure can be modified through MHD which improve the flow of fluid in a specific direction. The application of external magnetic field also plays a vital role in several industrial processes like, material manufacturing, metal casting etc. The MHD flow as well as the heat transfer through a channel by using a sheet which is permeable was analyzed by Chauhan and Agrawal [14]. They observed that the cooling rate can be controlled by two parameters such as magnetic number and suction parameter. The heat transfer in 2D MHD fluid flow using a permeable surface with quick change in slip velocity and temperature gradient was analyzed by [15]. they observed that, the thermal boundary layer can be hiked by modifying the shrinking parameter of the system. Attia [16] studied the heat transfer using MHD Couette flow in a special type of fluid called dusty fluid by assuming different physical parameters and found that the temperature of both dust particle and fluid changes significantly. The 2D MHD flow of an incompressible Williamson nanofliud with mass and heat transfer in a porous sheet was investigated by Shawky et al. [17]. Hayat et al. [18] considerd another fluid called upper convected Maxwell fluid and investigated the MHD flow of this fluid over a stretching sheet. Khashi'ie et al. [19] considerd a shrinking sheet in a porous medium and applied an external magnetic field normal

to the surface of the sheet and then examined the flow of mixed convection MHD stagnation point. The 2D mixed convection MHD boundary layer stagnation point flow in the existence of thermal radiation using a vertical plate which was filled with nanofluid has been demonstrated by Eftekhari and Moradi [20]. Kumar et al. [21] analyzed the impact of the transfer of heat in MHD Casson nanofluid using nonlinear surface. Aman et al. [22] investigated the flow of 2D incompressible viscous fluid using a shrinking surface in the existence of an external magnetic filed.

1.3 Stagnation Point

Stagnation point always exist on the flow field surface such that close to this point the fluid come to at rest. Therefor, the Stagnation point can be defined as, the point in the flow field where the fluid velocity become zero. The study of the flow of nanofluid close to the stagnation point has many practical applications, some of them are listed as, cooling of electronic devices by fan, solar receiver, the cooling of nuclear reactor at the time of emergency shutdown, and several hydrodynamic processes [23]. Due to these important applications of stagnation point flow has attracted a great attention of scientific community. Hiemenz [24] was the first mathematician who first time proposed the 2D stagnation point flow. Eckert [25] got the accurate solution by extending Hiemenz problem by adding the energy equation. Mahapatra and Gupta [27], In view of that Ishak et al. [26], and Hayat et al. [28] investigated the impact of the transfer of heat on stagnation point over a porous plate. Jafar et al. [29] scrutinized the laminar MHD stagnation point flow of viscous fluid by applying magnetic field normal to the flow direction. Ashraf and Kamal [30] analyzed the stagnation point flow of electrically conducting fluid with heat transfer over a porous surface along with magnetic effect. The numerical study of stagnation point flow using convective boundary condition over a stretching sheet has been analyzed by Mohamed et al. [31]. Seth et al. [32] considerd the exponentially non-isothermal sheet with uniform source of heat and magnetic field and studied the 2D stagnation point flow of incompressible, electrically conducting

viscous fluid with viscous dissipation. Rizwan et al. [33] investigated the influence of both radiation and MHD on the flow of stagnation point of nanofluid over a flat sheet. Ibrahim [34] discussed the transfer of heat of boundary layer nanofluid flow past a stretching surface along with the magnetic field, radiative heat transfer and convective heating effects. Iqbal et al. [35] analyzed the flow of stagnation point using fluid dissipation and thermal radiation in such a way that the flow direction is induced by an exponentially stretching surface.

1.4 Casson Fluid

Non-Newtonian fluid has wide range of application such as oil recovery, filtration, polymer engineering, ceramics production and petroleum production. It also performs a significant function in the design of solid matrix, heat geothermal energy production, nuclear waste disposal, petroleum reservoirs etc, [36]. Non-Newtonian fluids are more complex due to nonlinear relation between stress and strain as compared to Newtonian fluids. In order to study the non-Newtonian fluid, several models have been developed, but still no single model exits which could explain all the properties of this fluid. Theres exists a sub-class of non-Newtonian fluids called Casson fluid. This fluid has large viscosity which tends to infinity at zero rate of shear i.e., if the magnitude of shear stress is much weaker than the magnitude of applied stress it behaves like a solid. On the other hand, if shear stress become greater than the yield stress the fluid start flowing. Casson [37] first time developed the Casson model for various suspension of cylindrical particles. Soup, fruit juice, jelly, honey and tomatoes sauce are general example of Casson fluid. Benazir et al. [38] have analyzed the unsteady MHD Casson fluid flow over a flat plate and vertical cone over porous medium along with double dispersion effects. The laminar convective boundary layer non-Newtonian Casson fluid flow thermally fixed over a stretching sheet have been analyzed by Animasaun et al. [39] Afikuzzaman et al. [40] have investigated the unsteady flow of MHD fluid with hall current through parallel plates, and considering the magnetic field perpendicular to the plates. The influence of different physical parameters such as thermal radiation,

viscous dissipation and Joule heating on the flow of MHD Casson nanofluid has been investigated by Ghadikolaei et al. [41]. Mustafa [42] numerically analyzed the MHD flow of nanofluid using rotating disk. The heat transfer with MHD Casson fluid flow towards a nonlinear stretching sheet with temperature distribution over the sheet has been analyzed by Mustafa and Junaid [43]. Pramanik [44] has studied the heat transfer in the Casson nanofluid flow by including the the thermal radiation.

1.5 Soret and Dufour Effects

The Soret effect also known as thermal diffusion effect is a process in which various sized particles behave differently to the temperature gradient. It was Charles Soret who discovered this effect for the first time in 1879 [45]. He found that a tube containing salt solution is arranged in such a way that the two ends of the tube are at different temperature then the salt solution does not maintain its uniform composition. Near the cold end of the tube, the concentration of salt is more as compared to the hot end. In other words, heavy particles get separated from light particles under a temperature gradient.

The Dufour effect also known as the diffusion thermo effect is the energy flux caused by the concentration gradient. A change in temperature causes the concentration gradient. Both Soret and Dufour effect are mostly ignored in those studies in which we analyze the transfer of mass and heat, because both these effects have weaker magnitude when compared with Ficks and Fouriers laws. On the other hand, these two effects are assumed to be second order phenomena and their applications are more significant in areas such as nuclear waste disposal, geothermal energy, petrology and hydrology etc. The Soret effect has been contribute in the process of isotopes separation and mixture between lighter molecular weight gasses such as H_2 and He etc. and medium molecular weight gasses such as $N2$ and air etc. Recently the Dufour effect is observed to have considerable magnitude due to which it cannot be neglected in any kind of study that deal with the energy flux caused by the concentration gradient [46]. The Dufour and Soret effects were

analyzed by Dursunkaya and Worek [47] in a natural steady convection using vertical surface. The same effect was studied by Kafoussias and Villiams [48] using transfer of mass and heat with temperature dependent viscosity using a flat sheet in a uniform boundary layer flow. Abreu et al. [49] have analyzed both Dufour and Soret effect using free and forced convection flow. The dependence of mass and heat transfer on magnetic field from vertical surfaces by considering Dufour and Soret effects have been addressed by Postelnicu [50]. The Dufour and Soret effect with variable suction on mixed convection flow over a porous flat surface have been addressed by Alam and Rahman [51]. Recently, Lakshmi Narayana and Murthy [52] have investigated the Dufour and Soret effects on heat and mass transfer in a porous sheet.

1.6 Thesis Contributions

In this thesis, we provide a detail review of Ibrahim et al. [53] work and the study is extended by considering various others effects such as Soret effect, Dufour effect and inclined magnetic field. In this work, we convert a system of PDEs into nonlinear ODEs using similarity transformations. A well known shooting technique with fourth order RK method is used to obtained the numerical results. Implemented in Matlab software package. Using tables and graphs, the influence of various suitable physical parameter hase been discussed.

1.7 Layout of Thesis

This dissertation is further composed of four chapters as below:

Chapter 2 inludes basic definition, laws and concept which are useful in understanding upcoming work. The mathematical model and the shooting method are also developed in the last page of this chapter.

Chapter 3 provides a detailed review work of Ibrahim et al. [53]. In this work, an appropriate similarity transformation are used for the conversion of PDEs into ODEs and obtained the numerical results by solving the system of ODEs with the help of shooting method.

Chapter 4 extends the work of Ibrahim et al. [53] explained in Chapter 3 by including the effect of inclined magnetic field, Soret and Dufour. The similarity transformation has been utilized for the conversion of PDEs into ODEs. The converted ODEs are then solved by using the most familiar shooting technique.

Chapter 5 summarizes the whole study and includes the conclusion arising from the entire discussion.

Chapter 2

Fundamental Concepts and Governing Laws

In this chapter, some basic definition governing laws and dimensionless quantities are presented, which will be used in the next chapters. Dimensionless quantities are also discussed which have been used in subsequent chapters. Furthermore, a brief discussion has been done for the shooting method which has been used to find the numerical results.

2.1 Some Basic Definition

Definition 2.1. (**Fluid** [1])
"You will recall from physics that a substance exists in three primary phases. solid, liquid and gas. (At very high temperatures, it also exists as plasma) A substance in the liquid or gas phase is referred to as a fluid. Distinction between a solid and fluid is made on the basis of substances ability to resist an applied shear or (tangential) stress that tends to change its shape."

Definition 2.2. (**Fluid Kinematics** [54])
"The study of the fluids in motion, where pressure forces are not considered, is called fluid kinematics."

Definition 2.3. (**Fluid Mechanics** [54])

"Fluid mechanics is that branch of science which deals with the behavior of the fluids (liquids or gases) at rest as well as in motion. Thus this branch of science deals with the static, kinematics and dynamic aspects of fluids."

Definition 2.4. (**Fluid Dynamics** [55])

"It is the study of the motion of liquid, gases and plasma from one place to another. Fluid dynamics has a wide range of applications like calculating force and moments on aircraft, mass flow rate of petroleum passing through pipelines, prediction of weather, etc."

Definition 2.5. (**Hydrodynamics** [55])

"The study of the motion of fluids that are practically incompressible such as liquids, especially water and gases at low speeds is usually referred to as hydrodynamics."

Definition 2.6. (**Magnetohydrodynamics** [56])

"Magnetohydrodynamics (MHD) is concerned with the flow of electrically conducting fluids in the presence of magnetic field, either externally applied or generated within the fluid by inductive action."

2.2 Physical Properties of the Fluid

There are certain physical property of fluid which is describe below

Definition 2.7. (**Pressure** [57])

"The pressure exert on or by a fluid denoted by p as defined as the magnitude of force per unit area exerted in a direction normal to that area. If the normal force F is uniformly distributed across the plane area A, then the pressure called the average (or mean) pressure is simply the ratio of the normal force to the total area that is" $$p=\frac{F}{A}.$$

Definition 2.8. (**Stress** [57])

"The stress or stress vector is defined as the force per unit area of the surface

on which it acts. If the stress is uniformly distributed over the plane area A, the stress called the average stress is defined as"

$$\frac{F}{A}.$$

Definition 2.9. (**Temperature** [57])

"Temperature of a body is defined as a measure of the intensity of heat. Heat always flows from a region of higher temperature to one of the lower temperature. Physical state of a substance changes with temperature. For example, water at low temperature is ice, at higher temperature is water and at still a higher temperature is steam."

Definition 2.10. (**Density** [57])

"The density of a fluid denoted by ρ is defined as the mass per unit volume. Thus if m is the mass enclosed in a volume V, then

$$\rho = \frac{m}{V},$$

if the density at each point of the fluid is the same, then the density is said to be uniform."

Definition 2.11. (**Specific Weight** [57])

"The specific weight of a fluid denoted by γ is defined as the weight per unit volume. Thus if V is the volume of the fluid having weight w, then

$$\gamma = \frac{W}{V} = \frac{mg}{V} = \rho g$$

where g is the acceleration due to gravity. In other words, the specific weight is the force with which the earth attracts a unit volume."

Definition 2.12. (**Specific Volume** [57])

"The specific volume denoted by V_s is defined as the volume occupied by a unit mass of the fluid

$$V_s = \frac{1}{\rho},$$

in other words, the specific volume is the reciprocal of the density."

Definition 2.13. (**Compressibility** [57])

"The compressibility of a fluid is a measure of the change of its volume (and thus the density) under the action of external forces. If the volume (or the density) of a fluid changes when the pressure or temperature change, it is said to be compressible otherwise incompressibel."

Definition 2.14. (**Viscosity**)

"Is a physical property of fluids associated with shearing deformation of fluid particles subjected to the action of applied forces."

Definition 2.15. (**Kinematic Viscosity** [57])

"The ratio of the absolute viscosity μ to the density ρ is called the kinematic viscosity of the fluid and is denoted by ν and mathematically it can be written as"

$$\nu = \frac{\mu}{\rho}.$$

Definition 2.16. (**Dynamic Viscosity** [57])

"The extent which measures the resistance of fluid tending to cause the fluid to flow is called dynamic viscosity, also known as absolute viscosity. This resistance arises from the attractive forces between the molecules of the fluid. Usually liquids and gasses have non-zero viscosity. It is denoted by symbol μ and mathematically, it can be written as

$$\mu = \frac{\text{shear stress}}{\text{shear strain}},$$

here μ is called the coefficient of viscosity. Unit of viscosity in SI system is $\frac{kg}{ms}$ or Pascal-second."

2.3 Types of Fluid Flow

Definition 2.17. (**Compressible and Incompressible Flows** [58])

"A fluid flow during which the density of the fluid remains nearly constant is called compressible flow. A fluid whose density is practically independent of pressure (such as a liquid) is called an incompressible fluid. The flow of compressible fluid

(such as air) is not necessarily compressible since the density of a compressible fluid may still remain constant during flow."

Definition 2.18. (**Steady versus Unsteady Flow** [58])
"A process is said to be steady-flow if it involves no change with time anywhere within the system or at the system boundaries otherwise unsteady-flow."

Definition 2.19. (**Laminar and Turbulent Flow** [59])
"Fluid partical follows a smooth trajectory, the flow is then said to be laminar. Further increases in speed may lead to instability that eventually produces a more random type of flow that is called turbulent."

Definition 2.20. (**Viscous Fluid and Shear** [58])
"Viscosity is the measure of the internal friction of fluid. This friction become apparent when a layer of fluid is made to move in relation to another layer. The greater the friction, the greater the amount of force required to cause this movement, which is called shear."

Definition 2.21. (**Internal and External Flow** [58])
"The flow of an unbounded fluid over a surface such as a plate, a wire, or a pipe is external flow. The flow in a pipe or duct is internal flow if the fluid is completely bounded by solid surfaces."

Definition 2.22. (**Natural and Force Flow** [58])
"In forced flow, the fluids is forced to flow over a surface or in a tube by external means such as a pump or a fan. In natural flow, any fluid motion is caused by natural means such as the buoyancy effect manifests itself as the rise of the warmer fluid and the fall of the cooler fluid. The flow caused by winds is natural flow for the earth, but it is forced flow for bodies subjected to the winds since for the it makes no difference whether the air motion is caused by a fan or by the wind."

2.4 Types of Fluid

Definition 2.23. (**Ideal Fluid** [54])
"A fluid, which is incompressible and is having no viscosity, is known as an ideal fluid."

Definition 2.24. (**Real Fluid** [54])
"A fluid, which possesses viscosity, is known as real fluid. All the fluids, in actual practice, are real fluids."

Definition 2.25. (**Newtonian Fluid** [54])
"A real fluid, in which the shear stress is directly proportional to the rate of shear strain (or velocity gradient), is known as a Newtonian fluid. "

Definition 2.26. (**Non-Newtonian Fluid** [54])
"A real fluid, in which the shear stress is not directly proportional to the rate of shear strain (or velocity gradient), is known as a non-Newtonian fluid". Mathematically it can be express as":

$$\tau = k\left(\frac{\partial u}{\partial y}\right)^n.$$

Definition 2.27. Viscoplastic or Bingham Fluids
"These fluids show a linear relationship between shear stress and shear strain but need a yield stress to flow.
Examples of Bingham fluids are tooth paste, granular materials and fresh concrete."

Definition 2.28. Shear Thickening Fluids
"A small group of real liquids for which the velocity increases with the increasing shear rate such fluids are called shear thickening fluids.
Shear thickening fluids are also called dilatant fluids. Examples are corn starch and obleck."

Definition 2.29. Nanofluids
"Nanofluids are engineered colloids made of a base fluid and nanoparticles (1 −

100)nm. Nanofluids have higher thermal conductivity and single-phase heat transfer coefficients than their base fluids Metals, oxides, carbides, or carbon nanotubes are the typical nanoparticles which are used in nanofluids and oil, ethylene glycol and water are the examples of common base fluids."

2.5 Heat Transfer Mechanism and Properties

Definition 2.30. (**Heat** [60])
"In thermodynamics heat is defined as the form of energy that is transferred across the boundary of a system at a given temperature to another system (or the surroundings) at a lower temperature by virtue of the temperature difference between the two system."

Definition 2.31. (**Heat Transfer** [60])
"Heat transfer is that section of engineering science that studies the energy transport between material bodies due to a temperature difference."

Definition 2.32. (**Mixed Convection** [60])
"Mixed convection involves features from both Forced convection and Natural convection."

Definition 2.33. (**Natural Convection** [60])
"When fluid motion occurs because of a density variation caused by temperature differences, the situation is said to be a free, or natural, convection."

Definition 2.34. (**Forced Convection** [60])
"When fluid motion is caused by external force, such as pumping or blowing, the state is defined as being one of forced convection."

Definition 2.35. (**Modes of Heat Transfer** [60])
"There are three modes of heat transfer namely conduction, convection and radiation".

Definition 2.36. (**Conduction** [60])
"The conduction mode of heat transfer occurs either because of an exchange of

energy from one molecule to another, without the actual motion of the molecules, or because of the motion of the free electrons of they are present. This form of heat transfer occurs in solids, liquid and gases."

Definition 2.37. (**Convection** [60])
"Molecules present in liquids and gases have freedom of motion, and by moving from hot to cold region, they carry energy with them. The transfer of heat from one region to another, due to such macroscopic motion in a liquid and gas, added to the energy transfer by conduction within the fluid, is called heat transfer by convection."

Definition 2.38. (**Radiation** [60])
"All bodies emit thermal radiation at all temperature. This is the only mode in which both does not require a material medium for heat transfer to occure. The nature of thermal radiation is such that a propagation of energy, carried by electromagnetic waves, is emitted from the surface of the body. When these electromagnetic waves strike other body surface, a part is reflected, a part is transmitted and the remaining part absorbed."

2.6 Some Important Definition

Definition 2.39. (**Streamlines** [61])
"A streamline is a line everywhere tangent to the velocity field. For two-dimensional flows the slop of the streamline must be equal to the tangent of the angle that the velocity angle makes with the x-axis. "

Definition 2.40. (**Stream Function** [60, 61])
"Stream function is a very useful device in the study of fluid dynamics. Stream function is often used to draw the streamlines in order to better understand the flow pattern around a body. A stream function ψ is one which satisfies $u{=}\frac{\partial \psi}{\partial y}$, $v{=}u{=}\frac{\partial \psi}{\partial x}$. "

Definition 2.41. (**Isothermal Process** [54])
"If the change in density occurs at constant temperature, then the process is called

isothermal and relationship between pressure (P) and density (ρ) is given by $\frac{P}{\rho} =$ Constant."

Definition 2.42. (**Adiabatic Process** [54])
"If the change in density occurs with no heat exchange to and from the gas, the process is called adiabatic. And if no heat is generated within the gas due to friction, the relationship between pressure and density is given by
$\frac{p}{\rho^k} =$ Constant
where $k =$ Ratio of the specific heat of a gas at constant pressure and constant volume."

Definition 2.43. (**Viscous Dissipation** [1])
"Viscous dissipation represent the irreversible (in the thermodynamic sense) conversion of kinetic energy of the flow into internal energy of the fluid."

Definition 2.44. (**Thermal Conductivity** [1])
"Thermal conductivity k is a measure of the ability of a material to conduct heat. Mathematically:

$$k = \frac{q\nabla l}{S\nabla T}$$

where q is the heat passing through a surface area S and the effect of temperature difference ∇T over a distance is ∇l. Here l, S and ∇T all are assumed to be of unit measurement."

Definition 2.45. (**Joule Heating**)
"Joule heating is the energy dissipation that occurs with an electric current flowing through a resistor."

Definition 2.46. (**Thermal Diffusivity**)
"It measures the ability of material to conduct thermal energy relative to its ability to store energy means how fast or how easily heat can penetrate an object or substance. Mathematically:

$$\alpha = \frac{k}{\rho C_p},$$

where k is the thermal conductivity ρ is the density and C_p is the specific heat."

Definition 2.47. (**Newton's Law of Viscosity**)
"It states that the shear stress is proportional to the deformation rate of the fluid. Mathematically it is written as

$$\tau_{yx} = \mu \frac{du}{dy},$$

where the symbol τ_{yx} is the shear stress, x and y represents horizontal and vertical coordinates, u is the horizontal components of velocity, μ is the constant of proportionality termed as dynamic viscosity while $du\ dy$ is the deformation rate."

2.7 Boundary Layer

"Viscous effects are particularly important near the solid surfaces, where the strong interaction of the molecules of the fluid with molecules of the solid causes the relative velocity between the fluid and the solid to become almost exactly zero for a stationary surface. Therefore, the fluid velocity in the region near the wall must reduce to zero. This is called no slip condition. In that condition there is no relative motion between the fluid and the solid surface at their point of contact. It follows that the flow velocity varies with distance from the wall, from zero at the wall to its full value some distance away, so that significant velocity gradients are established close to the wall. In most cases this region is thin (compared to the typical body dimension), and it is called a boundary layer."

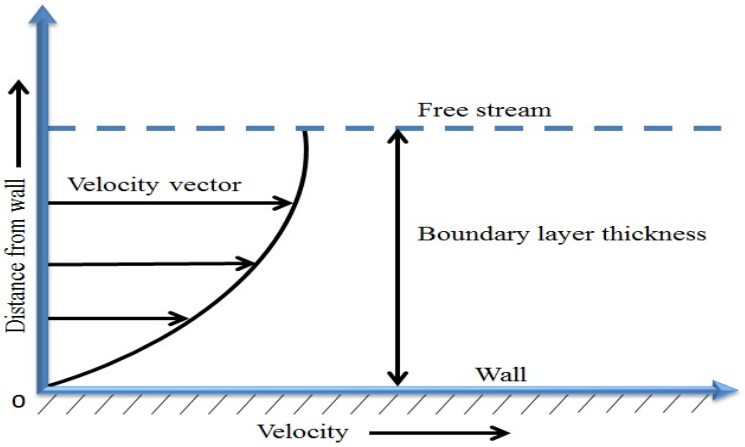

2.8 Laws of Conservation and Basic Equation

"There are three laws of conservation which are used to model the problems of fluid dynamics, and may be written in integral or differential form. Integral formulations of these laws consider the change of mass, momentum or energy within the control volume" [62].

2.9 Continuity Equation [62]

"The conservation of mass of fluid entering and leaving the control volume, the resulting mass balance is called the equation of continuity. This equation reflects the fact that mass is conserved. For any fluid, conservation of mass is expressed by the scaler equation

$$\frac{\partial \rho}{\partial t} + \nabla.(\rho \mathbf{V}) = 0. \tag{2.1}$$

For the steady flow above Eq. (2.1) can be written as

$$\nabla.(\rho \mathbf{V}) = \mathbf{0}. \tag{2.2}$$

For incompressible flow, Eq. (2.2) becomes

$$\nabla.\mathbf{V} = \mathbf{0}. \tag{2.3}$$

For incompressible and irrotational flow, the Eq. (2.3) is transformed in terms of velocity potential ψ, which is given by

$$\nabla^2\psi = 0. \tag{2.4}$$

Eq. (2.4) is known as Laplace equation."

2.10 Momentum Equation [1, 62]

"The product of the mass and the velocity of a body is called the linear momentum. Newton's second law states that the acceleration of a body is proportional to the net force acting on it and is inversely proportional to its mass, and that the rate of change of the momentum of a body is equal to the net force acting on the body. Therefore, the momentum of a system remains constant when the net force acting on it is zero, and thus the momentum of such systems is conserved. This is known as the conservation of momentum principal. For any fluid, the momentum equation is

$$\frac{\partial(\rho\mathbf{V})}{\partial t} + \nabla.\Big((\rho\mathbf{V})\mathbf{V}\Big) - \nabla.\mathbf{T} - \rho\mathbf{g} = \mathbf{0}. \tag{2.5}$$

Since $T = -p\mathbf{I} + \tau$, the momentum equation takes the form

$$\rho\left(\frac{\partial\mathbf{V}}{\partial t} + \mathbf{V}.\nabla\mathbf{V}\right) = \nabla.(-p\mathbf{I} + \tau) + \rho g. \tag{2.6}$$

Eq. (2.6) is a vector equation and can be decomposed further into three scalar components by taking the scalar product with the basis vectors of an appropriate orthogonal coordinate system. By setting $g = -g\nabla z$, where z is the distance from

an arbitrary reference elevation in the direction of gravity, Eq. (2.6) can be also expressed as

$$\rho\left(\frac{\partial \mathbf{V}}{\partial t} + \mathbf{V}.\nabla\mathbf{V}\right) = \nabla.(-p\mathbf{I} + \tau) + \nabla(-\rho g z). \tag{2.7}$$

The momentum equation then states that the acceleration of a particle following the motion is the result of a net force, expressed by the gradient of pressure,viscous and gravity forces."

2.11 Energy Equation [1]

"The energy conservation of a system can be expressed in rate form as:
Rate of change of energy in system or control volume=(Rate of in flow of energy-Rate of out flow of energy)+(Rate of heat addition due to conduction)+(Rate of internal heat generation with in control volume)+(Rate of work done by the forces acting on control volume).
Conservation of thermal energy is expressed by

$$\rho\left[\frac{\partial V}{\partial t} + \mathbf{v}.\nabla\mathbf{V}\right] = [\tau : \nabla\mathbf{v} + \mathbf{p}\nabla.\mathbf{v}] + \nabla(\mathbf{k}\nabla\mathbf{T}) \pm \hat{\mathbf{H}}_\mathbf{r}, \tag{2.8}$$

where V is the internal energy per unit mass, and H_r is the heat of reaction. By invoking the definition of the internal energy, dV=$C_v dT$, Eq. (2.8) becomes

$$\rho C_\nu\left(\frac{\partial T}{\partial t} + \mathbf{v}.\nabla\mathbf{T}\right) = \tau : \nabla\mathbf{v} + \mathbf{p}\nabla.\mathbf{v} + \nabla(\mathbf{k}\nabla\mathbf{T}) \pm \hat{\mathbf{H}}\mathbf{r}. \tag{2.9}$$

For heat conduction in solids, i.e., when $\mathbf{v} = \mathbf{0}$, $\nabla\mathbf{v}$=0 and $C_v = C$, the resulting equation is"

$$\rho C\frac{\partial T}{\partial t} = \nabla(k\nabla T) \pm \hat{H}_r. \tag{2.10}$$

2.12 Dimensionless Quantities

Definition 2.48. (**Prandtl Number** (Pr)) [63]

"This number expresses the ratio of the momentum diffusivity (viscosity) to the thermal diffusivity. Mathematically it can be written as

$$Pr = \frac{\nu}{\alpha},$$

where ν represent the kinematic viscosity and α denotes thermal diffusive heat transfers."

Definition 2.49. (**Skin Friction Coefficient** (C_f)) [63]

"Skin friction coefficient occurs between the fluid and the solid surface which leads to slow down the motion of the fluid. The skin friction coefficient can be defined as

$$C_f = \frac{\tau_\omega}{\rho U_\omega^2},$$

where τ_ω denotes the wall shear stress, ρ the density and U_ω the stretching velocity."

Definition 2.50. (**Eckert Number** (Ec)) [63]

"It expresses the ratio of kinetic energy to a thermal energy change. Mathematically

$$Ec = \frac{w_\infty^2}{C_p \Delta T},$$

where C_p is the specific heat, w_∞^2 velocity of fluid far from body, ΔT the temperature difference."

Definition 2.51. (**Biot Number** (Bi)) [63]

"We know that resistance of heat transfer is different inside of the material and at the surface. Their ratio is called biot number. Mathematically it as defined as

$$Bi = \frac{hL}{k},$$

here h is convective heat transfer, L represents the characteristic length and k the thermal conductivity fo the fluid."

Definition 2.52. (**Lewis Number** (Le)) [63]
"The Lewis number can be defined as the ratio of thermal diffusivity with molecular diffusivity. It helps us to find the relationship between mass and heat transfer coefficient. Mathematically

$$Le = \frac{\lambda}{\rho D_m C_p},$$

where λ is the convective heat transfer, D_m the mixture average diffusion coefficient, and c_p the specific heat capacity at constant pressure."

Definition 2.53. (**Nusselt Number** (N_u)) [63]
"It expresses the ratio of the total heat transfer in a system to the heat transfer by conduction. It characterizes the heat transfer by convection between a fluid and the environment close to it or, alternatively, the connection between the heat transfer intensity and the temperature field in a flow boundary layer, Mathematically

$$N_u = \frac{\alpha H}{\lambda},$$

where H is the characteristic length, α is the heat transfer coefficient, and λ is thermal conductivity."

Definition 2.54. (**Reynolds Number** (Re)) [63]
"This number expressed the ratio of the fluid inertia force to that of molecular friction (viscosity). It determines the character of the flow (laminar, turbulent and transient flows). Mathematically it can be written as

$$Re = \frac{u_0 H}{\nu},$$

where H is characteristic length, u_0 the flow velocity, and ν is density."

Definition 2.55. (**Schmidt Number** (Sc)) [63]
"This number expresses the ratio of momentum diffusivity (viscosity) and mass

diffusivity. It can be written as.

$$Sc = \frac{\nu}{D_m},$$

where ν is the kinematic viscosity and D_m is mass diffusivity."

Definition 2.56. (**Sherwood Number** (Sh)) [63]
"The Sherwood number can be defined as the ratio of total rate of mass transfer to the rate of diffusive mass transport. Mathematically

$$Sh = \frac{\beta L}{D},$$

where β is the mass transfer coefficient, L denotes the characteristic length and D stands for molecular diffusivity. It expresses the ratio of the heat transfer to the molecular diffusion. It characterizes the mass transfer intensity at the interface of phases."

2.13 Solution Methodology [64]

"Shooting method is used to solve the higher order nonlinear ordinary differential equations. To implement this technique, we first convert the higher order ODEs to the system of first order ODEs. After that we assume the missing initial conditions and the differential equations are then integrated numerically using the Runge-Kutta method as an initial value problem. The accuracy of the assumed missing initial condition is then checked by comparing the calculated values of the dependent variables at the terminal point with their given value there. If the boundary conditions are not fulfilled up to the required accuracy, with the new set of initial conditions, then they are modified by Newtons method. The process is repeated again until the required accuracy is achieved. To explain the shooting method, we consider the following general second order boundary value problem:

$$y''(x) = f(x, y, y'(x)) \tag{2.11}$$

along with the boundary conditions

$$y(0) = 0, \quad y(L) = B. \tag{2.12}$$

To have a system of first order ODEs, used the notations:

$$y = y_1, \quad y' = y_2. \tag{2.13}$$

By using the notations (2.13) in (2.11) and (2.12) can be written as

$$\left.\begin{aligned} y_1' &= y_2, \quad y_1(0) = 0, \\ y_2' &= f(x, y_1, y_2), \quad y_1(L) = B. \end{aligned}\right\} \tag{2.14}$$

Choose the missing initial condition $y_2(0) = h$ we have the following IVP

$$\left.\begin{aligned} y_1' &= y_2, \quad y_1(0) = 0, \\ y_2' &= f(x, y_1, y_2), \quad y_2(0) = h. \end{aligned}\right\} \tag{2.15}$$

Now, the initial value problem satisfy the boundary condition $y_2(L) = B$

$$y_1(L, h) - B = \phi(h) = 0. \tag{2.16}$$

To find an approximate root of (2.16) by the Newton's method, is written as

$$h_{n+1} = h_n - \frac{\phi(h_n)}{\phi'(h_n)}, \tag{2.17}$$

or

$$h_{n+1} = h_n - \frac{y_1(L, h_n) - B}{\frac{\partial}{\partial h}[y_1(L, h_n) - B]}. \tag{2.18}$$

To implement the Newton's method, consider the following notations

$$\frac{\partial y_1}{\partial h} = y_3, \quad \frac{\partial y_2}{\partial h} = y_4. \tag{2.19}$$

Differentiating Eq. (2.15) with respect to h we get the following four first order ODEs along with the associated initial conditions

$$\left.\begin{aligned} y_3' &= y_4, \quad y_3(0) = 0, \\ y_4' &= y_3\frac{\partial f}{\partial y_1} + y_4\frac{\partial f}{\partial y_2}, \quad y_4(0) = 1. \end{aligned}\right\} \tag{2.20}$$

Now, solving the IVP (2.20), we get y_3 *at* L. This value is actually the derivative of y_1 with respect to h compute at L. Using the value of $y_3(L, h)$ in Eq. (2.18), the modified value of h can be achieved. This new value of h is used to solve the (2.20) and the process is repeated until the require accuracy."

Chapter 3

Numerical Simulation of MHD Nanofluid Flow Induced by Stretching Surface

3.1 Introduction

The magnetohydrodynamics stagnation point nanofluid flow towards stretching surface with velocity slip and convective boundary condition has been investigated in this chapter. Using appropriate similarity transformation PDEs are converted into ODEs and shooting technique has been used to obtain the numerical results. Different physical parameters effects on concentration, velocity, and temperature of nanofluid flow have been presented graphicaly and discussed in detail. This chapter is a review of Ibrahim et al. [53].

3.2 Problem Formuation

We have considered a 2D steady incompressible MHD stagnation point flow of a Casson nanofluid over a stretching sheet. The sheet is placed in the plane $y = 0$, such that y-axis is normal to the sheet. The flow of nanofluid is constrained

to the surface $y > 0$, the origin is kept fixed while the sheet is stretching with velocity $u = U_w = ax^n$ with $n \geq 0$ and $U_\infty = bx^n$ is the free stream velocity where a and b are two positive constants. The slip velocity at the surface is taken as $U_{slip} = \left(\mu_B + \frac{P_y}{\sqrt{2\pi_c}}\right) \frac{\partial u}{\partial y}$. Whear π_c is the critical value of this product based on the non Newtonian model, μ_B is the plastic dynamic viscosity and p_y is the yield stress. The magnetic field $B(x) = B_0 x^{\frac{n-1}{2}}$ is applied normal to the sheet where B_0 is a constant. It is also assume that the magnetic Reynolds number is small and the induced magnetic field is negligible. A convective heating process is used to regulate the sheet temperature T_f. The nanoparticles concentration is C_w which is assumed to be constant. For y goes to infinity, the concentration and temperature of nanofluid is represented by T_∞ and C_∞ respectively.

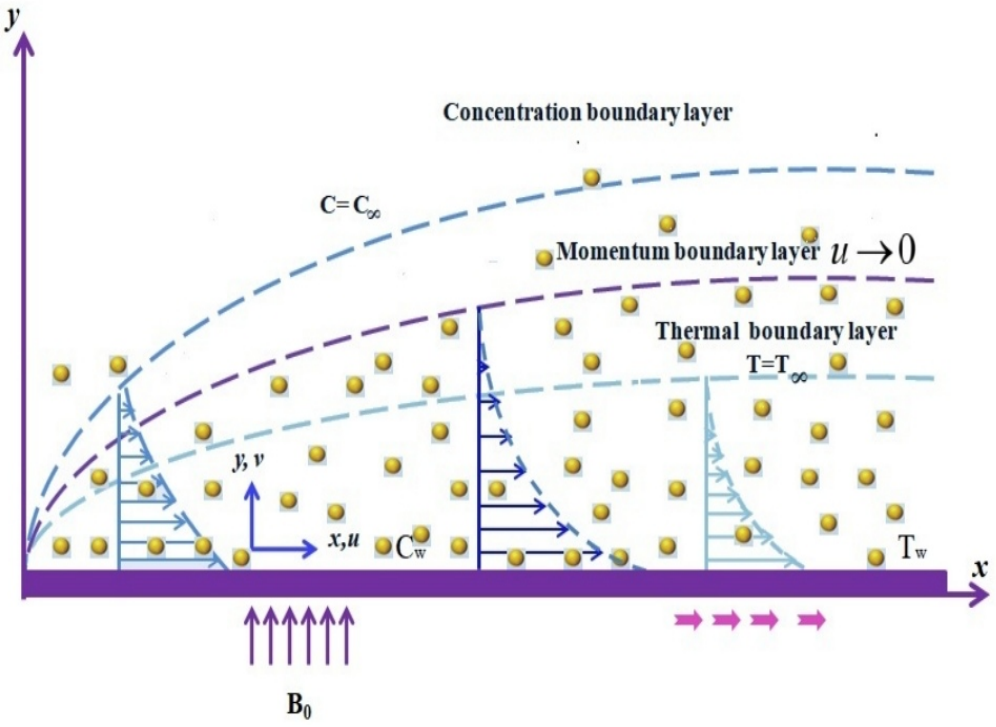

FIGURE 3.1: Flow model geometry.

The boundary layer equations in the light of above assumptions are

$$\frac{\partial u}{\partial x}+\frac{\partial v}{\partial y}=0, \tag{3.1}$$

$$u\frac{\partial u}{\partial x}+v\frac{\partial u}{\partial y}=\nu\left(1+\frac{1}{\beta}\right)\frac{\partial^2 u}{\partial y^2}+U_\infty\frac{\partial U_\infty}{\partial x}+\frac{\sigma B^2(x)}{\rho_f}(U_\infty-u), \tag{3.2}$$

$$\begin{aligned}u\frac{\partial T}{\partial x}+v\frac{\partial T}{\partial y}&=\alpha\frac{\partial^2 T}{\partial y^2}+\frac{\nu}{C_p}\left(1+\frac{1}{\beta}\right)\left(\frac{\partial u}{\partial y}\right)^2+\frac{1}{(\rho c)_f}\frac{Q_0}{(T-T_\infty)}\\&-\frac{1}{(\rho c)_f}\frac{\partial q_r}{\partial y}+\frac{(\rho c)_p}{(\rho c)_f}\left[D_B\frac{\partial C}{\partial y}\frac{\partial T}{\partial y}+\frac{D_T}{T_\infty}\left(\frac{\partial T}{\partial y}\right)^2\right],\end{aligned} \tag{3.3}$$

$$u\frac{\partial C}{\partial x}+v\frac{\partial C}{\partial y}=D_B\frac{\partial^2 C}{\partial y^2}+\frac{D_T}{T_\infty}\frac{\partial^2 T}{\partial y^2}-k_0(C-C_\infty). \tag{3.4}$$

The corresponding boundary conditions are:

$$\left.\begin{aligned}&\left.\begin{aligned}&u=U_w+U_{slip}=ax^n+\left(\mu_B+\frac{P_y}{\sqrt{2\pi_c}}\right)\frac{\partial u}{\partial y},\\&v=v_w,\ \ -k\frac{\partial T}{\partial y}=h_f(T_f-T),\ C=C_w,\end{aligned}\right\}\ \text{at}\ \ y=0,\\&u\to U_\infty=bx^n,\ v\to 0,\ T\to T_\infty,\ C\to C_\infty\ \text{as}\ y\to\infty.\end{aligned}\right\} \tag{3.5}$$

In the above equations, ν stands for kinematic viscosity, ρ_f for fluid density, α represent thermal diffusivity, C_p represents constant pressure at specific heat, k_0 denotes chemical reaction coefficient and $(\rho c)_f$ represents heat capacity, D_B represents Brownian diffusion coefficient, Q_0 shows volumetric heat generation, D_T thermophoresis diffusion coefficient, U_∞ represents free stream velocity n indicates nonlinear stretching parameter, σ shows the electrical conductivity, β represents the Casson fluid parameter, sheet temperature can be represented by T_w and T represents nanofluid temperature respectively.

3.3 Similarity Transformation

The following transformation [53] has been used to get ODEs from PDEs

$$\left.\begin{aligned} &u = ax^n f'(\xi),\ v = -\sqrt{\frac{a\nu(n+1)}{2}}x^{\frac{n-1}{2}}\left(f(\xi)+\frac{n-1}{n+1}\xi f'(\xi)\right), \\ &\xi = y\sqrt{\frac{a(n+1)}{2\nu}}x^{\frac{n-1}{2}}, \quad \psi = \sqrt{\frac{2a\nu}{(n+1)}}x^{\frac{n+1}{2}}f(\xi), \\ &\theta(\xi) = \frac{T-T_\infty}{T_f-T_\infty}, \qquad\qquad \phi(\xi) = \frac{C-C_\infty}{C_w-C_\infty}. \end{aligned}\right\} \tag{3.6}$$

The following assumptions are made for the calculation of velocity components along x and y direction as

$$\begin{aligned} u &= \frac{\partial\psi}{\partial y} \text{ and } v = -\frac{\partial\psi}{\partial x}. \\ u &= \frac{\partial}{\partial y}\left(\sqrt{\frac{2a\nu}{n+1}}x^{\frac{n+1}{2}}f(\xi)\right), \\ &= \sqrt{\frac{2a\nu}{n+1}}x^{\frac{n+1}{2}}f'(\xi)\frac{\partial\xi}{\partial y}, \\ &= \left(\sqrt{\frac{2a\nu}{n+1}}x^{\frac{n+1}{2}}f'(\xi)\right)\left(\sqrt{\frac{a(n+1)}{2\nu}}x^{\frac{n-1}{2}}\right), \\ &= ax^{\frac{n+1+n-1}{2}}f'(\xi), \\ &= ax^n f'(\xi). \end{aligned} \tag{3.7}$$

Similarly we can find

$$\begin{aligned} v &= -\frac{\partial\psi}{\partial x}, \\ v &= -\frac{\partial}{\partial x}\left[\sqrt{\frac{2a\nu}{n+1}}x^{\frac{n+1}{2}}f(\xi)\right], \\ &= -\sqrt{\frac{2a\nu}{n+1}}x^{\frac{n+1}{2}}f'(\xi)\frac{\partial}{\partial x}\left(y\sqrt{\frac{a(n+1)}{2\nu}}x^{\frac{n-1}{2}}\right) \\ &\qquad + f(\xi)\sqrt{\frac{2a\nu}{n+1}}\frac{n+1}{2}x^{\frac{n-1}{2}}, \end{aligned}$$

$$= -\sqrt{\frac{2a\nu}{n+1}}x^{\frac{n-1}{2}}\left[f'(\xi)y\sqrt{\frac{a(n+1)}{2\nu}}\frac{n-1}{2}x^{\frac{n-1}{2}} + f(\xi)\frac{n+1}{2}\right]. \tag{3.8}$$

Now we multiply and divide the right hand side of Eq. (3.8) by $2(n+1)$, then it becomes

$$= -\sqrt{\frac{a\nu(n+1)}{2}}x^{\frac{n-1}{2}}\left[f(\xi) + \frac{n-1}{n+1}\xi f'(\xi)\right].$$

From Eq. (3.1) we get

$$\begin{aligned}
&\frac{\partial u}{\partial x} + \frac{\partial v}{\partial y} = 0\\
&\frac{\partial u}{\partial x} = \frac{\partial}{\partial x}\left[ax^n f'(\xi)\right],\\
&= nax^{n-1}f'(\xi) + ax^n f''(\xi)\frac{\partial \xi}{\partial x},\\
&= nax^{n-1}f'(\xi) + ax^{n-1}f''(\xi)\xi\left(\frac{n-1}{2}\right). \qquad (3.9)\\
&\frac{\partial v}{\partial y} = -\left(\sqrt{\frac{a\nu(n+1)}{2}}x^{\frac{n-1}{2}}\right)f'(\xi) - \left(\sqrt{\frac{a\nu(n+1)}{2}}x^{\frac{n-1}{2}}\right)\frac{n-1}{n+1}f'(\xi)\\
&\qquad - \left(\sqrt{\frac{a\nu(n+1)}{2}}x^{\frac{n-1}{2}}\right)\left(\sqrt{\frac{a(n+1)}{2\nu}}x^{\frac{n-1}{2}}\right)\frac{n-1}{n+1}\xi f''(\xi),\\
&= -a\left(\frac{n+1}{2}\right)x^{n-1}\left[f'(\xi) + \frac{n-1}{n+1}f'(\xi) + \frac{n-1}{n+1}\xi f''(\xi)\right],\\
&= -a\left(\frac{n+1}{2}\right)x^{n-1}\left[\frac{2n}{n+1}f'(\xi) + \frac{n-1}{n+1}\xi f''(\xi)\right],\\
&= -ax^{n-1}nf'(\xi) - x^{n-1}a\left(\frac{n-1}{2}\right)\xi f''(\xi). \qquad (3.10)
\end{aligned}$$

Adding Eqs. (3.9) and (3.10) we get the follwing results

$$\begin{aligned}
\frac{\partial u}{\partial x} + \frac{\partial v}{\partial y} &= nax^{n-1}f'(\xi) + ax^{n-1}f''(\xi)(\xi)\left(\frac{n-1}{2}\right),\\
&\quad - ax^{n-1}nf'(\xi) - ax^{n-1}f''(\xi)(\xi)\left(\frac{n-1}{2}\right),\\
\frac{\partial u}{\partial x} + \frac{\partial v}{\partial y} &= 0.
\end{aligned}$$

We will use the following procedure for the conversion of Eq. (3.2) into dimensionless form

$$\frac{\partial u}{\partial x} = ax^{n-1}\left(nf'(\xi) + \frac{n-1}{2}\xi f''(\xi)\right),$$

Now we find $\frac{\partial u}{\partial y}$:

$$\begin{aligned}
\frac{\partial u}{\partial y} &= \frac{\partial}{\partial y}\left(ax^n f'(\xi)\right), \\
&= \left(ax^n f''(\xi)\frac{\partial \xi}{\partial y}\right), \\
&= ax^n\sqrt{\frac{a(n+1)}{2\nu}}x^{\frac{n-1}{2}}f''(\xi).
\end{aligned}$$

Differentiate again we have

$$\begin{aligned}
\frac{\partial^2 u}{\partial y^2} &= ax^n\sqrt{\frac{a(n+1)}{2\nu}}x^{\frac{n-1}{2}}f'''(\xi)\frac{\partial}{\partial y}\left(y\sqrt{\frac{a(n+1)}{2\nu}}x^{\frac{n-1}{2}}\right), \\
&= a^2x^{(2n-1)}\frac{n+1}{2\nu}f'''(\xi).
\end{aligned}$$

Taking left hand side of Eq. (3.2), we get the following form

$$\begin{aligned}
u\frac{\partial u}{\partial x} + v\frac{\partial u}{\partial y} &= ax^n f' ax^{n-1}\left(nf' + \frac{n-1}{2}\xi f''\right) \\
&\quad - \sqrt{\frac{a\nu(n+1)}{2}}x^{\frac{n-1}{2}}\left(f + \frac{n-1}{n+1}\xi f'\right)ax^n\sqrt{\frac{a(n+1)}{2\nu}}x^{\frac{n-1}{2}}f'', \\
&= ax^n f' ax^{n-1}\left(nf' + \frac{n-1}{2}\xi f''\right) \\
&\quad - \frac{a(n+1)}{2}x^{n-1}f''\left(f + \frac{n-1}{n+1}\xi f'\right)ax^n, \\
&= a^2x^{2n-1}f'\left(nf' + \frac{n-1}{2}\xi f''\right) \\
&\quad - a^2x^{2n-1}\frac{n+1}{2}f''\left(f + \frac{n-1}{n+1}\xi f'\right), \\
&= a^2x^{2n-1}\left(nf'^2 - \frac{n+1}{2}ff''\right).
\end{aligned}$$

Now taking the right hand side of Eq. (3.2), we have

$$\nu\left(1+\frac{1}{\beta}\right)\frac{\partial^2 u}{\partial y^2} = \nu\left(1+\frac{1}{\beta}\right)a^2x^{2n-1}\left(\frac{n+1}{2\nu}\right)f''',$$
$$\nu\left(1+\frac{1}{\beta}\right)\frac{\partial^2 u}{\partial y^2} = \left(1+\frac{1}{\beta}\right)a^2x^{2n-1}\left(\frac{n+1}{2}\right)f''',$$
$$U_\infty\frac{\partial U_\infty}{\partial x} = bx^n\frac{\partial}{\partial x}(bx^n),$$
$$U_\infty\frac{\partial U_\infty}{\partial x} = b^2nx^{2n-1}.$$

Using this values in Eq. (3.2), we have

$$u\frac{\partial u}{\partial y}+v\frac{\partial u}{\partial y} = \nu\left(1+\frac{1}{\beta}\right)\frac{\partial^2 u}{\partial y^2}+U_\infty\frac{\partial U_\infty}{\partial x}+\frac{\sigma B_0^2(x)}{\rho_f}(U_\infty-u),$$
$$a^2x^{2n-1}\left(nf'^2-\frac{n+1}{2}ff''\right) = a^2x^{2n-1}\left(1+\frac{1}{\beta}\right)\frac{n+1}{2}f'''$$
$$+bx^nnbx^{n-1}+\frac{\sigma B_0^2x^{n-1}}{\rho_f}(bx^n-ax^nf'). \tag{3.11}$$

Dividing each term of Eq. (3.11) by (a^2x^{2n-1}) then it becomes

$$\left(nf'^2-\frac{n+1}{2}ff''\right) = \left(1+\frac{1}{\beta}\right)\frac{n+1}{2}f'''+\frac{nb^2x^{2n-1}}{a^2x^{2n-1}}$$
$$+\frac{\sigma B_0^2x^{n-1}}{\rho_f}\left(\frac{bx^n-ax^nf'}{a^2x^{2n-1}}\right),$$
$$-\frac{n+1}{2}ff'' = \left(1+\frac{1}{\beta}\right)\frac{n+1}{2}f'''-nf'^2+n\left(\frac{b}{a}\right)^2$$
$$+\frac{\sigma B_0^2x^{n-1}}{\rho_f}\left(\frac{bx^n-ax^nf'}{a^2x^{2n-1}}\right). \tag{3.12}$$

Multiplying each term of Eq. (3.12) by $(\frac{2}{n+1})$, then we get

$$-ff'' = \left(1+\frac{1}{\beta}\right)f'''-\frac{2n}{n+1}f'^2+\frac{2n}{n+1}\left(\frac{b}{a}\right)^2$$
$$+\frac{2\sigma B_0^2x^{n-1}}{a\rho_f(n+1)}\left(\frac{bx^n-ax^nf'}{ax^{2n-1}}\right),$$

$$\left(1+\frac{1}{\beta}\right)f'''+ff''-\frac{2n}{n+1}\left(f'^2-A^2\right)$$
$$+\frac{2\sigma B_0^2 x^{n-1}}{a\rho_f(n+1)}\left(\frac{bx^{2n-1}-ax^{2n-1}f'}{ax^{2n-1}}\right)=0,$$
$$\left(1+\frac{1}{\beta}\right)f'''+ff''-\frac{2n}{n+1}\left(f'^2-A^2\right)+M\left(A-f'\right)=0. \tag{3.13}$$

Next we use the following detailed procedure to convert Eq. (3.3) into the dimensionless form

$$u\frac{\partial T}{\partial x}+v\frac{\partial T}{\partial y}=\alpha\frac{\partial^2 T}{\partial y^2}+\frac{\nu}{C_p}\left(1+\frac{1}{\beta}\right)\left(\frac{\partial u}{\partial y}\right)^2+\frac{1}{(\rho c)_f}\frac{Q_0}{(T-T\infty)}$$
$$-\frac{1}{(\rho c)_f}\frac{\partial q_r}{\partial y}+\frac{(\rho c)_p}{(\rho c)_f}\left[D_B\frac{\partial C}{\partial y}\frac{\partial T}{\partial y}+\frac{D_T}{T_\infty}\left(\frac{\partial T}{\partial y}\right)^2\right].$$

Here q_r represents the Rosseland radiative heat flux which can be define as

$$q_r=\frac{-4\sigma^*\partial T^4}{3k^*\partial y}.$$

In the above expression k^* is the absorption coefficient, σ^* is the Boltzmann constant. T^4 can be expanded about T_∞ by using Taylor series if temperature constant is very small. By ignoring the higher order terms, the reduced Taylor series gets the form

$$T^4=4T_\infty^3T-3T_\infty^4,$$
$$T=T_\infty+(T_f-T_\infty)\theta.$$
$$C=C_\infty+(C_w-C_\infty)\phi.$$
$$\frac{\partial T}{\partial x}=(T_f-T_\infty)\theta' y\sqrt{\frac{a(n+1)}{2\nu}}\left(\frac{n-1}{2}\right)x^{\frac{n-1}{2}}x^{-1},$$
$$=(T_f-T_\infty)\theta'\left(\frac{n-1}{2x}\right)\xi.$$
$$\frac{\partial C}{\partial y}=(C_w-C_\infty)\phi'\sqrt{\frac{a(n+1)}{2\nu}}x^{\frac{n-1}{2}},$$
$$\frac{\partial^2 C}{\partial y^2}=(C_w-C_\infty)\phi''\frac{a(n+1)}{2\nu}x^{n-1}.$$

$$\frac{\partial T}{\partial y} = (T_f - T_\infty)\theta' \sqrt{\frac{a(n+1)}{2\nu}} x^{\frac{n-1}{2}},$$
$$\frac{\partial^2 T}{\partial y^2} = (T_f - T_\infty)\theta'' \sqrt{\frac{a(n+1)}{2\nu}} x^{\frac{n-1}{2}} \sqrt{\frac{a(n+1)}{2\nu}} x^{\frac{n-1}{2}},$$
$$= (T_f - T_\infty)\theta'' \frac{a(n+1)}{2\nu} x^{n-1}.$$
$$q_r = \frac{-4\sigma^* \partial T^4}{3k^* \partial y},$$
$$T = T_\infty + (T_f - T_\infty)\theta,$$
$$\frac{\partial q_r}{\partial y} = \frac{-4\sigma^*}{3k^*} \frac{\partial^2}{\partial y^2} \left(4TT_\infty^3 - 3T_\infty^3 \right),$$
$$= \frac{-16\sigma^*}{3k^*} T_\infty^3 \left(T_f - T_\infty \right) \frac{a(n+1)}{2\nu} x^{n-1}\theta''.$$

Taking the left hand side of Eq. (3.3)

$$u\frac{\partial T}{\partial x} = ax^n f'(T_f - T_\infty)\theta' \left(\frac{n-1}{2x} \right) \xi,$$
$$= a(T_f - T_\infty) \left(\frac{n-1}{2} \right) \xi x^{n-1} f'\theta'. \tag{3.14}$$
$$v\frac{\partial T}{\partial y} = \left(- \sqrt{\frac{a\nu(n+1)}{2}} x^{\frac{n-1}{2}} f - \sqrt{\frac{a\nu(n+1)}{2}} x^{\frac{n-1}{2}} \frac{n-1}{n+1} \xi f' \right)$$
$$\left((T_f - T_\infty)\theta' \sqrt{\frac{a(n+1)}{2\nu}} x^{\frac{n-1}{2}} \right),$$
$$= -\frac{a(n+1)}{2} \left(f\theta' + \frac{n-1}{n+1} \xi f'\theta \right) (T_f - T_\infty) x^{n-1}. \tag{3.15}$$

Adding Eqs. (3.14) and (3.15) we get the following form

$$u\frac{\partial T}{\partial x} + v\frac{\partial T}{\partial y} = a(T_f - T_\infty) \left(\frac{n-1}{2} \right) \xi x^{n-1} f'\theta'$$
$$- \frac{a(n+1)}{2} \left(f\theta' + \frac{n-1}{n+1} \xi f'\theta \right) (T_f - T_\infty) x^{n-1},$$
$$= \frac{-a(n+1)}{2} (T_f - T_\infty) x^{n-1} f\theta'.$$

Using the procedure discussed above, Eq. (3.3) can be written as

$$\alpha \frac{\partial^2 T}{\partial y^2} = \alpha (T_f - T_\infty)\theta'' \frac{a(n+1)}{2\nu} x^{n-1}.$$

$$\frac{\partial C}{\partial y}\frac{\partial T}{\partial y} = (T_f - T_\infty)(C_w - C_\infty)\phi'\theta'\frac{a(n+1)}{2\nu}x^{n-1}.$$

$$\frac{(\rho c)_p}{(\rho c)_f}\left[D_B\frac{\partial C}{\partial y}\frac{\partial T}{\partial y} + \frac{D_T}{T_\infty}\left(\frac{\partial T}{\partial y}\right)^2\right] = \frac{D_T}{T_\infty}(T_w - T_\infty)^2\frac{a(n+1)}{2\nu}x^{n-1}\theta'^2 + \frac{(\rho c)_p}{(\rho c)_f}D_B(C_w - C_\infty)(T_w - T_\infty)\phi'\theta'\frac{a(n+1)}{2\nu}x^{n-1},$$

$$\frac{\nu}{C_p}\left(1+\frac{1}{\beta}\right)\left(\frac{\partial u}{\partial y}\right)^2 = \frac{\nu}{C_p}\left(1+\frac{1}{\beta}\right)a^2x^{3n-1}f''^2\frac{a(n+1)}{2\nu},$$

$$= \frac{1}{C_p}\left(1+\frac{1}{\beta}\right)a^2x^{3n-1}f''^2\frac{a(n+1)}{2},$$

$$= \frac{1}{C_p}\left(1+\frac{1}{\beta}\right)a^2x^{2n}f''^2\frac{a(n+1)}{2}x^{n-1},$$

$$\frac{1}{(\rho_c)_f}\frac{\partial q_r}{\partial y} = \frac{1}{(\rho_c)_f}\frac{-16\sigma^*}{3k^*}T_\infty^3\left(T_w - T_\infty\right)\frac{a(n+1)}{2\nu}x^{n-1}\theta''.$$

Putting all of the above values in Eq. (3.3) we get

$$\begin{aligned}\frac{-a(n+1)}{2}(T_f - T_\infty)x^{n-1}f\theta' &= \alpha(T_f - T_\infty)\theta''\frac{a(n+1)}{2\nu}x^{n-1} \\ &+ \frac{(\rho c)_p}{(\rho c)_f}\left[D_B(C_w - C_\infty)(T_f - T_\infty)\phi'\theta'\frac{a(n+1)}{2\nu}x^{n-1}\right] \\ &+ \frac{(\rho c)_p}{(\rho c)_f}\left[\frac{D_T}{T_\infty}(T_f - T_\infty)^2\frac{a(n+1)}{2\nu}x^{n-1}\theta'^2\right] \\ &+ \frac{1}{C_p}\left(1+\frac{1}{\beta}\right)a^2x^{2n}f''^2\frac{a(n+1)}{2}x^{n-1} + \frac{1}{(\rho_c)_f}Q_0(T_w - T_\infty)\theta \\ &- \frac{1}{(\rho c)_f}\frac{16\sigma^*}{3k^*}T_\infty^3\left(T_f - T_\infty\right)\frac{a(n+1)}{2\nu}x^{n-1}\theta''. \end{aligned} \tag{3.16}$$

Dividing both side of Eq. (3.16) by $(T_f - T_\infty)\frac{2}{a(n+1)}$ we have

$$\frac{1}{Pr}\theta'' + \frac{4}{3}R\frac{1}{Pr}\theta'' + Nb\phi'\theta' + Nt\theta'^2 + f\theta' + \frac{2}{n+1}Q\theta + \frac{U_w^2}{C_p(T_w - T_\infty)}\left(1+\frac{1}{\beta}\right)f''^2 = 0.$$

The dimensional form of Eq. (3.3) is given below

$$\left(1+\frac{4}{3}R\right)\theta'' + Prf\theta' + PrNb\phi'\theta' + PrNt\theta'^2 + \left(1+\frac{1}{\beta}\right)PrEcf''^2 + PrQ\theta = 0. \tag{3.17}$$

Now we use the following procedure to convert Eq. (3.4) into the dimensionless form:

$$\begin{aligned}
\frac{\partial C}{\partial x} &= \Big(C_w - C_\infty\Big)\phi'(\xi)\frac{\partial \xi}{\partial x},\\
&= \Big(C_w - C_\infty\Big)\phi'(\xi) y\sqrt{\frac{a(n+1)}{2\nu}}\Big(\frac{n-1}{2}\Big)x^{\frac{n-1}{2}}x^{-1},\\
&= \phi'(\xi)\Big(C_w - C_\infty\Big)\frac{\xi}{x}\Big(\frac{n-1}{2}\Big).\\
\frac{\partial C}{\partial y} &= \Big(C_w - C_\infty\Big)\phi'(\xi)\frac{\partial \xi}{\partial y},\\
&= \phi'(\xi)\Big(C_w - C_\infty\Big)\sqrt{\frac{a(n+1)}{2\nu}}x^{\frac{n-1}{2}}.
\end{aligned} \tag{3.18}$$

Differentiate again Eq. (3.18) then it becomes

$$\begin{aligned}
\frac{\partial^2 C}{\partial y^2} &= \phi''(\xi)\Big(C_w - C_\infty\Big)\sqrt{\frac{a(n+1)}{2\nu}}x^{\frac{n-1}{2}}\sqrt{\frac{a(n+1)}{2\nu}}x^{\frac{n-1}{2}},\\
&= \phi''(\xi)\Big(C_w - C_\infty\Big)\frac{a(n+1)}{2\nu}x^{n-1},\\
u\frac{\partial C}{\partial x} &= ax^{n-1}\Big(C_w - C_\infty\Big)\Big(\frac{n-1}{2}\Big)\xi f'(\xi)\phi'(\xi).
\end{aligned} \tag{3.19}$$

$$\begin{aligned}
v\frac{\partial C}{\partial y} &= -\sqrt{\frac{a\nu(n+1)}{2}}x^{n-1}\Big[f(\xi) + \frac{n-1}{n+1}\xi f'(\xi)\Big]\\
&\quad \Big(C_w - C_\infty\Big)\phi'(\xi)\sqrt{\frac{a(n+1)}{2\nu}}x^{\frac{n-1}{2}},\\
v\frac{\partial C}{\partial y} &= -\frac{a(n+1)}{2}x^{n-1}\Big(C_w - C_\infty\Big)\phi'(\xi)\Big[f(\xi) + \frac{n-1}{n+1}\xi f'(\xi)\Big].
\end{aligned} \tag{3.20}$$

Adding Eqs. (3.19) and (3.20), we have

$$\begin{aligned}
u\frac{\partial C}{\partial x} + v\frac{\partial C}{\partial y} &= ax^{n-1}\Big(C_w - C_\infty\Big)\Big(\frac{n-1}{2}\Big)\xi f'(\xi)\phi'(\xi)\\
&\quad - \frac{a(n+1)}{2}x^{n-1}\Big(C_w - C_\infty\Big)\phi'(\xi)\Big[f(\xi) + \frac{n-1}{n+1}\xi f'(\xi)\Big],\\
u\frac{\partial C}{\partial x} + v\frac{\partial C}{\partial y} &= -\frac{a(n+1)}{2}x^{n-1}\Big(C_w - C_\infty\Big)f(\xi)\phi'(\xi).
\end{aligned}$$

Similarly Eq. (3.4) can be expressed as

$$\frac{D_T}{T_\infty}\frac{\partial^2 T}{\partial y^2} = \frac{D_T}{T_\infty}\left[\Big(T_w - T_\infty\Big)\theta''(\xi)\frac{a(n+1)}{2\nu}x^{n-1}\right].$$

Putting all of the above values in Eq. (3.4)

$$\frac{-a(n+1)}{2}x^{n-1}\Big(C_w - C_\infty\Big)f(\xi)\phi'(\xi) = D_B\Big(C_w - C_\infty\Big)\frac{a(n+1)}{2\nu}x^{n-1}\phi''(\xi) + \frac{D_T}{T_\infty}\frac{a(n+1)}{2\nu}\Big(T_w - T_\infty\Big)x^{n-1}\theta''(\xi) - K_0\Big(C_w - C_\infty\Big). \tag{3.21}$$

Dividing both sides of Eq. (3.21) by $\frac{2}{a(n+1)}x^{n-1}(C_w - C_\infty)$

$$\begin{aligned}
&\frac{-\nu}{D_B}f\phi' = \left[\frac{(\rho_c)_p}{(\rho_c)_f}\frac{D_T}{T_{(\infty)}}(T_w - T_\infty)\theta'' - \frac{\nu}{D_B}\frac{2K_0\nu x}{(n+1)(ax^n)}\phi\right],\\
&-Lef\phi' = \left[\phi'' + \frac{N_t}{N_b}\theta'' - Le\gamma\phi\right],\\
&\phi'' + Lef\phi' + \frac{N_t}{N_b}\theta'' - Le\gamma\phi = 0.
\end{aligned} \tag{3.22}$$

Consider the boundary conditions

- $V(x,y) = V_w \qquad at\ y = 0,$

$$\Rightarrow -\sqrt{\frac{a\nu(n+1)}{2}}x^{\frac{n-1}{2}}\left(f(\xi) + \frac{n-1}{n+1}\xi f'(\xi)\right) = V_w \qquad at\ \ \xi = 0,$$

$$\Rightarrow f(0) = S, \qquad \left(\because \quad S = -\frac{V_w}{\sqrt{\frac{a\nu(n+1)}{2}}x^{\frac{n-1}{2}}}\right)$$

$$\Rightarrow f(0) = -\frac{V_w}{\sqrt{\frac{a\nu(n+1)}{2}}x^{\frac{n-1}{2}}}, \qquad \left(\because \quad V_w = -\sqrt{\frac{a\nu(n+1)}{2}}x^{\frac{n-1}{2}}S\right)$$

$$\Rightarrow f(0) = -\frac{-\sqrt{\frac{a\nu(n+1)}{2}}x^{\frac{n-1}{2}}S}{\sqrt{\frac{a\nu(n+1)}{2}}x^{\frac{n-1}{2}}},$$

$$\Rightarrow f(0) = S.$$

- $u(x,y) = U_w + U_{slip} = ax^n + \left(\mu_B + \frac{P_y}{\sqrt{2\pi_c}}\right)\frac{\partial u}{\partial y} \qquad at\ \ y = 0,$

$$\Rightarrow ax^n + \left(\mu_B + \frac{P_y}{\sqrt{2\pi_c}}\right)\frac{\partial}{\partial y}\Big(ax^n f'(\xi)\Big), \qquad \left(\because \quad u = U_w = ax^n\right)$$

$$\Rightarrow ax^n + \left(\mu_B + \frac{P_y}{\sqrt{2\pi_c}}\right) ax^n f''(\xi)\frac{\partial \xi}{\partial y},$$

$$\Rightarrow ax^n + \left(\mu_B + \frac{P_y}{\sqrt{2\pi_c}}\right) ax^n \sqrt{\frac{a(n+1)}{2\nu}} x^{\frac{n-1}{2}} f''(\xi) \qquad at \quad \xi = 0,$$

$$\Rightarrow f'(0) = 1 + \left(\mu_B + \frac{P_y}{\sqrt{2\pi_c}}\right) \sqrt{\frac{a(n+1)}{2\nu}} x^{\frac{n-1}{2}} f''(0),$$

$$\Rightarrow f'(0) = 1 + \left(1 + \frac{P_y}{\mu_B\sqrt{2\pi_c}}\right) \mu_B \sqrt{\frac{a(n+1)}{2\nu}} x^{\frac{n-1}{2}} f''(0),$$

$$\Rightarrow f'(0) = 1 + \left(\mu_B + \frac{P_y}{\sqrt{2\pi_c}}\right) \sqrt{\frac{a(n+1)}{2\nu}} x^{\frac{n-1}{2}} f''(0),$$

$$\Rightarrow f'(0) = 1 + \left(1 + \frac{P_y}{\mu_B\sqrt{2\pi_c}}\right) \mu_B \sqrt{\frac{a(n+1)}{2\nu}} x^{\frac{n-1}{2}} f''(0),$$

$$\Rightarrow f'(0) = 1 + \left(1 + \frac{\frac{1}{\mu_B\sqrt{2\pi_c}}}{P_y}\right) \delta f''(0),$$

$$\Rightarrow f'(0) = 1 + \left(1 + \frac{1}{\beta}\right) \delta f''(0).$$

- $-K\dfrac{\partial T}{\partial y} = h_f(T_f - T) \qquad \text{at} \quad y = 0,$

$$\Rightarrow -K(T_f - T_\infty)\theta'(\xi)\sqrt{\frac{a(n+1)}{2\nu}} x^{\frac{n-1}{2}} = h_f\Big((T_f - T_\infty) - (T_f - T_\infty)\theta(\xi)\Big) \text{ at } \xi = 0,$$

$$\Rightarrow -K\sqrt{\frac{a(n+1)}{2\nu}} x^{\frac{n-1}{2}} \theta'(0) = h_f(1 - \theta(0)),$$

$$\Rightarrow \theta'(0) = -\frac{h_f}{K\sqrt{\frac{a(n+1)}{2\nu}} x^{\frac{n-1}{2}}}(1 - \theta(0)),$$

$$\Rightarrow \theta'(0) = -Bi(1 - \theta(0)).$$

- $C(x, y) = C_w \qquad \text{at} \quad y = 0,$

$$\Rightarrow C_\infty + (C_w - C_\infty)\phi(\xi) = C_w \quad \text{at} \quad \xi = 0,$$

$$\Rightarrow \phi(0) = 1.$$

- $u(x, y) \to U_\infty = bx^n \qquad \text{as} \quad y \to \infty,$

$$\Rightarrow ax^n f'(\xi) \to bx^n \qquad as \quad \xi \to \infty, \qquad \left(\because \quad u = U_\infty = ax^n\right)$$

$$\Rightarrow f'(\xi) \to \frac{b}{a} \qquad \text{as} \quad \xi \to \infty,$$

$$\Rightarrow f'(\xi) \to A \qquad as \quad \xi \to \infty. \qquad \left(\because \quad A = \frac{b}{a}\right)$$

- $V(x, y) \to 0 \qquad as \quad y \to \infty,$

$$\Rightarrow -\sqrt{\frac{a\nu(n+1)}{2}} x^{\frac{n-1}{2}} \left(f(\xi) + \frac{n-1}{n+1}\xi f'(\xi)\right) \to 0 \quad as \quad \xi \to \infty,$$

- $T(x,y) \to T_\infty \quad \text{as} \quad y \to \infty,$

$\Rightarrow T_\infty + (T_f - T_\infty)\theta(\xi) \to T_\infty \quad \text{as} \quad \xi \to \infty,$

$\Rightarrow \theta(\xi) \to 0 \qquad \text{as} \quad \xi \to \infty.$

- $C(x,y) \to C_\infty \qquad \text{as} \quad y \to \infty,$

$\Rightarrow C_\infty + (C_w - C_\infty)\phi(\xi) \to \qquad \text{as} \quad \xi \to \infty,$

$\Rightarrow \phi(\xi) \to 0 \qquad \text{as} \quad \xi \to \infty.$

The dimensional form of the Eqs. (3.13), (3.17) and (3.22) are:

$$\left(1+\frac{1}{\beta}\right)f''' + ff'' - \frac{2n}{n+1}\left(f'^2 - A^2\right) + M\left(A - f'\right) = 0, \tag{3.23}$$

$$\left(1+\frac{4}{3}R\right)\theta'' + Prf\theta' + PrNb\phi'\theta' + PrNt\theta'^2 + \left(1+\frac{1}{\beta}\right)PrEcf''^2 + PrQ\theta = 0, \tag{3.24}$$

$$\phi'' + Lef\phi' + \frac{N_t}{N_b}\theta'' - Le\gamma\phi = 0. \tag{3.25}$$

The corresponding boundary condition becomes

$$\left.\begin{array}{l} f(0) = S,\ f'(0) = 1 + \delta\left(1+\frac{1}{\beta}\right)f''(0), \\ \theta'(0) = -Bi(1-\theta(0)),\quad \phi(0) = 1, \end{array}\right\} \ at\ \xi = 0, \\ f'(\infty) \to A,\ \theta(\infty) \to 0,\ \phi(\infty) \to 0,\ as\ \xi \to \infty. \Bigg\} \tag{3.26}$$

In the above Eqs. (3.23)-(3.26) R represents the radiation parameter, Pr stands for Prandtl number, Bi the Biot number, Ec for Eckert number, Nb represents Brownian motion parameter, Nt the thermophoresis parameter, Q represents the heat generation, Le stands for the Lewis number, A denotes velocity ratio number and S is the suction parameter, these parameter are formulated as:

$$A = \frac{b}{a},\ M = \frac{2\sigma B_0^2}{a\rho_f(n+1)},\ Nb = \frac{(\rho c)_p D_B(C_w - C_\infty)}{\nu(\rho c)_f},\ R = \frac{4\sigma^* T_\infty^3}{k^* k},\ Le = \frac{\nu}{D_B},$$

$$Q = \frac{2xQ_0}{(\rho c)_f(n+1)U_w},\ Ec = \frac{U_w^2}{C_p(T_f - T_\infty)},\ Nt = \frac{(\rho c)_p D_T(T_f - T_\infty)}{\nu(\rho c)_f T_\infty},$$

$$Pr = \frac{\nu}{\alpha},\ Bi = \frac{h_f}{k}\sqrt{\frac{2\nu}{a(n+1)}}\frac{1}{x^{\frac{n-1}{2}}}.$$

3.4 Physical Quantities of Interest

Mathematical form of skin coefficient friction is

$$C_f = \frac{\tau_w}{\rho U_w^2}. \tag{3.27}$$

Mathematical form of Nusselt number is

$$Nu_x = \frac{xq_w}{k(T_f - T_\infty)}. \tag{3.28}$$

And the Sherwood number is

$$Sh_x = \frac{xq_m}{D_B(C_w - C_\infty)}. \tag{3.29}$$

In the above equations q_w represents the heat flux, T_w the shear stress, and q_m denotes the mass flux which are defined as

$$\left.\begin{aligned} &\tau_w = \mu\left(1+\frac{1}{\beta}\right)\left(\frac{\partial u}{\partial y}\right)_{y=0,} \quad q_w = \left(-\left(k+\frac{16\sigma^* T_\infty^3}{3k^*}\right)\left(\frac{\partial T}{\partial y}\right)\right)_{y=0}, \\ &q_m = -D_B\left(\frac{\partial C}{\partial y}\right)_{y=0}. \end{aligned}\right\} \tag{3.30}$$

Use the following procedure to convert the above formulae into dimensional form

- $$\tau_w == \mu\left(1+\frac{1}{\beta}\right) a x^n a^{\frac{1}{2}} \sqrt{\frac{n+1}{2\nu}}\, x^{\frac{n-1}{2}} f''(0). \tag{3.31}$$
- $$\begin{aligned} q_w &= \left(-\left(k+\frac{16\sigma^* T_\infty^3}{3k^*}\right)\left(T_f - T_\infty\right)\sqrt{\frac{a(n+1)}{2\nu}}\, x^{\frac{n-1}{2}}\theta'(0)\right), \\ &= \left(-\left(k+\frac{4}{3}\frac{4\sigma^* T_\infty^3}{k^*}\right)\left(T_f - T_\infty\right) a^{\frac{1}{2}}\sqrt{\frac{n+1}{2\nu}}\, x^{\frac{n-1}{2}}\theta'(0)\right). \end{aligned} \tag{3.32}$$
- $$\begin{aligned} q_m &= -D_B\left(C_w - C_\infty\right) x^{\frac{n-1}{2}}\sqrt{\frac{a(n+1)}{2\nu}}\,\phi'(0), \\ &= -D_B\left(C_w - C_\infty\right) x^{\frac{n-1}{2}} a^{\frac{1}{2}}\sqrt{\frac{n+1}{2\nu}}\,\phi'(0). \end{aligned} \tag{3.33}$$

We obtained the following dimensionless form for Nusselt number sherwood number and skin friction coefficient by inserting Eqs. (3.31)-(3.33) in Eq. (3.30),

- $C_f = \frac{\tau_w}{\rho U_w^2}$,

$$= \frac{\mu\left(1+\frac{1}{\beta}\right)ax^n a^{\frac{1}{2}}\sqrt{\frac{n+1}{2\nu}}x^{\frac{n-1}{2}}f''(0)}{\rho a^2 x^{2n}}, \qquad (\because \quad U_w = ax^n)$$

$$= \frac{\mu}{\rho}\left(1+\frac{1}{\beta}\right)ax^n a^{\frac{1}{2}}\sqrt{\frac{n+1}{2\nu}}x^{\frac{n-1}{2}}a^{-2}x^{-2n}f''(0),$$

$$= \nu\left(1+\frac{1}{\beta}\right)a^{\frac{-1}{2}}\sqrt{\frac{n+1}{2\nu}}x^{\frac{-n-1}{2}}f''(0), \qquad (\because \quad \frac{\mu}{\rho} = \nu)$$

$$= \nu\left(1+\frac{1}{\beta}\right)\sqrt{\frac{n+1}{2}}\frac{1}{\sqrt{\nu}}a^{\frac{-1}{2}}x^{\frac{-n}{2}}x^{\frac{-1}{2}}f''(0),$$

$$= \sqrt{\nu}\sqrt{\nu}\left(1+\frac{1}{\beta}\right)\sqrt{\frac{n+1}{2}}\frac{1}{\sqrt{\nu}}a^{\frac{-1}{2}}x^{\frac{-n}{2}}x^{\frac{-1}{2}}f''(0),$$

$$= \frac{\left(1+\frac{1}{\beta}\right)\sqrt{\frac{n+1}{2}}\frac{1}{\sqrt{\nu}}a^{\frac{-1}{2}}x^{\frac{-n}{2}}x^{\frac{-1}{2}}f''(0)}{\nu^{\frac{-1}{2}}},$$

$$= \left(\frac{ax^n x}{\nu}\right)^{\frac{-1}{2}}\left(1+\frac{1}{\beta}\right)\sqrt{\frac{n+1}{2}}f''(0),$$

$$= Re_x^{\frac{-1}{2}}\left(1+\frac{1}{\beta}\right)\sqrt{\frac{n+1}{2}}f''(0), \qquad (\because \quad Re_x = \frac{ax^n}{\nu})$$

$$\Rightarrow \quad Re_x^{\frac{1}{2}}C_f\sqrt{\frac{2}{n+1}} = \left(1+\frac{1}{\beta}\right)f''(0). \tag{3.34}$$

- $Nu_x = \frac{xq_w}{K(T_f - T_\infty)}$,

$$= \frac{x\left(-\left(k+\frac{4}{3}\frac{4\sigma^* T_\infty^3}{k^*}\right)\left(T_f - T_\infty\right)a^{\frac{1}{2}}\sqrt{\frac{n+1}{2\nu}}x^{\frac{n-1}{2}}\theta'(0)\right)}{k(T_f - T_\infty)},$$

$$= \frac{-k\left(1+\frac{4}{3}\frac{4\sigma^* T_\infty^3}{k^* k}\right)\left(T_f - T_\infty\right)a^{\frac{1}{2}}\sqrt{\frac{n+1}{2\nu}}x^{\frac{n-1}{2}}x\theta'(0)}{k(T_f - T_\infty)},$$

$$= -\left(1+\frac{4}{3}R\right)a^{\frac{1}{2}}\sqrt{\frac{n+1}{2\nu}}x^{\frac{n+1}{2}}\theta'(0), \qquad (\because \quad \frac{4\sigma^* T_\infty^3}{k^* k} = R)$$

$$= -\left(1+\frac{4}{3}R\right)a^{\frac{1}{2}}x^{\frac{n}{2}}x^{\frac{1}{2}}\sqrt{\frac{n+1}{2}}\frac{1}{\sqrt{\nu}}\theta'(0),$$

$$= -\left(1+\frac{4}{3}R\right)\left(\frac{ax^n x)}{\nu}\right)^{\frac{1}{2}}\sqrt{\frac{n+1}{2}}\theta'(0),$$

$$Nu_x = -\left(1+\frac{4}{3}R\right)Re_x^{\frac{1}{2}}\sqrt{\frac{n+1}{2}}\theta'(0),$$

$$\Rightarrow \quad Re_x^{\frac{-1}{2}} Nu_x \sqrt{\frac{2}{n+1}} = -\left(1+\frac{4}{3}R\right)\theta'(0). \tag{3.35}$$

- $Sh_x = \dfrac{xq_m}{D_B(C_w - C_\infty)}$,

$$= \frac{-xD_B\left(C_w - C_\infty\right)x^{\frac{n-1}{2}}a^{\frac{1}{2}}\sqrt{\frac{n+1}{2\nu}}\phi'(0)}{D_B(C_w - C_\infty)},$$

$$= -x^{\frac{n+1}{2}}a^{\frac{1}{2}}\sqrt{\frac{n+1}{2}}\frac{1}{\sqrt{\nu}}\phi'(0),$$

$$= -x^{\frac{n}{2}}x^{\frac{1}{2}}a^{\frac{1}{2}}\sqrt{\frac{n+1}{2}}\frac{1}{\sqrt{\nu}}\phi'(0),$$

$$= \frac{-x^{\frac{n}{2}}x^{\frac{1}{2}}a^{\frac{1}{2}}\sqrt{\frac{n+1}{2}}\phi'(0)}{\nu^{\frac{1}{2}}},$$

$$= \left(\frac{-ax^n x}{\nu}\right)^{\frac{1}{2}}\sqrt{\frac{n+1}{2}}\phi'(0),$$

$$= \left(\frac{U_w x}{\nu}\right)^{\frac{1}{2}}\sqrt{\frac{n+1}{2}}\phi'(0) \qquad (\because \quad U_w x = ax^n),$$

$$= Re_x^{\frac{-1}{2}}\sqrt{\frac{n+1}{2}}\phi'(0),$$

$$\Rightarrow \quad Re_x^{\frac{-1}{2}} Sh_x \sqrt{\frac{n+1}{2}} = -\phi'(0). \tag{3.36}$$

The Reynolds number can be defined as $Re_x = \frac{U_w x}{\nu}$.

3.5 Solution Methodology

The system of nonlinear ODEs (3.23)-(3.25) along with boundary condition (3.26) are converted into first order ODEs. The first order system of ODEs with appropriate boundary condition are solved by using shooting method. We adopt the following procedure:

$$f''' = \frac{-ff'' + \frac{2n}{n+1}(f'^2 - A^2) - M(A - f')}{(1+\frac{1}{\beta})}, \tag{3.37}$$

$$\theta'' = \frac{-Pr[f\theta' + Nb\theta'\phi' + Nt\theta'^2 + (1+\frac{1}{\beta})Ecf''^2 + Q\theta]}{(1+\frac{4}{3}R)}, \tag{3.38}$$

$$\phi'' = -Lef\phi' - \frac{Nt}{Nb}\theta'' + Le\gamma\phi. \tag{3.39}$$

$$\tag{3.40}$$

The suitable boundary conditions are

$$\left.\begin{array}{l} f(0)=S,\ f'(0)=1+\delta(1+\dfrac{1}{\beta})f''(0), \\ \theta'(0)=-Bi(1-\theta(0)),\quad \phi(0)=1, \\ f'\to A,\ \theta\to 0,\ \phi\to 0,\quad as\ \ \xi\to\infty. \end{array}\right\} at\ \xi=0, \tag{3.41}$$

Since Eq. (3.37) is a function of f and its derivatives, which can be solved individually by shooting method. The solution of Eq. (3.37) can be used in Eq. (3.38) and Eq. (3.39) as a recognize input. We have notice two initial conditions given at ξ=0 in the above third order ODE, Eq. (3.37) give the unknown condition $f''(0)$ which is represented by P. We have introduced the following symbols for further simplification.

$$f=y_1, f'=y_2, f''=y_3, \frac{\partial f}{\partial P}=y_4, \frac{\partial f'}{\partial P}=y_5, \frac{\partial f''}{\partial P}=y_6.$$

The above system of ODEs and the corresponding initial condition can be written as

$$\left.\begin{array}{ll} y_1'=y_2, & y_1(0)=S, \\ y_2'=y_3, & y_2(0)=1+\delta\left(1+\dfrac{1}{\beta}\right)P, \\ y_3'=\dfrac{1}{(1+\frac{1}{\beta})}[-y_1y_2+\dfrac{2n}{n+1}(y_2^2-A^2)-M(A-y_2)], & y_3(0)=P, \\ y_4'=y_5, & y_4(0)=0, \\ y_5'=y_6, & y_5(0)=\delta\left(1+\dfrac{1}{\beta}\right), \\ y_6'=\dfrac{1}{(1+\frac{1}{\beta})}[-y_1y_6-y_4y_3+\dfrac{2n}{n+1}(2y_2y_5)+My_5], & y_6(0)=1. \end{array}\right\} \tag{3.42}$$

For the solution of above initial value problem we use Runge Kutta method of order four. For finding the initial condition we take P=$P^{(0)}$. For calculating the

root we used Newton method which is given by the following iteration

$$P^{(n+1)} = P^{(n)} - \left(\frac{y_2(\xi_\infty, P^{(n)}) - A}{y_5(\xi_\infty, P^{(n)})} \right). \tag{3.43}$$

The approximate solution of Eq. (3.37) can be obtained by converting the unbounded domain $[0,\ \infty]$ into bounded domain $[0,\ \xi_{max}]$, where ξ_{max} is chosen such that no considrable changes are obtained going beyond. In order to apply numerical method for the solution of Eqs. (3.38) and Eq. (3.39), we denote the missing initial condition $\theta(0)$ and $\phi(0)$ by q and r, respectively and different notations have been used which are given below

$$\left.\begin{aligned} &\theta = Y_1,\ \theta' = Y_2,\ \phi = Y_3,\ \phi' = Y_4,\ \frac{\partial\theta}{\partial q} = Y_5,\ \frac{\partial\theta'}{\partial q} = Y_6,\ \frac{\partial\phi}{\partial q} = Y_7,\\ &\frac{\partial\phi'}{\partial q} = Y_8,\ \frac{\partial\theta}{\partial r} = Y_9,\ \frac{\partial\theta'}{\partial r} = Y_{10},\ \frac{\partial\phi}{\partial r} = Y_{11},\ \frac{\partial\phi'}{\partial r} = Y_{12}. \end{aligned}\right\} \tag{3.44}$$

Using these notations, we get a system of first order ODEs which are given below

$$\begin{aligned}
&Y_1' = Y_2, && Y_1(0) = q,\\
&Y_2' = \frac{-Pr}{(1+\frac{4}{3}R)}\left[y_1Y_2 + NbY_2Y_4 + \left(1+\frac{1}{\beta}\right)Ecy_3^2 + NtY_2^2 + QY_1\right], && Y_2(0) = -Bi(1-q),\\
&Y_3' = Y_4, && Y_3(0) = 1,\\
&Y_4' = -Ley_1Y_4 + \frac{3NtPr}{Nb(3+4R)}\Big[y_1Y_2 + NbY_2Y_4 + NtY_2^2\\
&+ (1+\frac{1}{\beta})Ecy_3^2 + QY_1\Big] + Le\gamma Y_3, && Y_4(0) = r,\\
&Y_5' = Y_6, && Y_5(0) = 1,\\
&Y_6' = \frac{-3Pr}{(3+4R)}\Big[y_1Y_6 + Nb(Y_6Y_4 + Y_2Y_8)\\
&+ 2NtY_2Y_6 + QY_5\Big], && Y_6(0) = Bi,\\
&Y_7' = Y_8, && Y_7(0) = 0,
\end{aligned}$$

$$Y_8' = -Ley_1Y_8 + \frac{3NtPr}{Nb(3+4R)}\Big[y_1Y_6 + Nb(Y_6Y_4 + Y_2Y_8)$$
$$+ 2NtY_2Y_6 + QY_5\Big] + Le\gamma Y_7, \qquad Y_8(0) = 0,$$
$$Y_9' = Y_{10}, \qquad Y_9(0) = 0,$$
$$Y_{10}' = \frac{-3Pr}{(3+4R)}\Big[y_1Y_{10} + Nb(Y_{10}Y_4 + Y_2Y_{12})$$
$$+ 2NtY_2Y_10 + QY_9\Big], \qquad Y_{10}(0) = 0,$$
$$Y_{11}' = Y_{12}, \qquad Y_{11}(0) = 0,$$
$$Y_{12}' = -Ley_1Y_{12+}\frac{3NtPr}{Nb(3+4R)}\Big[y_1Y_{10} + Nb(Y_{10}Y_4 + Y_2Y_{12})$$
$$+ 2NtY_2Y_{10} + QY_9\Big] + Le\gamma Y_{11}, \qquad Y_{12}(0) = 1.$$

In order to solve the above initial value problem, we used RK4 method and the missing conditions are chosen such that

$$(Z_1(q,r))_{\xi=\xi_\infty} = 0, \qquad (Z_3(q,r))_{\xi=\xi_\infty} = 0. \tag{3.45}$$

The above set of equations can be solved by using Newtons method with following iterative formula:

$$\begin{bmatrix} q^{(n+1)} \\ r^{(n+1)} \end{bmatrix} = \begin{bmatrix} q^{(n)} \\ r^{(n)} \end{bmatrix} - \begin{bmatrix} \frac{\partial Y_1(q,r)}{\partial q} & \frac{\partial Y_1(q,r)}{\partial r} \\ \frac{\partial Y_3(q,r)}{\partial q} & \frac{\partial Y_3(q,r)}{\partial r} \end{bmatrix}^{-1} \begin{bmatrix} Y_1 \\ Y_3 \end{bmatrix}_{(q^{(n)},r^{(n)},\xi_\infty)}$$
$$\Rightarrow \begin{bmatrix} q^{(n+1)} \\ r^{(n+1)} \end{bmatrix} = \begin{bmatrix} q^{(n)} \\ r^{(n)} \end{bmatrix} - \begin{bmatrix} Y_5 & Y_9 \\ Y_7 & Y_{11} \end{bmatrix}^{-1} \begin{bmatrix} Y_1 \\ Y_3 \end{bmatrix}_{(q^{(n)},r^{(n)},\xi_\infty)}.$$

The stopping criteria for the shooting method is set as:

$$max\{|(Y_1(\xi_\infty)|,\ |Y_3(\xi_\infty))|\} < \epsilon,$$

where ϵ is a small positive number. From now onward ϵ has been taken as 10^{-8} whereas ξ_∞ is set as 7.

3.6 Results and Discussion

The numerical results of the equations in the previous sections are discussed in this section by using the graphs and tables. The numerical computations are done for the influence of different important parameters such as, thermal radiation R, nonlinear parameter n, Casson fluid parameter β, thermophoresis parameter Nt, magnetic paramter M, velocity parameter, skin friction coefficient, Brownian parameter, Sherwood and Nusselt number. These physical parameters have a direct effect on concentration, temperature and velocity distribution.

Skin-Friction Coefficient, Nusselt Number and Sherood Numbers

δ	R	Nb	Nt	Ec	Q	Bi	γ	$-\left(1+\frac{1}{\beta}\right)f''(0)$	$-\left(1+\frac{4}{3}R\right)\theta'(0)$	$-\phi'(0)$
0.1	0.1	0.2	0.2	0.1	0.1	0.5	0.2	1.61508	0.31881	0.78212
0.5								0.86635	0.31584	0.73225
1.0								0.55611	0.29743	0.69361
	0.5							0.80773	0.47534	0.85635
	0.7							0.80773	0.54226	0.86696
		0.5						0.80773	0.52735	0.91883
		0.1						0.80773	0.30714	0.75428
			0.3					0.80773	0.49898	0.93392
			0.5					0.80773	0.31618	0.75528
				0.5				0.80773	0.37008	0.82365
				1.0				0.80773	0.47926	0.94256
					-0.2			0.80773	0.51145	0.92416
					0.0			0.80773	0.35468	0.83659
						0.1		0.80773	0.15916	0.94445
						2.0		0.80773	0.52619	0.82931
							0.0	0.80773	0.52985	0.72444
							0.5	0.80773	0.52180	0.96569

TABLE 3.1: Computed numerical data of skin friction coefficient, Nusselt and Sherwood number for $M = 0.5$, $\beta = 1.0$, $S = 1.0$, $A = 0.2$, $n = 2.0$.

Table 3.1 describes the computed numerical results of Nusselts number, sherwood number and skin friction coefficient using different physical parameters given in the table. The skin friction coefficient is $-(1+1/\beta)f''(0)$, the Nusselt number is $-(1+\frac{4}{3}R)\theta'(0)$ and the Sherwood number is $-\phi'(0)$. The values of skin friction coefficient, Nusselt number and Sherwood number changes by changing the physical parameters. As given in the table, the skin friction coefficient gradually depressed by taking large values of slip parameter, Brownian parameter, chemical reaction parameter, thermophoresis parameter and Biot number, however for thermal radiation and Ekert number no change has been observed in the skin friction coefficient. The table clearly shows gradual decrease in Nusselt and Sherwood number by enhancing the numerical values of various physical parameters.

δ	R	Nb	Nt	Ec	Q	Bi	γ	I_f	I_θ	I_ϕ
0.1	0.1	0.2	0.2	0.1	0.1	0.5	0.2	[-0.9, 0.2]	[0, 3]	[1, 3]
0.5								[-0.5, 0.1]	[1, 2]	[1, 2]
1.0								[-0.3, 0]	[0, 2]	[1, 2]
	0.5							[-0.3, 0.2]	[1, 3]	[1, 3]
	0.7							[-0.3, 0.2]	[1, 3]	[0, 3]
		0.5						[-0.3, 0.2]	[1, 3]	[1, 3]
		0.1						[-0.3, 0.2]	[0, 4]	[0, 4]
			0.3					[-0.3, 0.2]	[1, 6]	[1, 6]
			0.5					[-0.3, 0.2]	[1, 5]	[1, 5]
				0.5				[-0.3, 0.2]	[1, 4]	[1, 6]
				1.0				[-0.3, 0.2]	[1, 7]	[1, 7]
					-0.2			[-0.3, 0.2]	[1, 7]	[1, 7]
					0.0			[-0.3, 0.2]	[1, 8]	[1, 8]
						0.1		[-0.3, 0.2]	[1, 8]	[1, 8]
						2.0		[-0.3, 0.2]	[1, 5]	[1, 4]
							0.0	[-0.3, 0.2]	[1, 9]	[1, 8]
							0.5	[-0.3, 0.2]	[0, 6]	[1, 8]

TABLE 3.2: The intervals for the initial guesses for the missing initial conditions when $M = 0.5$, $\beta = 1.0$, $S = 1.0$, $A = 0.2$, $n = 2.0$.

Table 3.2 shows the interval I_f, I_θ and I_ϕ by choosing the missing initial conditions as $f''(0)$, $\theta'(0)$ and $\phi'(0)$ respectively. The interval mentioned above offer a considerable flexibility for the choice of initial guesses.

Effect of Casson Parameter β

Figure 3.2 analyzes the impact of β on dimensional velocity profile. The velocity of the fluid decreases by increasing the numerical value of β. Physically, this means that fluid viscosity increases due to accelerating values of β which in turn decelerate the nanofluid velocity profile. Furthermore, the present phenomena convert to Newtonian fluid as β approaches to inifinity. Figure 3.3 illustrates the relationship between energy profile and β. It is seen that the temperature distribution of the fluid increases by gradually increasing the value of β. Actually, by increasing value of β the thermal boundary thickness increase due to which the surface temperature increases. Figure 3.4 demonstrates the behavior of β on the concentration field. The nanoparticle volume fraction is observed to be increased for the higher estimation of β.

Effect of Magnetic Number M

Figure 3.5 shows the relationship between M on dimensionless velocity profile $f'(\xi)$, we see that the velocity profile of the fluid depressed continuously by accelerating the value of magnetic field. Generally, the increasing value of M creates the Lorentz force and the collision between the conducting molecules increase in the presence of this force due to which the temperature of the fluid increases and the velocity decreases at the boundary layer. Figure 3.6 illustrates the dependence of energy profile on magnetic parameter M. From the graph, we see that gradually enhancement of M causes an increase in the temperature. Physically, the greater magnetic number induces an opposing force normally known as the Lorentz force which significantly increase both boundary layer thickness and temperature profile of the nanofluid. Figure 3.7 analyzes the behavior of concentration distribution for ascending values of M. The graph shows that the fluid concentration distribution is enhanced with mounting values of M.

Effect of Eckert Number Ec

Figure 3.23 illustrates the impact of Ec on temperature profile of the fluid. The graph clearly shows that the temperature distribution is enhanced by mounting values of Ec. Actually, Ec can be written as a ratio of kinetic energy of the fluid particle and thermal energy. The increasing value of Ec means, we have increased the kinetic energy of the fluid particle, as a result the thermal boundary layer thickness is enhanced.

Effect of Thermophoresis Parameter Nt

Figure 3.26 investigates the dependence of temperature distribution on Nt. The plot shows that the temperature profile of the fluid is escalating with boosting values of Nt. Actualy, reason of this behavior is that the nanoparticle at the hot boundary side have been moved towards the cold boundary side and the thermal boundary layer become thicker in the existence of Nt. Figure 3.27 depicts the visualization of Nt on the concentration distribution. It is noticed that by gradually increasing Nt the concentration distribution also increases. Generally, in the presence of Nt exert forces on each other, as a result particles move from hotter to colder region of the fluid and has been noticed an increment in the concentration distribution.

Effect of Biot Number Bi

Figures 3.28 and 3.29 are drawn to analyze the impact of Bi on both energy and concentration distribution of the fluid respectively. Physically, Bi can be written as a ratio of convection to conduction. The convection is taking place on the surface while the conduction is taking place inside the surface. Thus the boosting value of Bi accelerates both temperature and concentration profile.

Effect of Velocity Slip Parameter δ

Figure 3.17 shows the relationship between slip parameter and dimensionless velocity distribution. The velocity is observed to be a reducing function of δ. It can be generalized as the fractional resistance between fluid particles and the flow surface increases as a result the velocity profile of the fluid decreases. Figure 3.18 shows that the energy profile is accelerated by gradually uprising the value of δ.

Effect of Radiation Parameter R

Figure 3.20 analyzes the impact of R on energy distribution. The gradually rising value of R enhances the energy distribution of the fluid. Actually, the heat energy exhausted from the fluid due to large value of R and as a result the energy distribution increased.

Effect of Prandtl Number Pr

Figure 3.21 explores the impact of Pr on energy distribution. Since, the Pr can be written as a ratio of kinematic diffusivity to heat diffusivity. The gradually increasing value of Pr increase the fluid density and decreasing thermal diffusivity and as a result the energy distribution is enhanced.

Effect of Heat Generation/Absorption Coefficient Q

Figure 3.22 illustrates the relationship between Q and temperature profile of the fluid. The plot clearly shows a reduction in temperature distribution of the fluid for negative value of Q. In the same way heat generation occurs for the positive value of Q. Due to these behaviors the temperature of the fluid gradually increases.

Effect of Brownian Motion Parameter Nb

Figure 3.24 is drawn to illustrate the relationship between Nb and temperature distribution. The temperature distribution is enhanced with rising value of Nb. Physically, Nb is associated with movement of the fluid nanoparticles. The kinetic energy of the fluid particles increases with boosting values of Nb, due to which the temperature distribution of the fluid increases. Figure 3.25 is drawn to analyze the effect of Nb on concentration profile, which shows that the increasing value of Nb produce a reduction in concentration distribution.

Effect of Suction Parameter S

Figures 3.11-3.13 show the relationship between S and velocity, S and temperature and S and concentration profile respectively. From the graphs it is observed that increasing the numerical value of S a decrement in the velocity, temperature and concentration profile of the fluid occur.

Effect of Lewis Number Le

Figure 3.30 analyzed the relation between the Lewis number Le and concentration distribution. Concentration profile decreased for high value of Le and thus we have get a small molecular diffusivity. Generally concentration profile is a decreasing function of Lewis number.

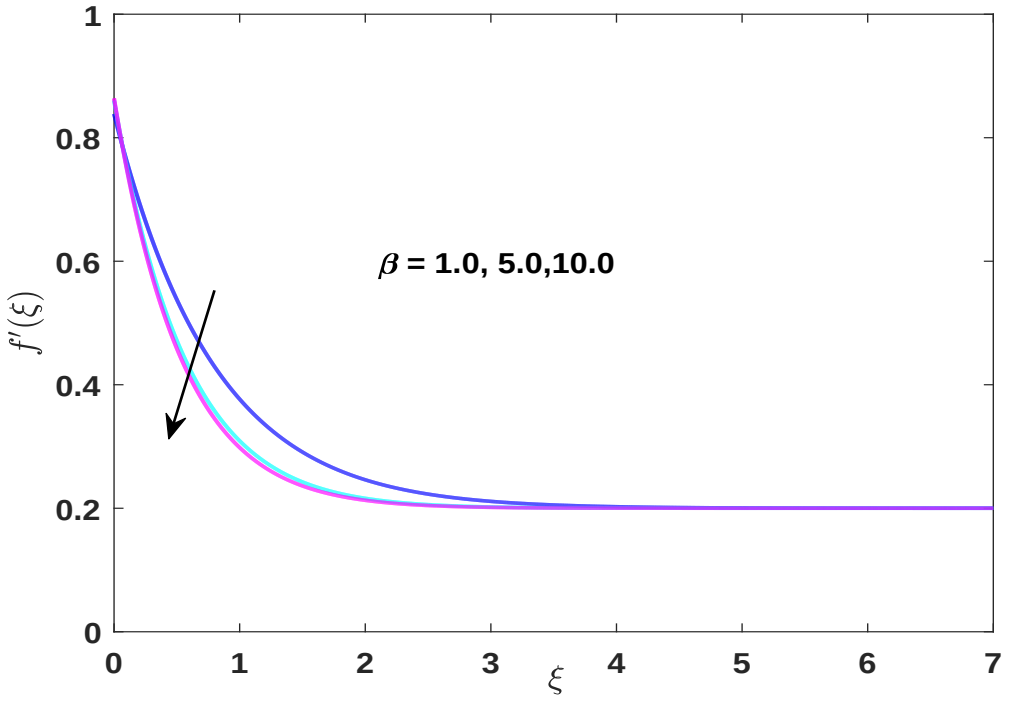

FIGURE 3.2: Influence of β on $f'(\xi)$.

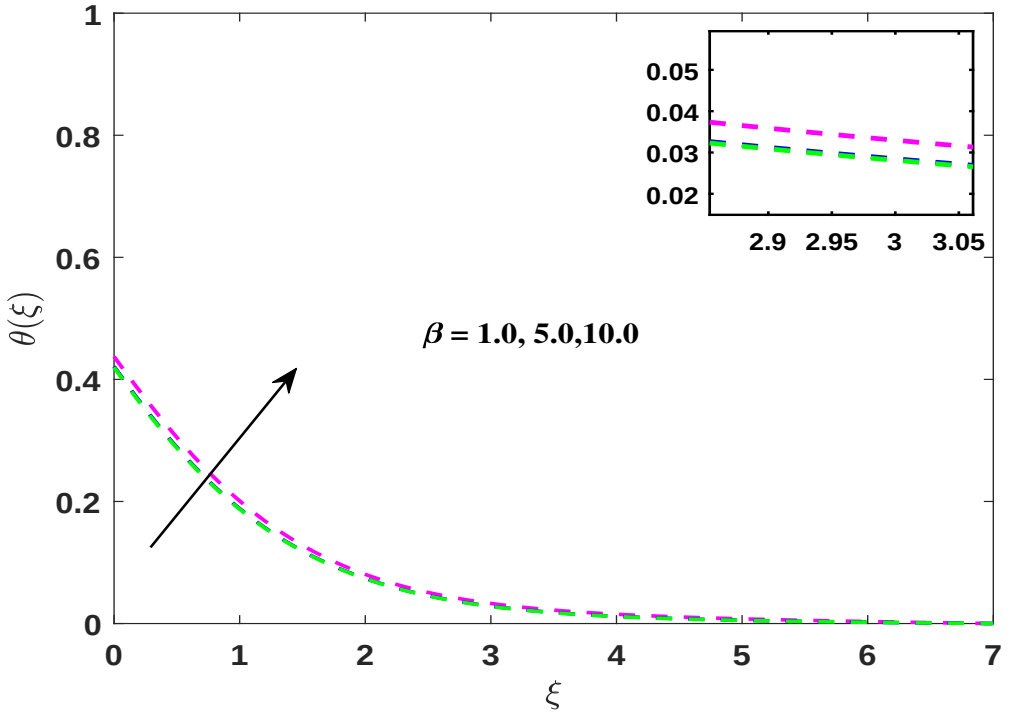

FIGURE 3.3: Influence of β on $\theta(\xi)$.

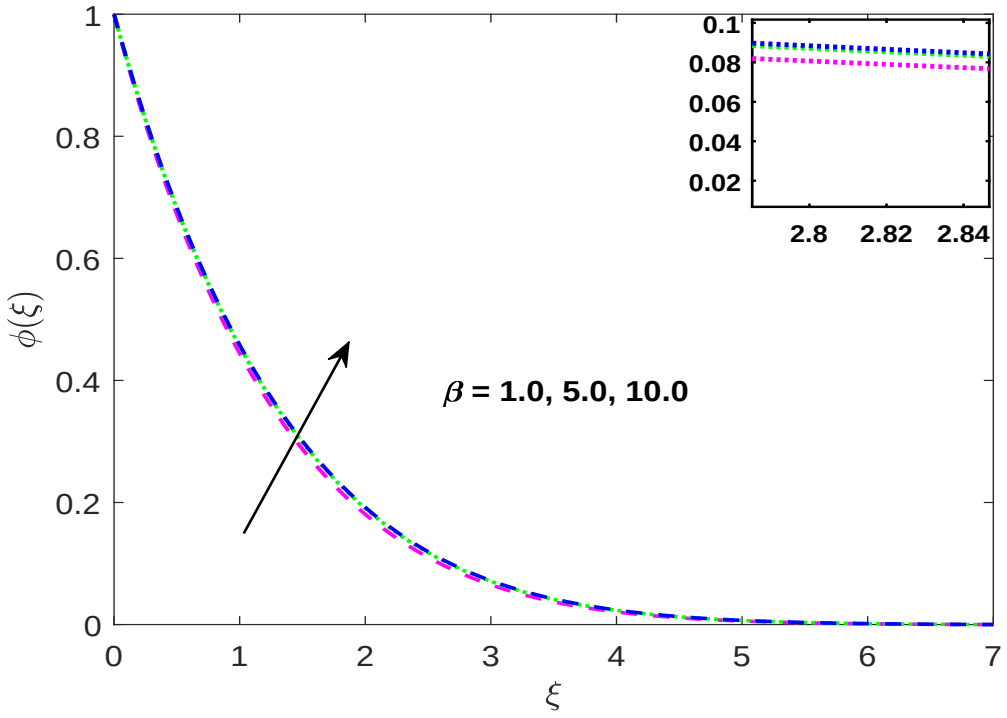

FIGURE 3.4: Influence of β on $\phi(\xi)$.

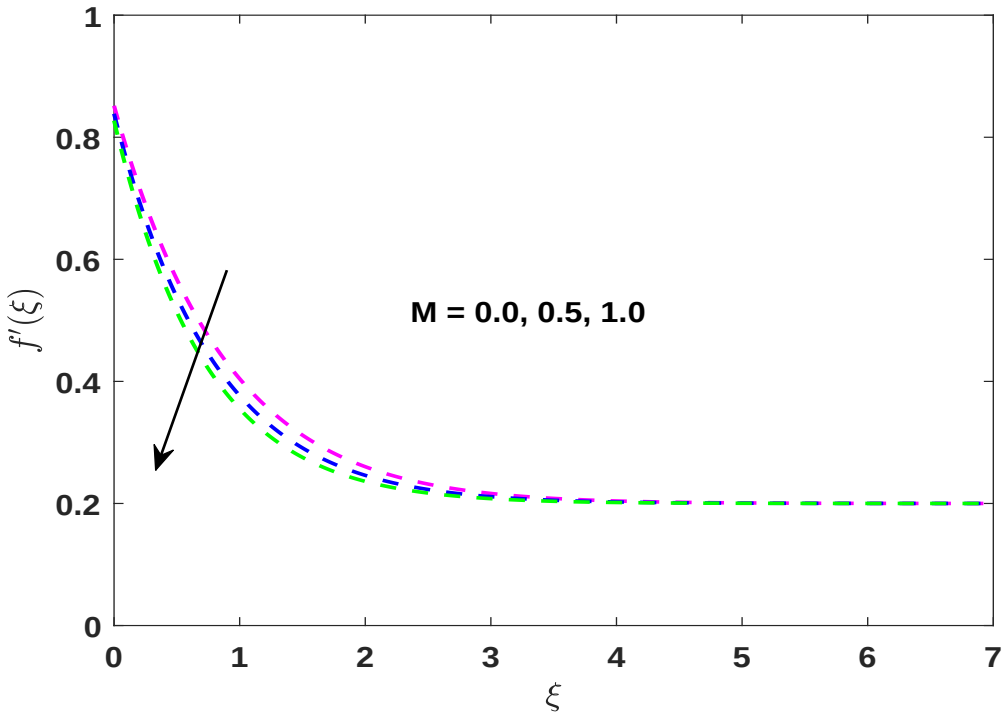

FIGURE 3.5: Influence of M on $f'(\xi)$.

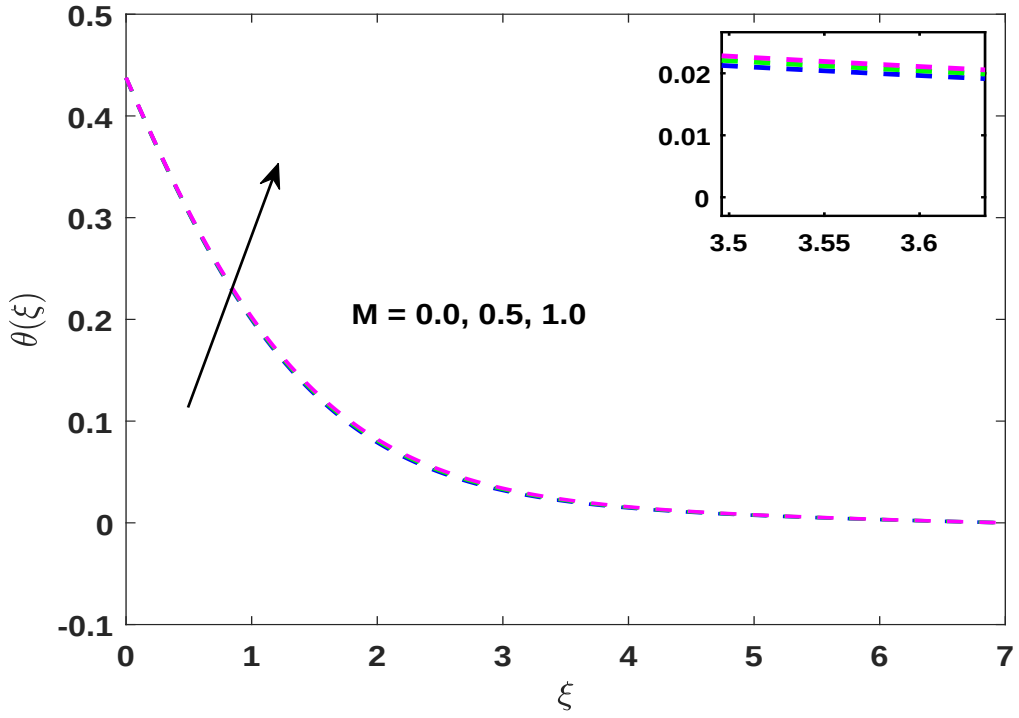

FIGURE 3.6: Influence of M on $\theta(\xi)$.

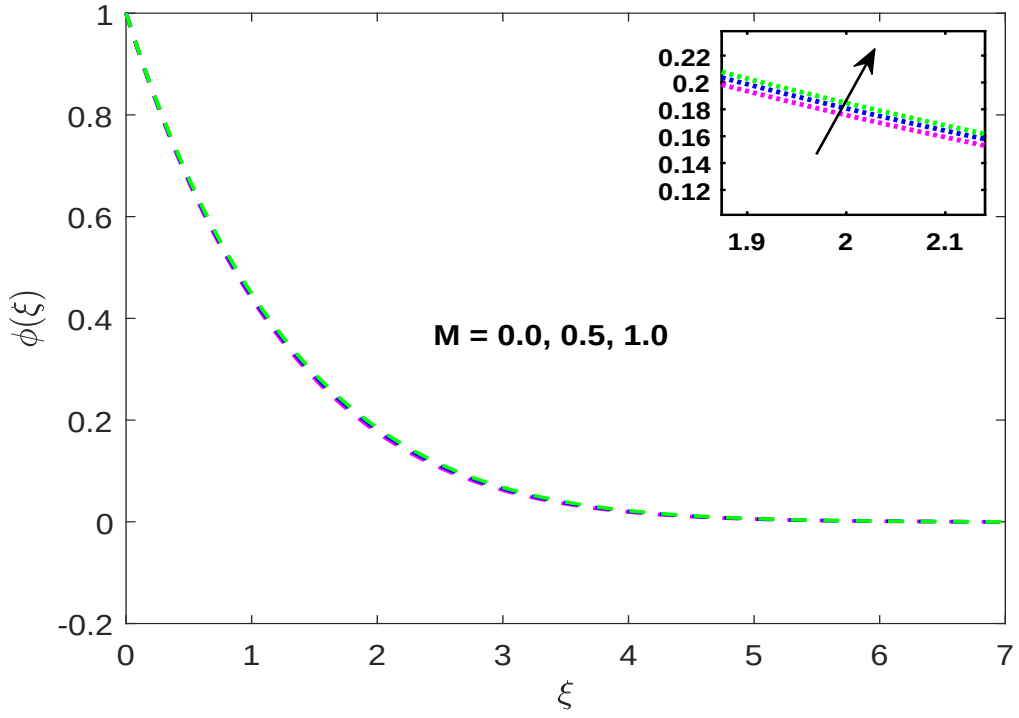

FIGURE 3.7: Influence of M on $\phi(\xi)$.

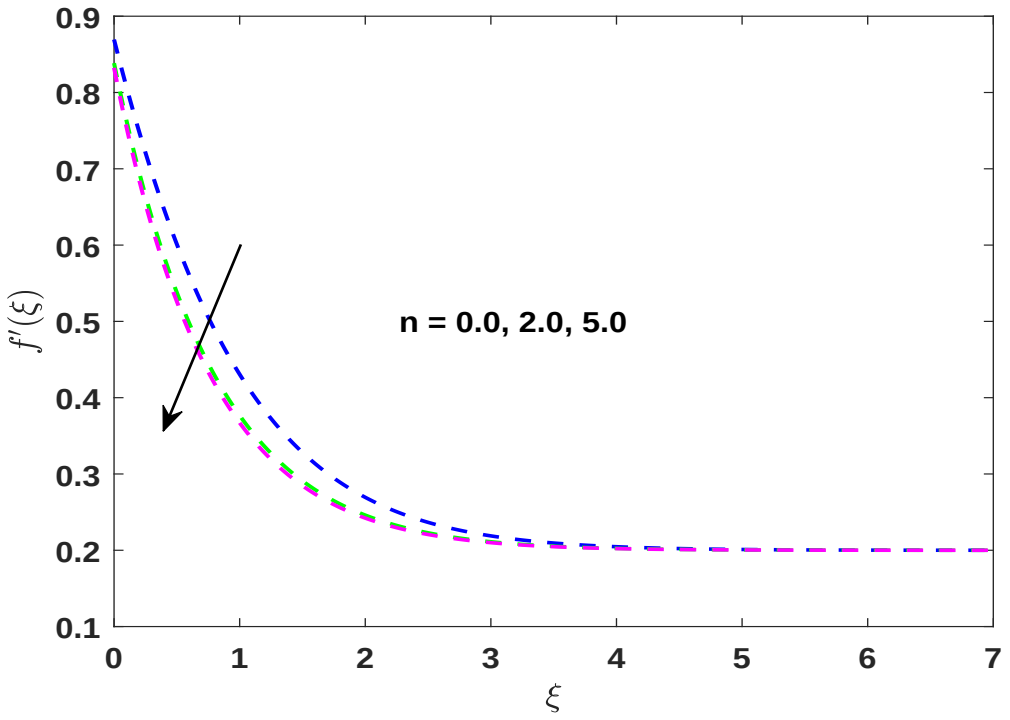

FIGURE 3.8: Influence of n on $f'(\xi)$.

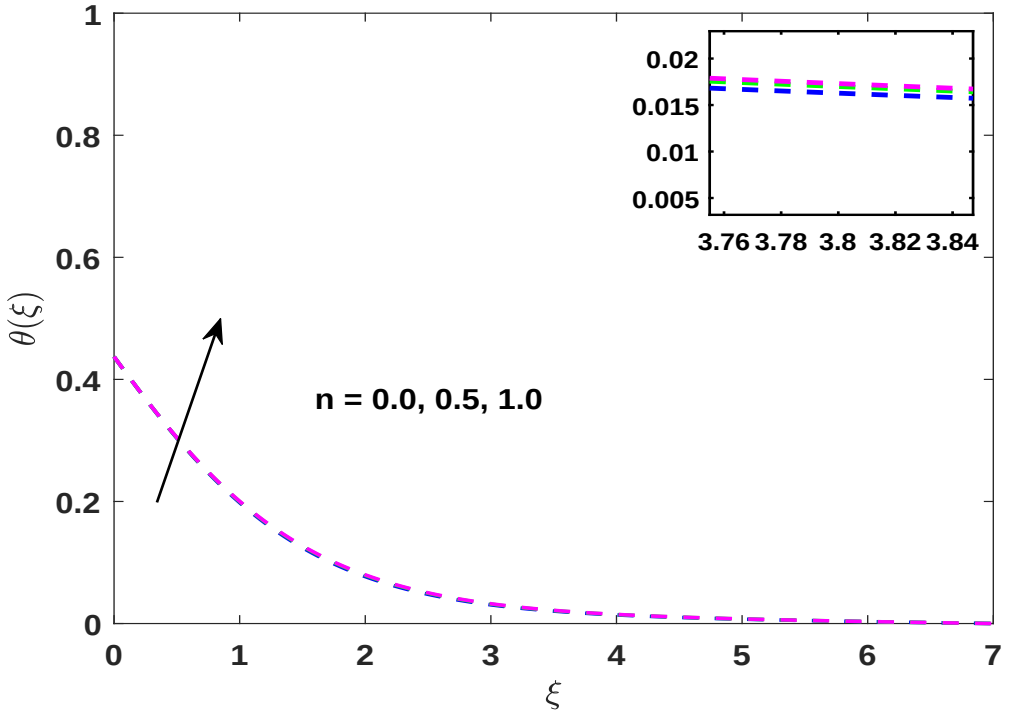

FIGURE 3.9: Influence of n on $\theta(\xi)$.

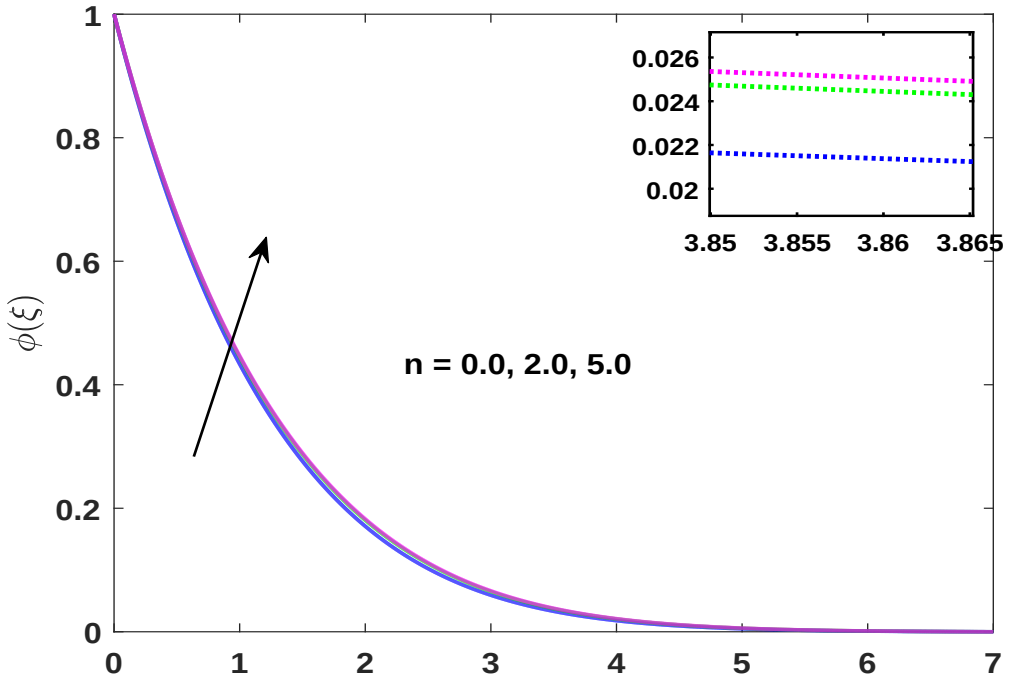

FIGURE 3.10: Influence of n on $\phi(\xi)$.

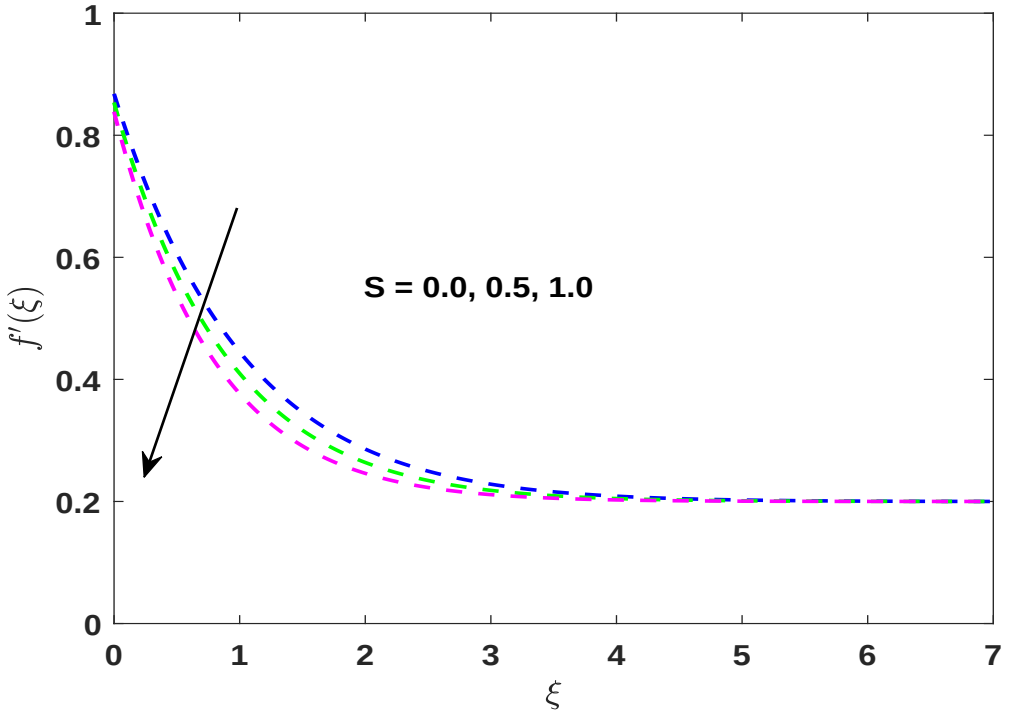

FIGURE 3.11: Influence of S on $f'(\xi)$.

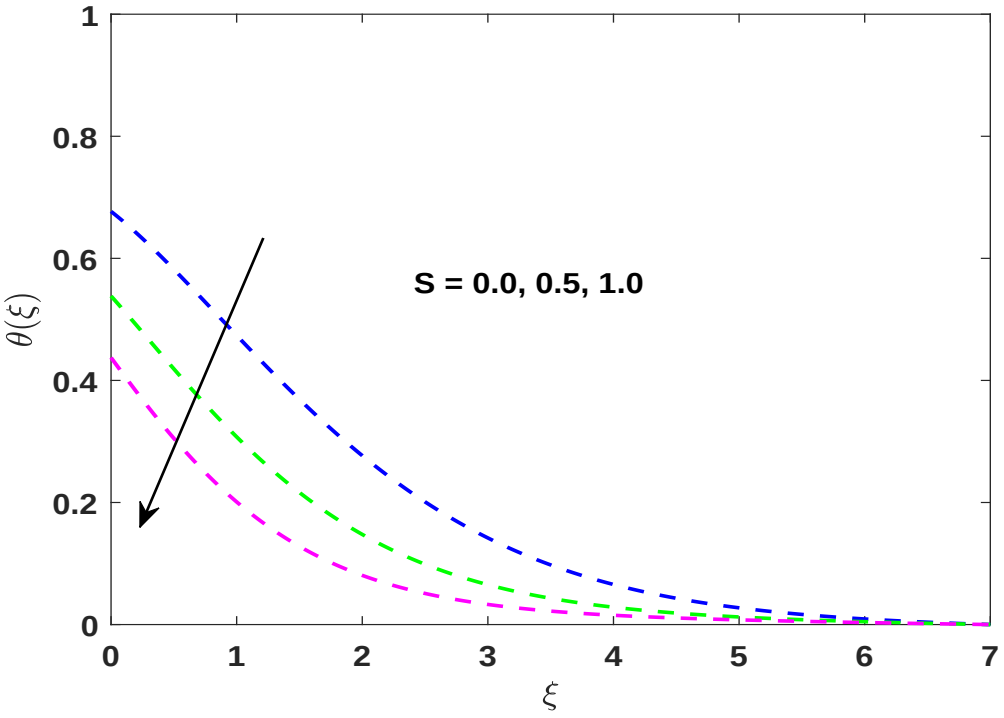

FIGURE 3.12: Influence of S on $\theta(\xi)$.

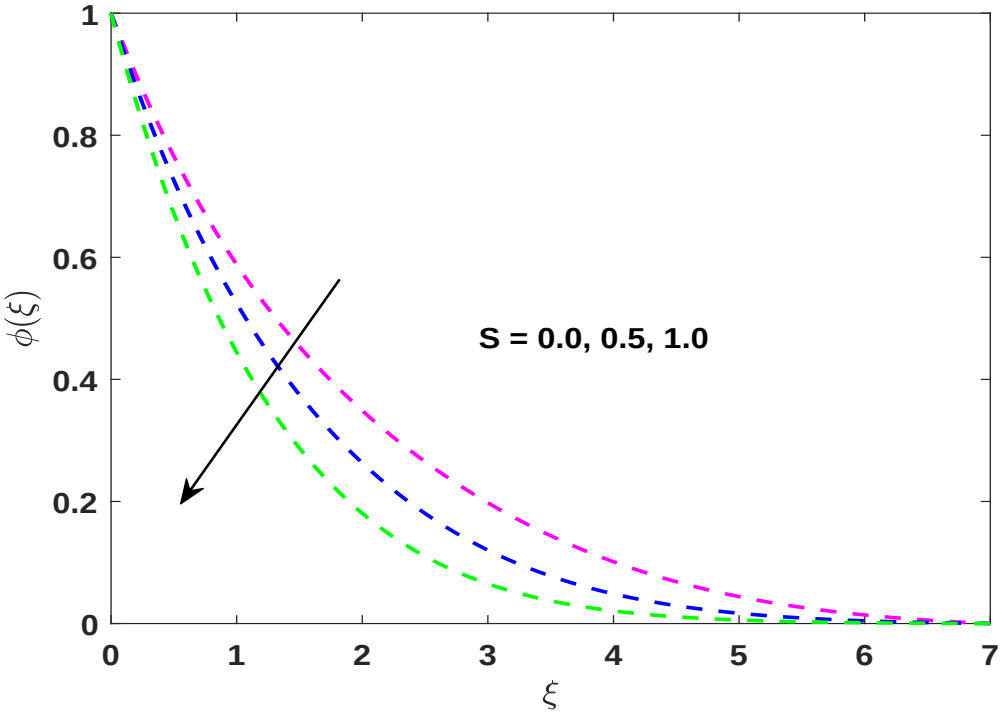

FIGURE 3.13: Influence of S on $\phi(\xi)$.

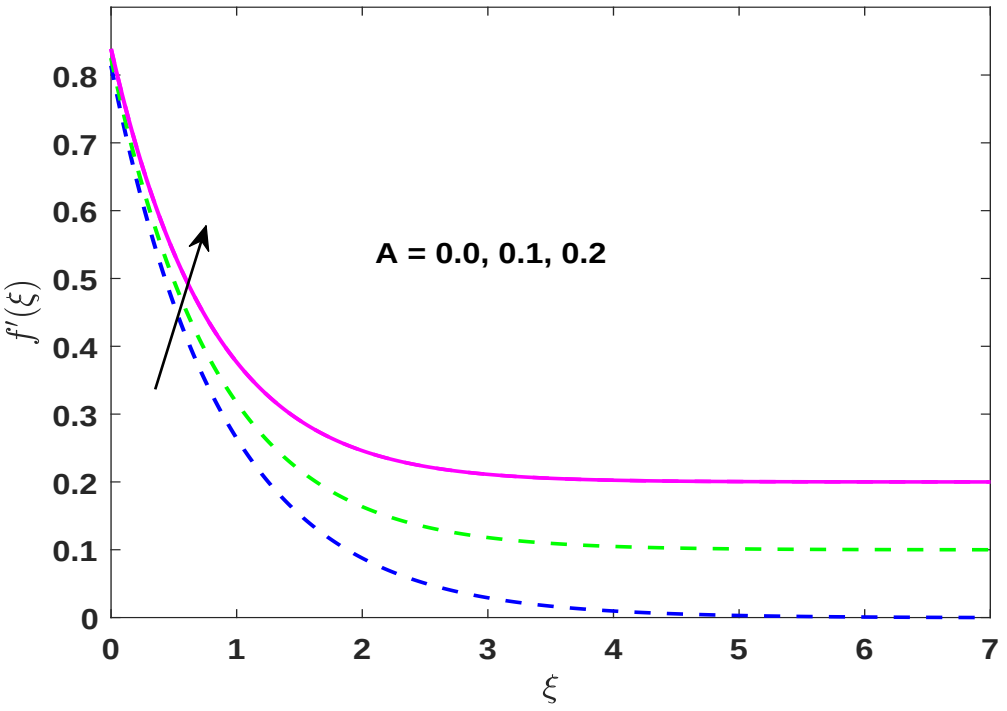

FIGURE 3.14: Influence of A on $f'(\xi)$.

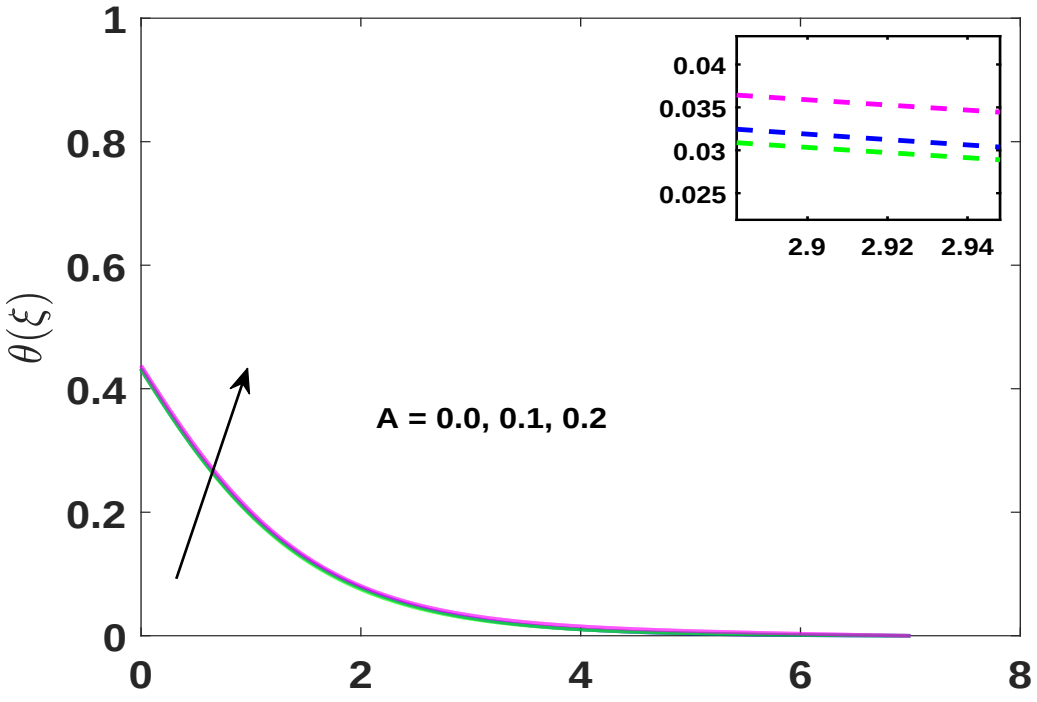

FIGURE 3.15: Influence of A on $\theta(\xi)$.

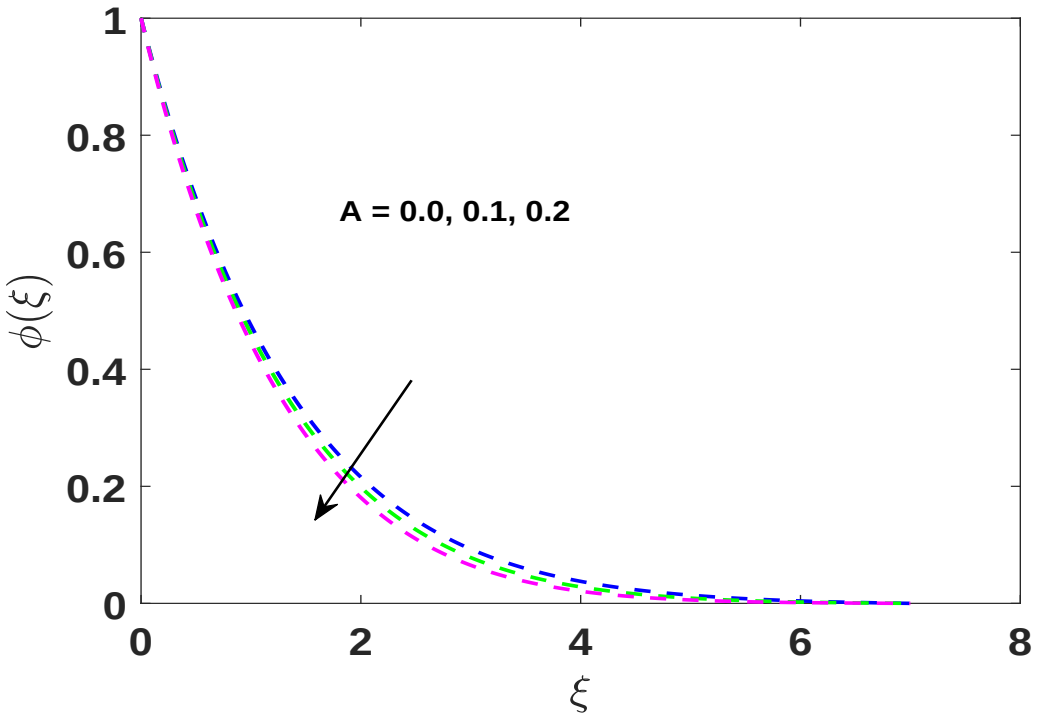

FIGURE 3.16: Influence of A on $\phi(\xi)$.

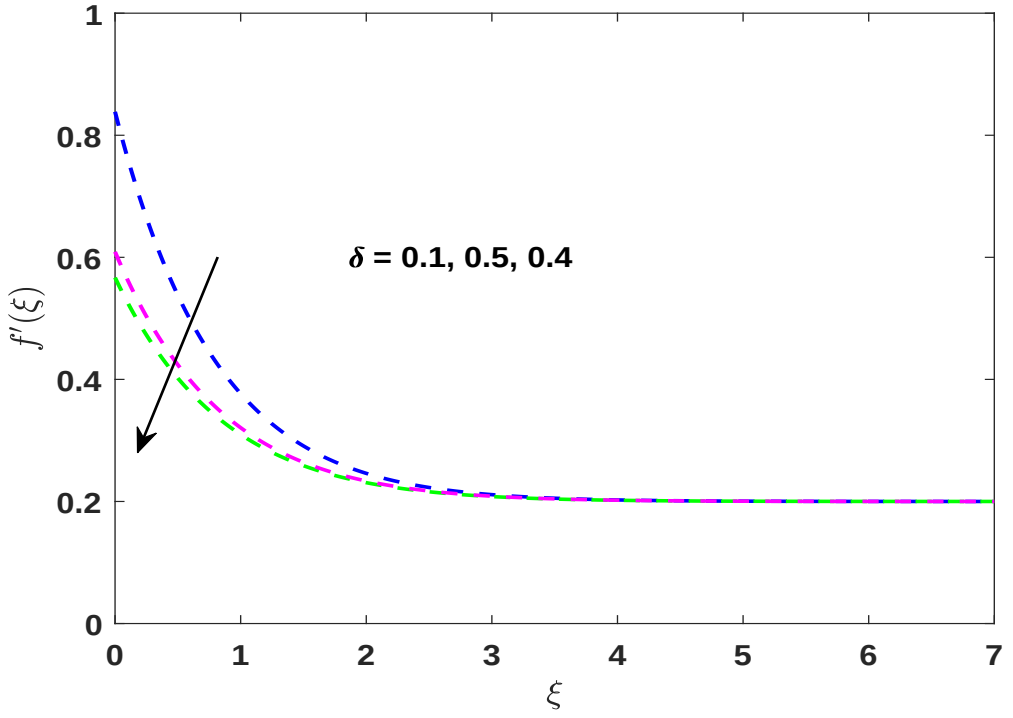

FIGURE 3.17: Influence of δ on $f'(\xi)$.

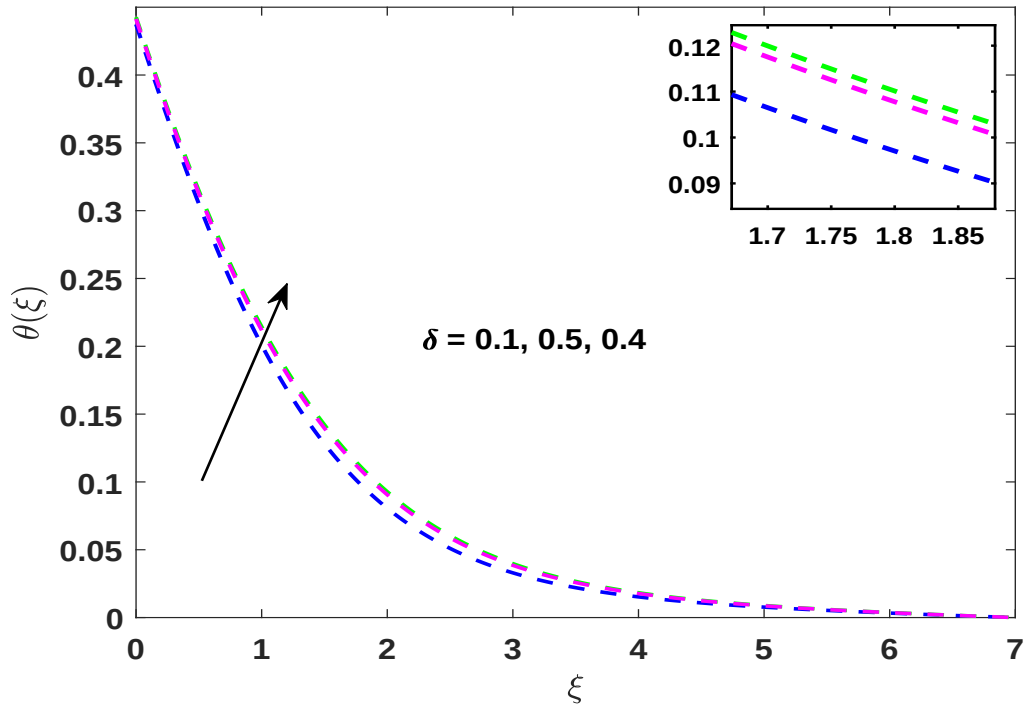

FIGURE 3.18: Influence of δ on $\theta(\xi)$.

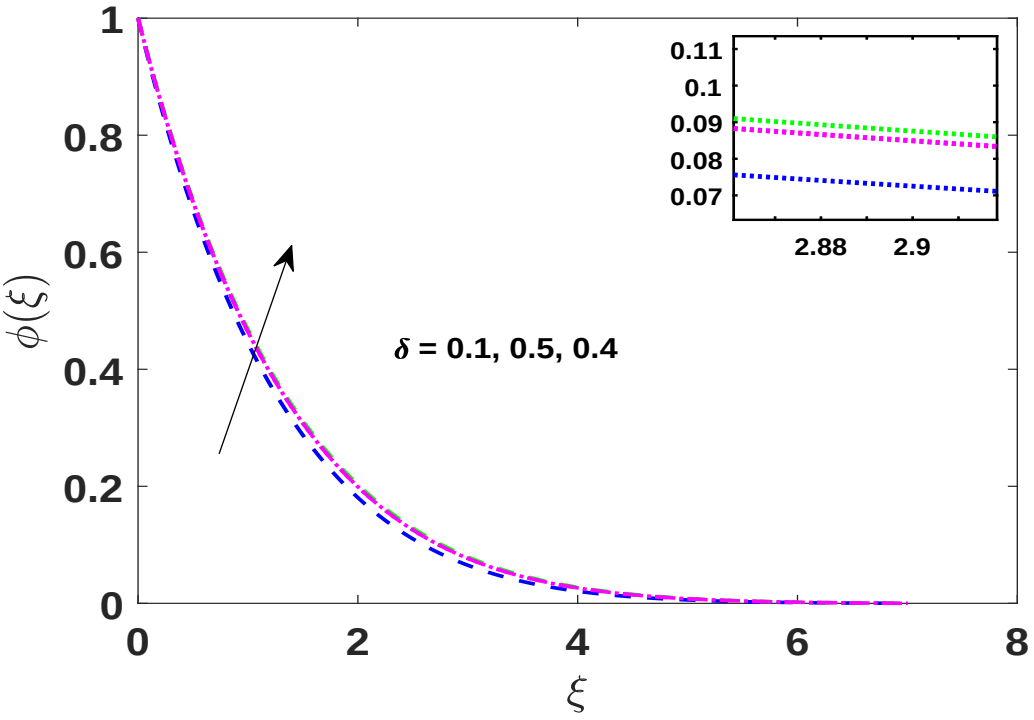

FIGURE 3.19: Influence of δ on $\phi(\xi)$.

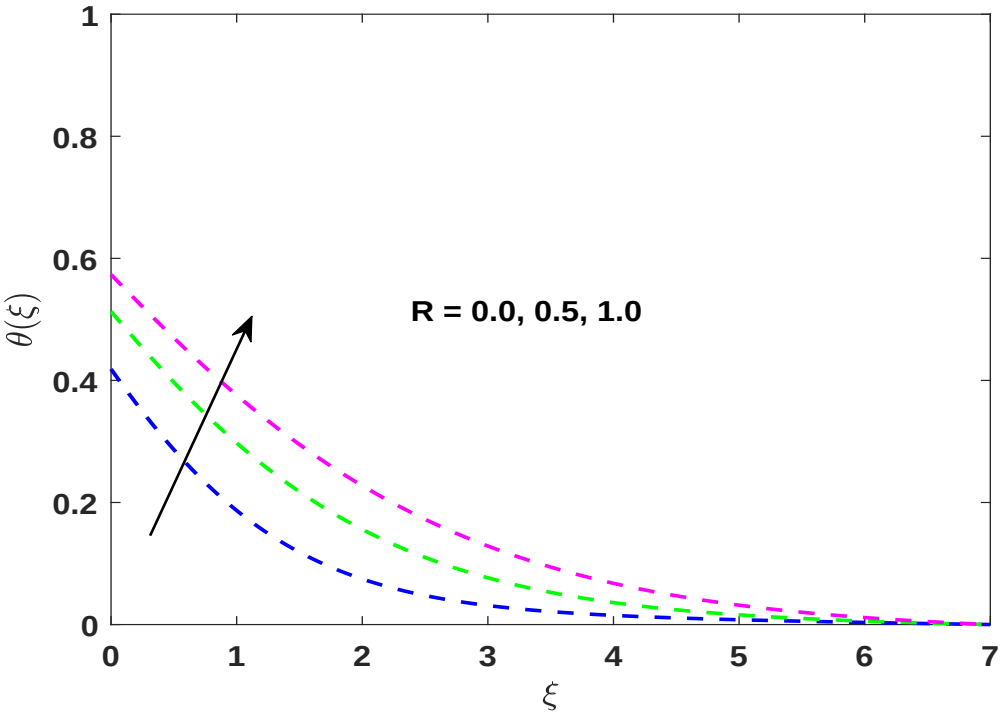

FIGURE 3.20: Influence of R on $\theta(\xi)$.

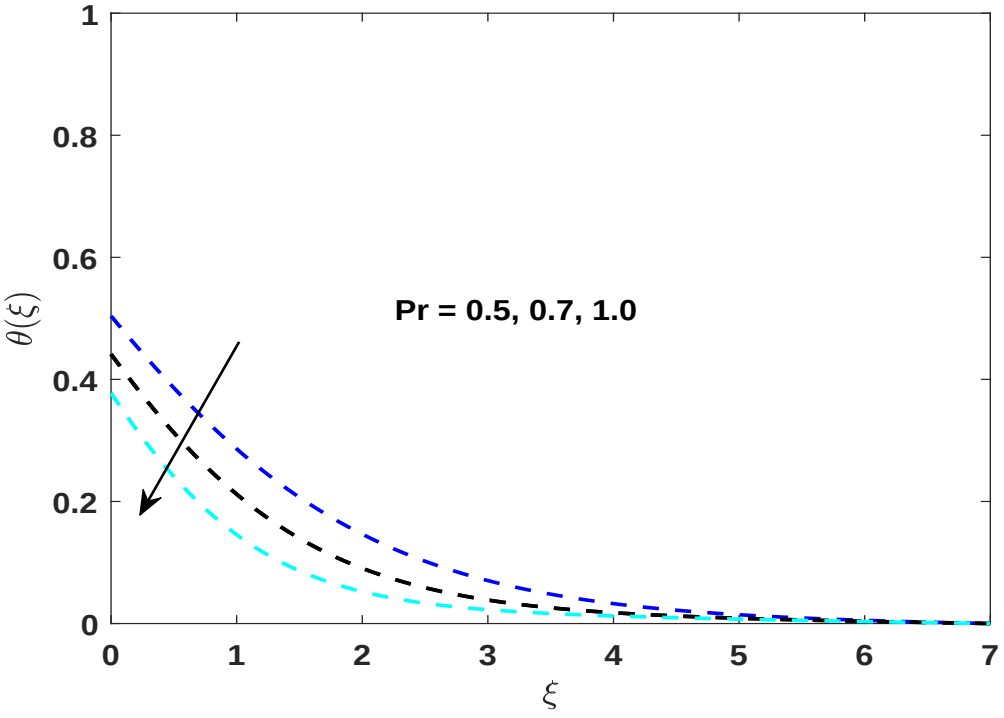

FIGURE 3.21: Influence of Pr on $\theta(\xi)$.

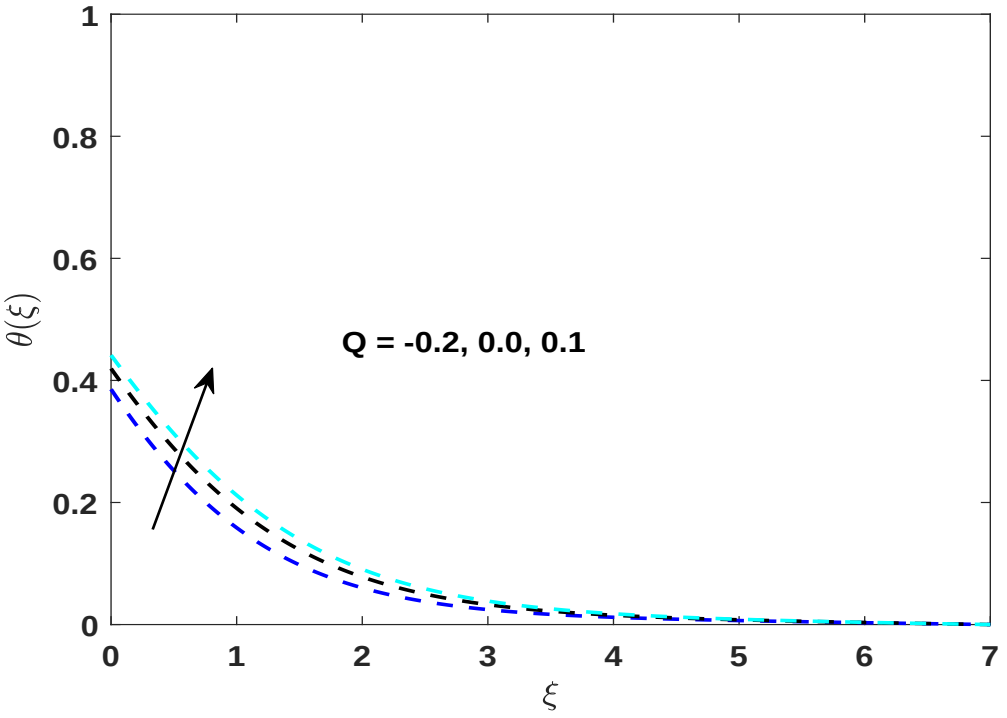

FIGURE 3.22: Effect of Q on $\theta(\xi)$.

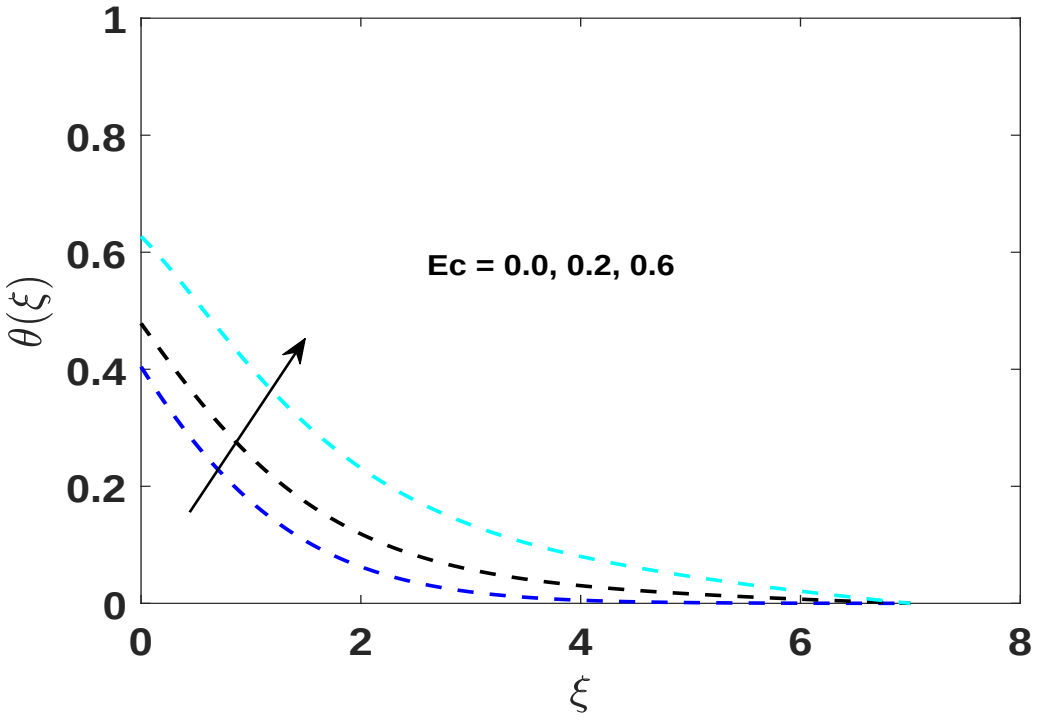

FIGURE 3.23: Influence of Ec on $\theta(\xi)$.

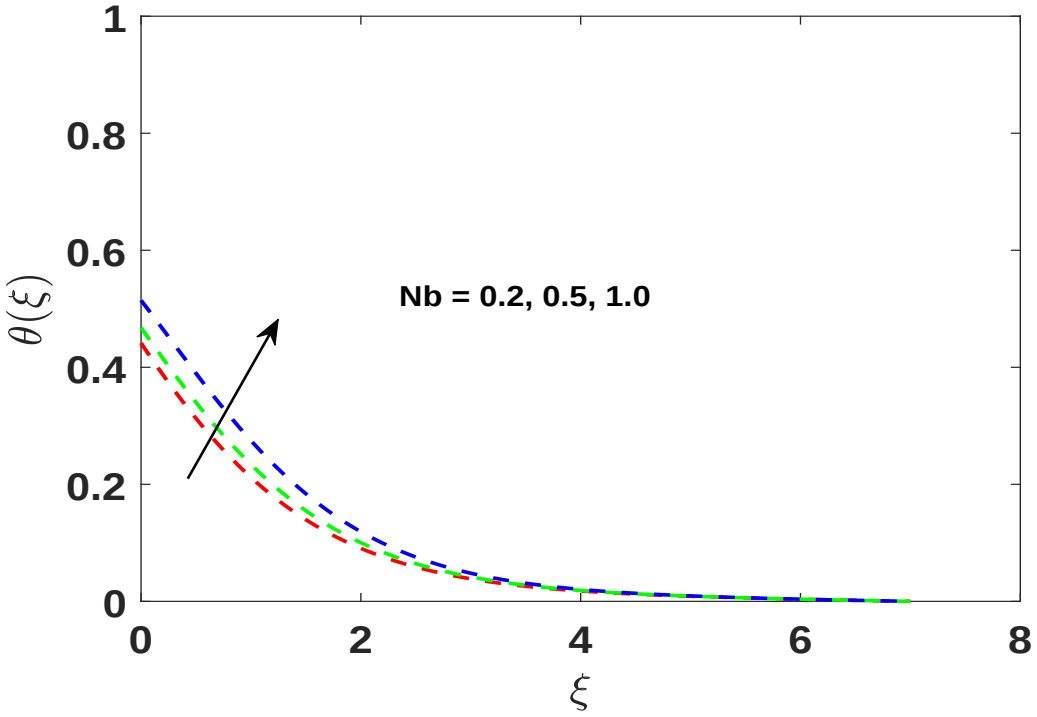

FIGURE 3.24: Influence of Nb on $\theta(\xi)$.

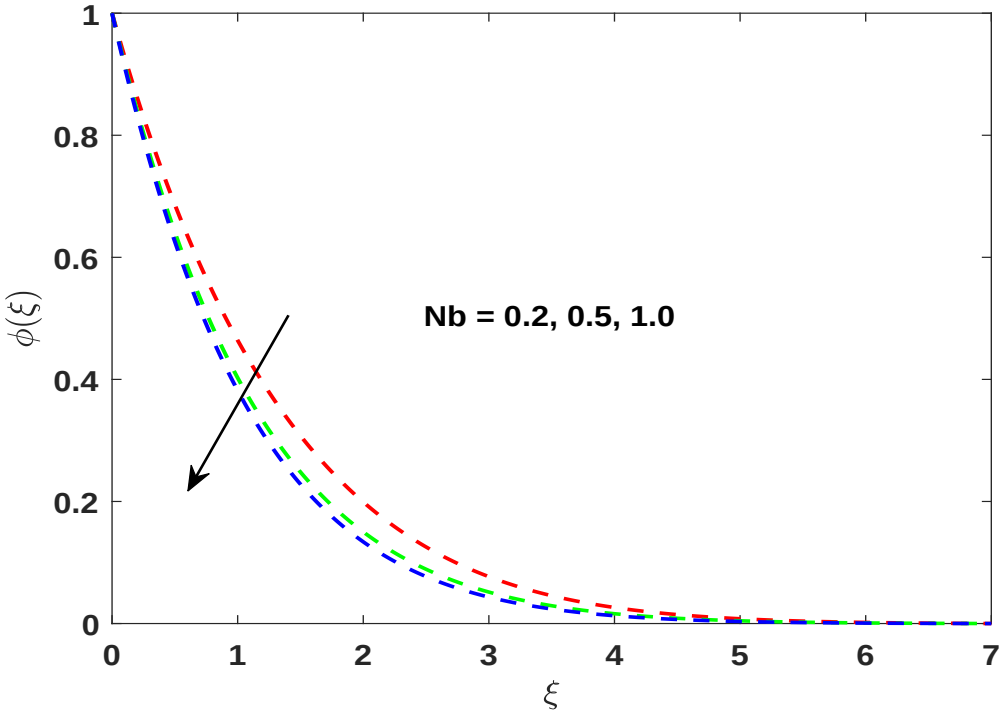

FIGURE 3.25: Influence of Nb on $\phi(\xi)$.

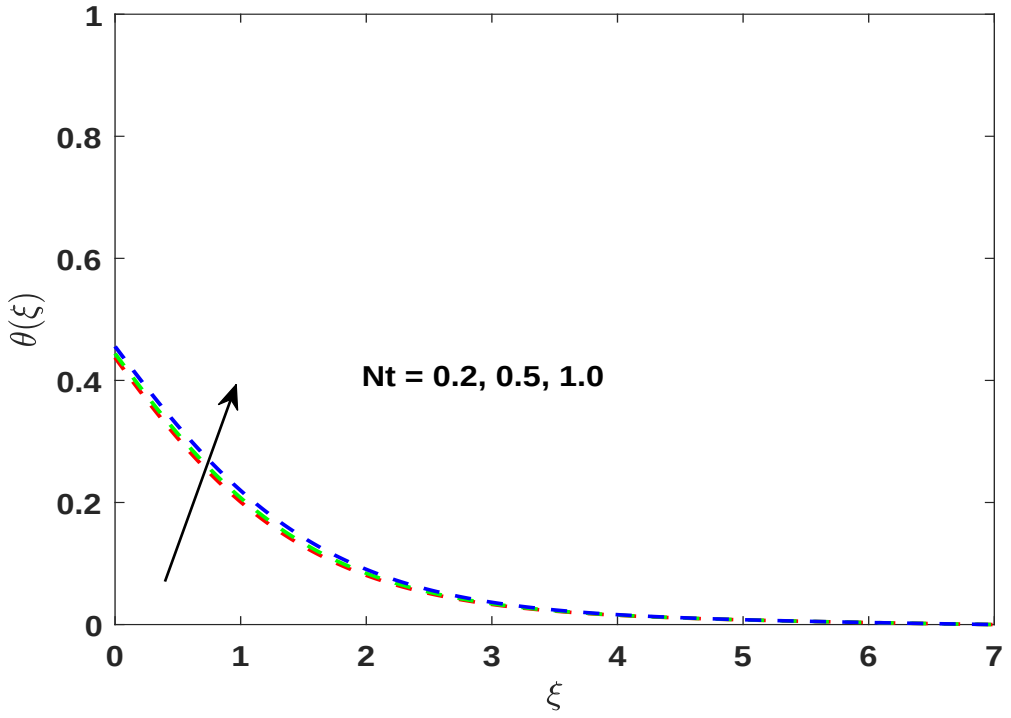

FIGURE 3.26: Influence of Nt on $\theta(\xi)$.

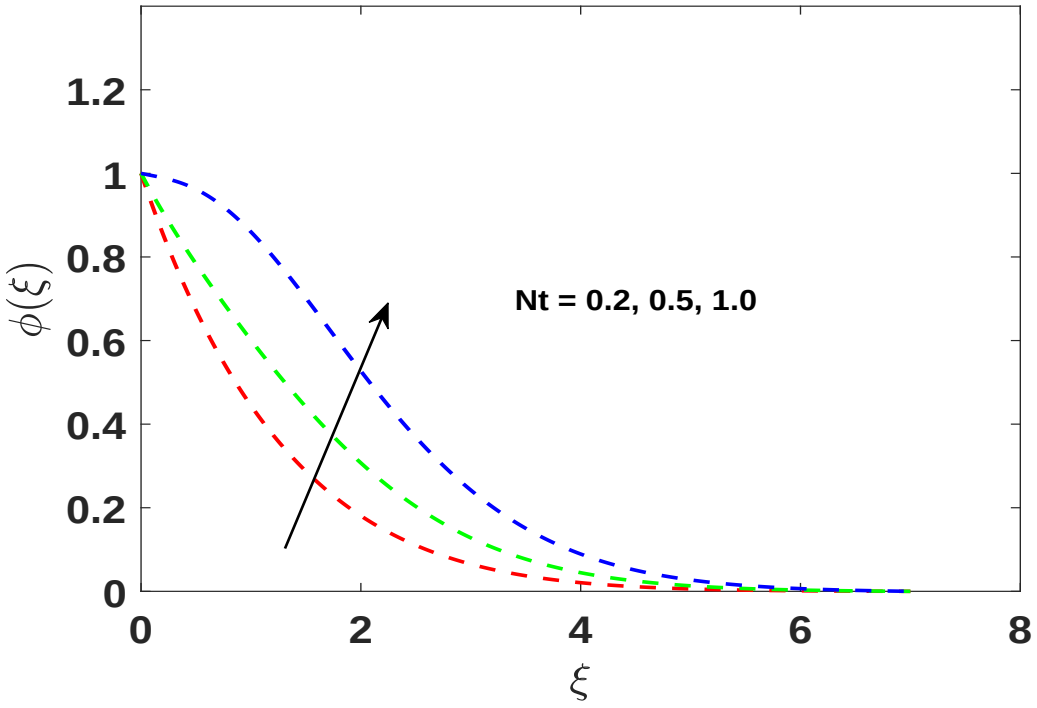

FIGURE 3.27: Influence of Nt on $\phi(\xi)$.

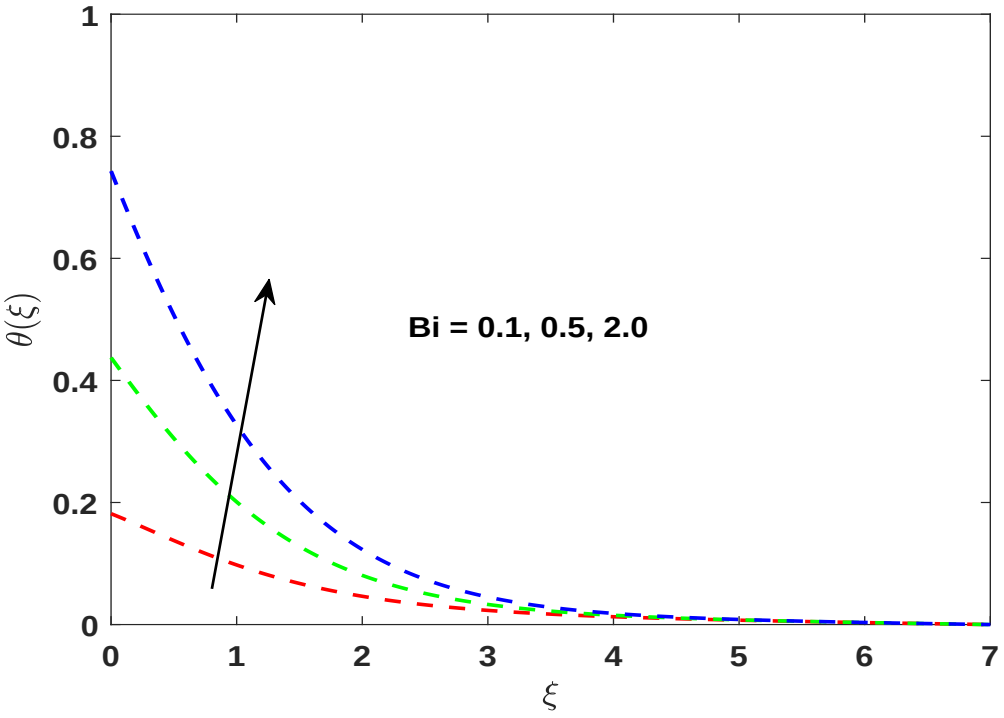

FIGURE 3.28: Effect of Bi on $\theta(\xi)$.

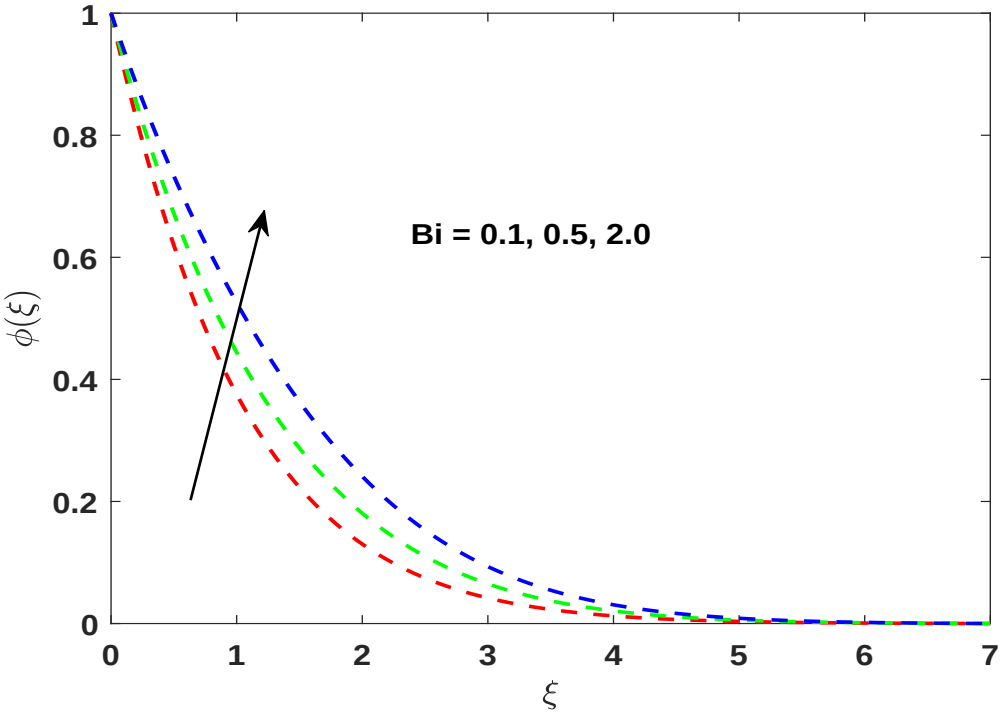

FIGURE 3.29: Influence of Bi on $\phi(\xi)$.

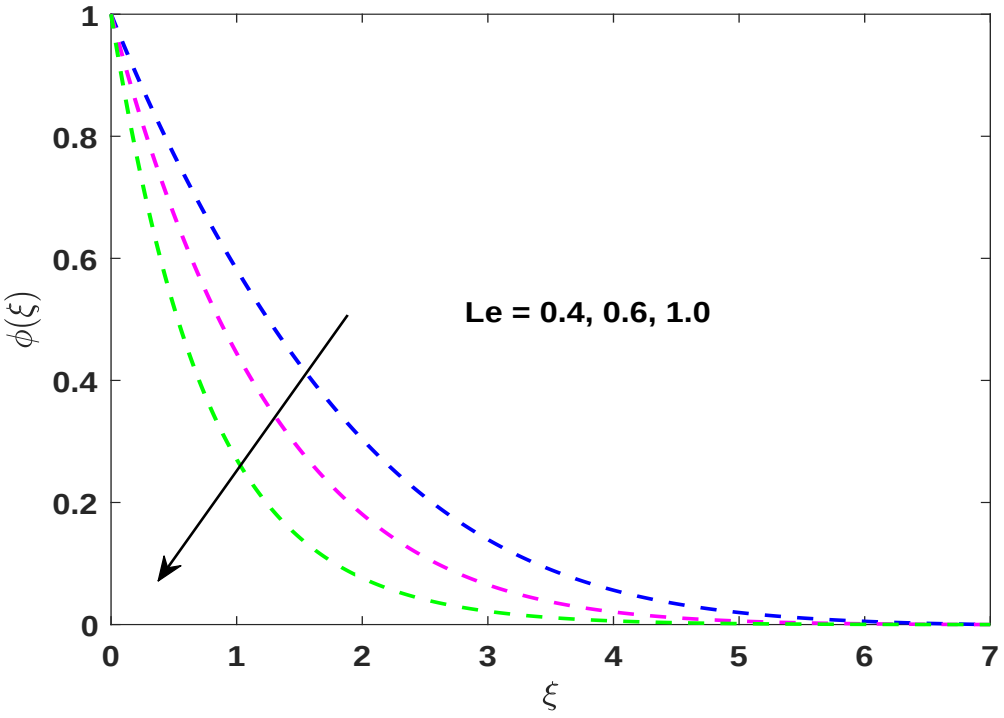

FIGURE 3.30: Influence of Le on $\phi(\xi)$.

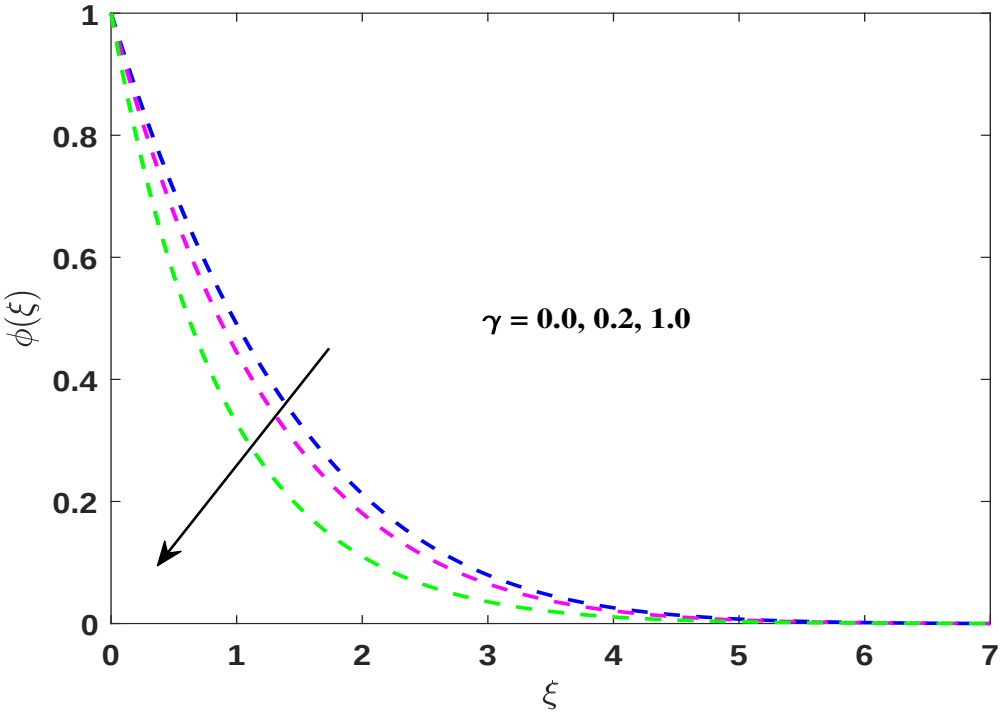

FIGURE 3.31: Influence of γ on $\phi(\xi)$.

Chapter 4

MHD Casson Nanofluid Flow with Dufour and Soret Effect

4.1 Introduction

The flow model of Ibrahim et al. [53] has been extended in this chapter by including additional effect of inclined magnetic field, Soret and Dufour. The MHD stagnation point flow using both slip velocity and convective boundary condition has been investigated. Furthermore, by using similarity variable a set of ODEs is obtained by converting the nonlinear PDEs of concentration, momentum and temperature. We will also use the well known shooting technique for the calculation of the numerical solution of these model ODEs. The influence of different parameters of the modeled equations on velocity, temperature, concentration, skin friction coefficient, Nusselt and Sherwood number will be discussed in detail in the result and discussion section.

4.2 Problem Formuation

The problem is formulated in the following way. We consider a 2D steady and incompressible flow of MHD stagnation point using a stretching sheet. The sheet

is displaced (in the plane $y = 0$) in such a way that the flow is constrained in the plane $y > 0$. The sheet is also stretched with velocity $u{=}U_w{=}ax^n$, with free stream velocity $U_\infty{=}bx^n$, where a and b are two positive constants and the stretching parameter $n \geq 0$. The slip velocity is given by $U_{slip}{=}\left(\mu_B + \frac{P_y}{\sqrt{2\pi_c}}\right)$ $\frac{\partial u}{\partial y}$ which is along x-axis where $B(x){=}B_0 x^{\frac{n-1}{2}}$ and B_0 is constant. The inclined magnetic field is applied to the sheet with an acute angle ω, $\left(0 \leq \omega \leq \frac{\pi}{2}\right)$. The induced magnetic field is neglected by assuming a small magnetic number. The nanoparticle concentration is consdier to be constant and the wall temperature can be regularized by a convective heating process. For extremely large value of y (i.e. $y \to \infty$) the nanoparticle concentration and temperature will be represented by C_∞ and T_∞ respectively.

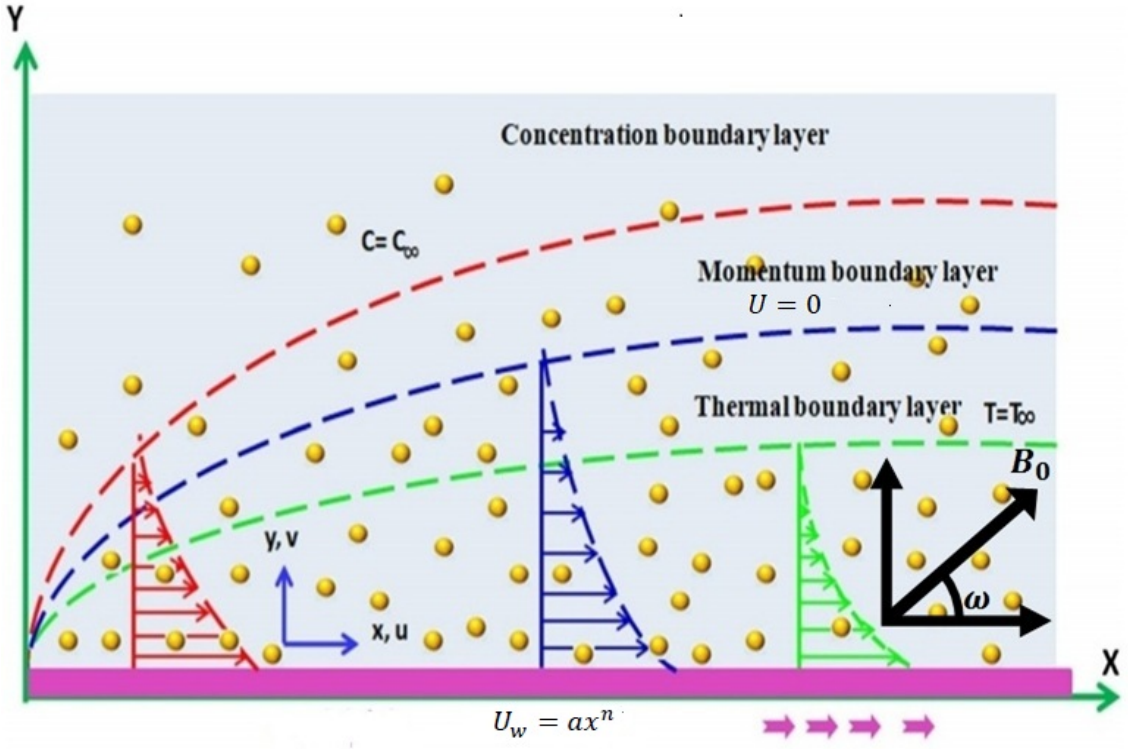

FIGURE 4.1: Geometry of physical model.

Under the light of above constraint the related governing equations are as follows:

$$\frac{\partial u}{\partial x}+\frac{\partial v}{\partial y}=0, \tag{4.1}$$

$$u\frac{\partial u}{\partial x}+v\frac{\partial u}{\partial y}=\nu\left(1+\frac{1}{\beta}\right)\frac{\partial^2 u}{\partial y^2}-\frac{\sigma B_0^2(x)}{\rho}u\sin^2\omega, \tag{4.2}$$

$$\begin{aligned}u\frac{\partial T}{\partial x}+v\frac{\partial T}{\partial y}=&\frac{D_m}{C_pC_s}K_T\frac{\partial^2 C}{\partial y^2}+\frac{\nu}{C_p}\left(1+\frac{1}{\beta}\right)\left(\frac{\partial u}{\partial y}\right)^2+\frac{\sigma B_0^2}{\rho}u^2\sin^2\omega\\&+\frac{(\rho c)_p}{(\rho c)_f}\left[D_B\frac{\partial C}{\partial y}\frac{\partial T}{\partial y}+\frac{D_T}{T_\infty}\left(\frac{\partial T}{\partial y}\right)^2\right]-\frac{1}{(\rho c)_f}\frac{\partial q_r}{\partial y}+\alpha\frac{\partial^2 T}{\partial y^2},\end{aligned} \tag{4.3}$$

$$u\frac{\partial C}{\partial x}+v\frac{\partial C}{\partial y}=D_B\frac{\partial^2 C}{\partial y^2}+\frac{D_mK_T}{T_m}\frac{\partial^2 T}{\partial y^2}-K_0(C-C_\infty). \tag{4.4}$$

And the boundary conditions are [53]:

$$\left.\begin{aligned}&U=ax^n,\ v=v_w,\ -k\frac{\partial T}{\partial y}=h_f(T_f-T),\ C=C_w\ \Big\}\text{ at } y=0,\\&u\to U_\infty,\ v\to 0,\ T\to T_\infty,\ C\to C_\infty \text{ as } \quad y\to\infty.\end{aligned}\right\} \tag{4.5}$$

In the above equations ω represents the inclination angle, the mass diffusivity is denoted by D_m , C_s stands for concentration susceptibility, C_p represents specific heat, K_T denotes the thermal-diffusion ratio, T_m stands for mean fluid temperature, etc.

4.3 Similarity Transformation

We adopt the below similarity variable for the conversion of PDEs and its related boundary condition into the ordinary differential equation [53]:

$$\left.\begin{aligned}&u=ax^nf'(\xi),\ v=-\sqrt{\frac{a\nu(n+1)}{2}}x^{\frac{n-1}{2}}\left(f(\xi)+\frac{n-1}{n+1}\xi f'(\xi)\right),\\&\xi=y\sqrt{\frac{a(n+1)}{2\nu}}x^{\frac{n-1}{2}},\quad \psi=\sqrt{\frac{2a\nu}{(n+1)}}x^{\frac{n+1}{2}}f(\xi),\\&\theta(\xi)=\frac{T-T_\infty}{T_f-T_\infty},\qquad \phi(\xi)=\frac{C-C_\infty}{C_w-C_\infty}.\end{aligned}\right\} \tag{4.6}$$

Velocity components intems of streem function are define as

$$u = \frac{\partial \psi}{\partial y}, \quad v = -\frac{\partial \psi}{\partial x}.$$

Detailed procedure for the confirmation of continuity Eq. (4.1) has been discussed in Chapter 3. We used the same procedure to convert Eq. (4.2) into the dimensionless form, differentiating u w.r.t x, we have

$$\frac{\partial u}{\partial x} = ax^{n-1}\left(nf'(\xi) + \frac{n-1}{2}\xi f''(\xi)\right).$$

Now differentiating u w.r.t y, we get

$$\frac{\partial u}{\partial y} = ax^{n}\sqrt{\frac{a(n+1)}{2\nu}}x^{\frac{n-1}{2}}f''(\xi),$$
$$\frac{\partial^2 u}{\partial y^2} = a^2x^{2n-1}\frac{n+1}{2\nu}f'''(\xi).$$

We can also write the left hand side of Eq. (4.2) as

$$u\frac{\partial u}{\partial x} + v\frac{\partial u}{\partial y} = a^2x^{2n-1}\left[nf'^2 - \frac{n+1}{2}ff''\right].$$

In order to convert the right hand side of Eq. (4.2) into dimensionaless form we used the same procedure i.e.,

$$\nu\left(1+\frac{1}{\beta}\right)\frac{\partial^2 u}{\partial y^2} = \left(1+\frac{1}{\beta}\right)a^2x^{2n-1}\left(\frac{n+1}{2}\right)f''', \tag{4.7}$$

$$\frac{\sigma B_0^2(x)}{\rho}u\sin^2\omega = \frac{\sigma B_0^2 x^{n-1}}{\rho}ax^n f'\sin^2\omega. \tag{4.8}$$

Putting Eqs. (4.7)-(4.8) in Eq. (4.2) we get the following dimensionless form

$$\left(1+\frac{1}{\beta}\right)f''' + ff'' - \frac{2n}{n+1}f'^2 - Mf'\sin^2\omega = 0.$$

The same procedure is be used to convert Eq. (4.3) into the dimensionless form

- $T = T_\infty + (T_f - T_\infty)\theta,$
- $C = C_\infty + (C_w - C_\infty)\phi.$
- $\dfrac{\partial T}{\partial x} = (T_f - T_\infty)\theta'\left(\dfrac{n-1}{2x}\right)\xi,$
- $\dfrac{\partial^2 T}{\partial y^2} = (T_f - T_\infty)\theta''\dfrac{a(n+1)}{2\nu}x^{n-1}.$
- $\dfrac{\partial^2 C}{\partial y^2} = (C_w - C_\infty)\phi''\dfrac{a(n+1)}{2\nu}x^{n-1}.$

Taking the left hand side of Eq. (4.3)

$$u\frac{\partial T}{\partial x} = a(T_f - T_\infty)\left(\frac{n-1}{2}\right)\xi x^{n-1}f'\theta'. \tag{4.9}$$

$$v\frac{\partial T}{\partial y} = -\frac{a(n+1)}{2}\left(f\theta' + \frac{n-1}{n+1}\xi f'\theta\right)(T_f - T_\infty)x^{n-1}. \tag{4.10}$$

Adding Eqs. (4.9)-(4.10) we get the left hand side of Eq. (4.3)

$$u\frac{\partial T}{\partial x} + v\frac{\partial T}{\partial y} = \frac{-a(n+1)}{2}(T_f - T_\infty)x^{n-1}f\theta'. \tag{4.11}$$

Similarly, we have used the same proces to convert the right hand side of Eq. (4.3) into dimensional form

$$\alpha\frac{\partial^2 T}{\partial y^2} = \alpha(T_w - T_\infty)\theta''\frac{a(n+1)}{2\nu}x^{n-1}, \tag{4.12}$$

$$\frac{\nu}{C_p}\left(1+\frac{1}{\beta}\right)\left(\frac{\partial u}{\partial y}\right)^2 = \frac{1}{C_p}\left(1+\frac{1}{\beta}\right)a^2x^{2n}f''^2\frac{a(n+1)}{2}x^{n-1},$$

$$\frac{1}{(\rho_c)_f}\frac{\partial q_r}{\partial y} = \frac{1}{(\rho_c)_f}\frac{-16\sigma^*}{3k^*}T_\infty^3\left(T_w - T_\infty\right)\frac{a(n+1)}{2\nu}x^{n-1}\theta'',$$

$$\frac{\sigma B_0^2(x)}{\rho}u^2\sin^2\omega = \frac{\sigma B_0^2(x)a^2x^{2n}f'^2\sin^2\omega}{\rho},$$

$$\frac{D_mK_T}{C_pC_s}\frac{\partial^2 C}{\partial y^2} = \frac{D_mK_T}{C_pC_s}(C_w - C_\infty)\frac{a(n+1)}{2\nu}x^{n-1}\theta''. \tag{4.13}$$

Using Eqs. (4.11)-(4.14) in (4.3) the following form is obtained

$$\begin{aligned}
&\frac{-a(n+1)}{2}(T_f - T_\infty)x^{n-1} f\theta' = \alpha(T_f - T_\infty)\theta''\frac{a(n+1)}{2\nu}x^{n-1} \\
&\quad + \frac{(\rho c)_p}{(\rho c)_f}\left[D_B(C_w - C_\infty)(T_w - T_\infty)\phi'\theta'\frac{a(n+1)}{2\nu}x^{n-1}\right] \\
&\quad + \frac{(\rho c)_p}{(\rho c)_f}\left[\frac{D_T}{T_\infty}(T_w - T_\infty)^2\frac{a(n+1)}{2\nu}x^{n-1}\theta'^2\right] \\
&+ \frac{1}{C_p}\left(1+\frac{1}{\beta}\right)a^2x^{2n}f''^2\frac{a(n+1)}{2}x^{n-1} + \frac{\sigma B_0^2(x)a^2x^{2n}f'^2\sin^2\omega}{\rho} \\
&- \frac{1}{(\rho_c)_f}\frac{16\sigma^*}{3k^*}T_\infty^3\left(T_f - T_\infty\right)\frac{a(n+1)}{2\nu}x^{n-1}\theta'' \\
&\qquad + \frac{D_m K_T}{C_p C_s}(C_w - C_\infty)\frac{a(n+1)}{2\nu}x^{n-1}\theta''. \qquad (4.14)
\end{aligned}$$

Dividing each terms of Eq. (4.14) by $\frac{2}{a(n+1)x^{n-1}(T_f - T_\infty)}$, we get

$$\begin{aligned}
&\frac{1}{Pr}\theta'' + \frac{4}{3}R\frac{1}{Pr}\theta'' + Nb\phi'\theta' + Nt\theta'^2 + f\theta' \\
&\qquad + \left(1+\frac{1}{\beta}\right)Ecf''^2 MEcf'^2\sin^2\omega + D_u\phi'' = 0. \qquad (4.15)
\end{aligned}$$

Multiplying each terms of Eq. (4.15) by Pr, we get

$$\begin{aligned}
&\left(1+\frac{4}{3}R\right)\theta'' + Prf\theta' + PrNb\phi'\theta' + PrNt\theta'^2 \\
&\qquad + \left(1+\frac{1}{\beta}\right)PrEcf''^2 + MPrEcf'^2\sin^2\omega + PrDu\phi'' = 0. \qquad (4.16)
\end{aligned}$$

Eq. (4.4) can also be converted into dimensionless form as:

- $\dfrac{\partial C}{\partial x} = \phi'(\xi)\left(C_w - C_\infty\right)\dfrac{\xi}{x}\left(\dfrac{n-1}{2}\right)$,
- $\dfrac{\partial^2 C}{\partial y^2} = \phi''(\xi)\left(C_w - C_\infty\right)\dfrac{a(n+1)}{2\nu}x^{n-1}$.

In the same way we can find $\frac{\partial T}{\partial y}$, as

- $\dfrac{\partial T}{\partial y} = \left(T_w - T_\infty\right)\theta'(\xi)\sqrt{\dfrac{a(n+1)}{2\nu}}x^{\frac{n-1}{2}}$,

$$u\frac{\partial C}{\partial x} = ax^{n-1}\Big(C_w - C_\infty\Big)\left(\frac{n-1}{2}\right)\xi f'(\xi)\phi'(\xi). \tag{4.17}$$

$$v\frac{\partial C}{\partial y} = -\frac{a(n+1)}{2}x^{n-1}\Big(C_w - C_\infty\Big)\phi'(\xi)\left[f(\xi) + \frac{n-1}{n+1}\xi f'(\xi)\right]. \tag{4.18}$$

Similarly Eq. (4.4) takes the form

$$u\frac{\partial C}{\partial x} + v\frac{\partial C}{\partial y} = -\frac{a(n+1)}{2}x^{n-1}\Big(C_w - C_\infty\Big)f\phi'.$$

The following procedure can be used to convert the right hand side of Eq. (4.4) into dimensionless form

$$D_B\frac{\partial^2 C}{\partial y^2} = D_B\left[\Big(C_w - C_\infty\Big)\phi''(\xi)\frac{a(n+1)}{2\nu}x^{n-1}\right],$$

$$\frac{D_m K_T}{T_m}\frac{\partial^2 T}{\partial y^2} = \frac{D_m K_T}{T_m}\left[\Big(T_f - T_\infty\Big)\theta''(\xi)\frac{a(n+1)}{2\nu}x^{n-1}\right],$$

$$K_0(C - C_\infty)\phi = K_0(C_w - C_\infty)\phi.$$

Using all of the above values in Eq. (4.4), it becomes

$$\frac{-a(n+1)}{2}x^{n-1}\Big(C_w - C_\infty\Big)f(\xi)\phi'(\xi) = D_B\Big(C_w - C_\infty\Big)\frac{a(n+1)}{2\nu}x^{n-1}\phi''(\xi) + \frac{D_m K_T}{T_m}\frac{a(n+1)}{2\nu}\Big(T_f - T_\infty\Big)x^{n-1}\theta''(\xi) - K_0\Big(C_w - C_\infty\Big). \tag{4.19}$$

Dividing each terms of Eq. (4.19) by $\frac{2}{a(n+1)x^{n-1}(C_w - C_\infty)}$, we get

$$-f\theta' = \frac{1}{Sc}\phi'' + Sr\theta'' - \gamma\phi. \tag{4.20}$$

Multiplying each terms of Eq. (4.20) by Sc, we get the dimensional form

$$-Scf\phi' = \phi'' + ScSr\theta'' - Sc\gamma\phi,$$

$$\phi'' + scf\phi' + ScSr\theta'' - Sc\gamma\phi = 0. \tag{4.21}$$

Ultimatelly, the ODEs explaning the proposed flow problem are given by

$$\left(1+\frac{1}{\beta}\right)f'''+ff''-\frac{2n}{n+1}f'^2-Mf'\sin^2\omega=0, \tag{4.22}$$

$$\left(1+\frac{4}{3}R\right)\theta''+Prf\theta'+PrNb\phi'\theta'+PrNt\theta'^2$$
$$+\left(1+\frac{1}{\beta}\right)PrEcf''^2+MPrEcf'^2\sin^2\omega+PrDu\phi''=0, \tag{4.23}$$

$$\phi''+scf\phi'+ScSr\theta''-Sc\gamma\phi=0. \tag{4.24}$$

The transformed boundary conditions are given below

$$\left.\begin{array}{ll} f(0)=S, \quad f'(0)=1, & \\ \theta'(0)=-Bi(1-\theta(0)), \ \phi(0)=1, & \end{array}\right\} \quad at \quad \xi=0, \left.\begin{array}{l} \\ \\ \end{array}\right\}$$
$$f'\to A, \ \theta\to 0, \ \phi\to 0, \quad as \quad \xi\to\infty. \tag{4.25}$$

4.4 Numerical Treatment

We solve Eqs. (4.22)-(4.24) using the boundary condition (4.25) with the help of shooting technique. Firstly, Eq. (4.22) is numerically solved, and then the obtained result of f, f' and f'' are used in Eqs. (4.23)-(4.24) for numerical usage of Eq. (4.22) The initial missing condition at $f''(0)$ which has been indicated by h with following notation.

$$f=g_1, f'=g_2, f''=g_3, \frac{\partial f}{\partial h}=g_4, \frac{\partial f'}{\partial h}=g_5, \frac{\partial f''}{\partial h}=g_6. \tag{4.26}$$

Eq. (4.22) can be converted into a system of there first order ODEs by using the above symbols. The three first order ODEs belong to Eq. (4.22), while the remaining three first order ODEs can be obtained by differentiating w.r.t h

$$g_1'=g_2, \qquad g_1(0)=S,$$
$$g_2'=g_3, \qquad g_2(0)=1,$$
$$g_3'=\frac{\beta}{(1+\beta)}[-g_1g_3+\frac{2n}{n+1}g_2^2+Mg_2\sin^2\omega], \qquad g_3(0)=h,$$

$$
\begin{aligned}
g_4' &= g_5, & g_4(0) &= 0,\\
g_5' &= g_6, & g_5(0) &= 0,\\
g_6' &= \frac{\beta}{(1+\beta)}[-g_1 g_6 - g_4 g_3 + \frac{4n}{n+1} g_2 g_5 + M g_5 \sin^2\omega], & g_6(0) &= 1.
\end{aligned}
$$

The above IVP can be solve by applying RK4 method. The missing condition of above equations can be taken at $h = h^{(0)}$, and Newtons method can be used for finding the roots. The Newtons method is given by the following iterative scheme

$$
\begin{aligned}
h^{(n+1)} &= h^{(n)} - \frac{(g_2(\xi_\infty))_{h=h^{(n)}} - A}{\left(\frac{\partial g_2(\xi_\infty)}{\partial h}\right)_{h=h^{(n)}}},\\
h^{(n+1)} &= h^{(n)} - \frac{(g_2(\xi_\infty))_{h=h^{(n)}} - A}{(g_2(\xi_\infty))_{h=h^{(n)}}}.
\end{aligned} \tag{4.27}
$$

The approximate numerical solution of Eq. (4.22) can be obtained by considering the domain of the problem i.e $[0, \xi_\infty]$, where ξ_∞ is chosen such that no considrable changes are obtaned going beyond. For the shooting method, the stopping criteria is defined as follows

$$
|(g_2(\xi_\infty))_{h=h^{(n)}} - A| < \epsilon, \tag{4.28}
$$

where ϵ is a small positive real number. Since Eqs. (4.23)-(4.24) are coupled system, therefore we can solve it numerically. The initial missing condition at $\theta(0)$ and $\phi(0)$ can be represented by p and q respectively, the following notation are considered

$$
\left.
\begin{aligned}
&\theta = Z_1, \theta' = Z_2, \phi = Z_3, \phi' = Z_4, \frac{\partial\theta}{\partial p} = Z_5, \frac{\partial\theta'}{\partial p} = Z_6, \frac{\partial\phi}{\partial p} = Z_7,\\
&\frac{\partial\phi'}{\partial p} = Z_8, \frac{\partial\theta}{\partial q} = Z_9, \frac{\partial\theta'}{\partial q} = Z_{10}, \frac{\partial\phi}{\partial q} = Z_{11}, \frac{\partial\phi'}{\partial q} = Z_{12}.
\end{aligned}
\right\} \tag{4.29}
$$

Using the above notations, the resulting system of first order ODEs is given below

$$Z_1' = Z_2, \qquad Z_1(0) = p,$$

$$\frac{-3Pr}{(3+4R) - PrDuScSr}\Big[g_1 Z_2 + NbZ_2Z_4 + \left(1+\frac{1}{\beta}\right)Ecg_3^2 + NtZ_2^2 + MEcg_2^2\sin^2\omega - DuScg_1Z_4 + DuSc\gamma Z_3\Big], \qquad Z_2(0) = -Bi(1-p),$$

$$Z_3' = Z_4, \qquad Z_3(0) = 1,$$

$$Z_4' = \frac{-3Sc}{(3+4R) - ScSrPrDu}\Big[g_1 Z_4\left(1+\frac{4}{3}R\right) - SrPrNtZ_2^2 - SrPrg_1Z_2 - SrPrNbZ_2Z_4 - \gamma Z_3\left(1+\frac{4}{3}R\right) - Sr\left(1+\frac{1}{\beta}\right)PrEcg_3^2 - SrMPrEcg_2^2\sin^2\omega\Big], \qquad Z_4(0) = q,$$

$$Z_5' = Z_6, \qquad Z_5(0) = 1,$$

$$Z_6' = \frac{-3Pr}{(3+4R) - PrDuScSr}\Big[g_1 Z_6 + Nb(Z_6Z_4 + Z_2Z_8) + 2NtZ_2Z_6 - (DuScg_1Z_8) + DuSc\gamma Z_7\Big], \qquad Z_6(0) = Bi,$$

$$Z_7' = Z_8, \qquad Z_7(0) = 0,$$

$$Z_8' = \frac{-3Sc}{(3+4R) - ScSrPrDu}\Big[g_1 Z_8\left(1+\frac{4}{3}R\right) - \gamma Z_7\left(1+\frac{4}{3}R\right) - SrPrg_1Z_6 - SrPrNb(Z_6Z_4 + Z_2Z_8) - 2SrPrNtZ_2Z_6\Big], \qquad Z_8(0) = 0,$$

$$Z_9' = Z_{10}, \qquad Z_9(0) = 0,$$

$$Z_{10}' = \frac{-3Pr}{(3+4R) - PrDuScSr}\Big[g_1 Z_{10} + Nb(Z_{10}Z_4 + Z_2Z_{12}) + 2NtZ_2Z_{10} - DuScg_1Z_{12} + DuSc\gamma Z_{11}\Big], \qquad Z_{10}(0) = 0,$$

$$Z_{11}' = Z_{12}, \qquad Z_{11}(0) = 0,$$

$$Z_{12}' = \frac{-3Sc}{(3+4R) - ScSrPrDu}\Big[g_1 Z_{12}\left(1+\frac{4}{3}R\right) - \gamma Z_{11}\left(1+\frac{4}{3}R\right) - SrPrg_1Z_{10} - SrPrNb(Z_2Z_{12} + Z_4Z_{10}) - 2SrPrNtZ_2Z_{10}\Big], \qquad Z_{12}(0) = 1.$$

The above initial value problem is solved by using $RK4$ method, and the missing condition can be taken as

$$(Z_1(p,q))_{\xi=\xi_\infty} = 0, \qquad (Z_3(p,q))_{\xi=\xi_\infty} = 0. \tag{4.30}$$

We have to solve the above Eq. (4.27) by apply the Newtons iteration scheme which is given as

$$\begin{bmatrix} p^{(n+1)} \\ q^{(n+1)} \end{bmatrix} = \begin{bmatrix} p^{(n)} \\ q^{(n)} \end{bmatrix} - \begin{bmatrix} \frac{\partial Z_1(p,q)}{\partial p} & \frac{\partial Z_1(p,q)}{\partial q} \\ \frac{\partial Z_3(p,q)}{\partial p} & \frac{\partial Z_3(p,q)}{\partial q} \end{bmatrix}^{-1} \begin{bmatrix} Z_1 \\ Z_3 \end{bmatrix}_{(p^{(n)},q^{(n)},\xi_\infty)},$$

$$\Rightarrow \begin{bmatrix} p^{(n+1)} \\ q^{(n+1)} \end{bmatrix} = \begin{bmatrix} p^{(n)} \\ q^{(n)} \end{bmatrix} - \begin{bmatrix} Z_1 & Z_9 \\ Z_7 & Z_11 \end{bmatrix}^{-1} \begin{bmatrix} Z_1 \\ Z_3 \end{bmatrix}_{(p^{(n)},q^{(n)},\xi_\infty)}.$$

The above iterative process is repeated until the following stopping criteria is met

$$max\{|Z_1(\xi_\infty)|, |Z_3(\xi_\infty)|\} < \epsilon,$$

where $\epsilon = 10^{-8}$ is set for the numerical calculation.

4.5 Results and Discussion

In this section, numerical results of velocity, temperature, concentration, skin friction coefficient Nusselt number and Sherwood number have been studied in detail with the help of graphs and tables by considering various physical parameters.

Skin-Friction Coefficient, Nusselt and Sherwood Numbers

Table 4.1 shows the computed numerical data for skin coefficient for different values of physical parameters such as n, M, β, S, A and ω. For raising values of n, M, and S the skin friction gradually increases while the skin friction depressed by enhancing the values of A, β and ω in both directions.

n	M	β	S	A	ω	$-(1+\frac{1}{\beta})f''(0)$	I_f
0.2	0.1	0.2	1	0.2	$\frac{\pi}{3}$	2.337123	[-1.5, 9.2]
0.6						2.711615	[-0.7, 3.5]
1.0						2.913409	[-0.7, 6.6]
	0.4					3.191963	[-0.7, 6.3]
	0.6					3.464128	[-0.8, 6.4]
		0.3				2.957716	[-0.8, 4.5]
		0.5				2.572221	[-1.0, 3.1]
			1.5			2.863085	[-1.1, 3.6]
			1.9			3.108925	[-1.3, 4.4]
				0.5		2.940977	[-1.3, 4.4]
				0.7		2.843137	[-1.3, 4.5]
					$\frac{\pi}{4}$	2.663075	[-1.2, 4.6]
					$\frac{\pi}{6}$	2.465694	[-1.2, 4.9]

TABLE 4.1: Computed results of skin friction coefficient $-(1+\frac{1}{\beta})f''(0)$.

Table 4.1 portray the interval I_f where from the missing initial condition $f''(0)$ can be chosen. It is noteworthy that the interval mentioned offer a considerable flexibility for the choice of initial guess.

Pr	Sc	Nb	Nt	β	Ec	Sr	Du	ω	Bi	γ	R	M	$-P_1\theta'(0)$	$-\phi'(0)$
4	0.2	0.1	0.1	0.2	0.1	0.2	0.3	$\frac{\pi}{3}$	1	0.4	0.5	0.1	1.287968	0.479813
4.4													1.327190	0.478839
5													1.361308	0.477962
	0.6												1.144816	1.021156
	0.7												1.092316	1.145211
		0.2											1.051265	1.148343
		0.5											0.916251	1.158577
			0.2										0.888380	1.160649
			0.3										0.858901	1.162830
				0.4									0.865538	1.153484
				0.6									0.866650	1.147477
					0.2								0.700094	1.155134
					0.3								0.531320	1.162944
						0.4							0.536205	1.144024
						0.6							0.541944	1.120584
							0.4						0.350612	1.156127
							0.5						0.131489	1.1961034
								$\frac{\pi}{4}$					0.610360	1.211267
								$\frac{\pi}{5}$					0.178357	1.220928
									1.2				0.201251	1.217480
									1.4				0.221553	1.214424
										0.6			0.066776	1.343398
										0.8			0.078029	1.462533
											1.4		0.0758084	1.433549
											1.9		0.242720	1.411537
												0.3	0.118069	1.400869
												0.9	0.223836	1.374641

TABLE 4.2: The computed result of Sherwood and Nusselt numbers for $A = 0.2$, $n = 0.2$, $S = 1$, where $P_1 = -(1 + \frac{4}{3}R)$,

Table 4.2 describes the impact of various physical parameters on Nusselt and Sherwood number. For the gradually mounting values of Pr, β, Sr, R and Bi, the Nusselt number gradually grows on the other hand Sherwood number is reduced. Furthermore for ascending values of Sc, Nb, Nt, Ec, Du, ω, γ and M Nusselt number depresses while its oppose Sherwood number increasing.

Pr	Sc	Nb	Nt	β	Ec	Sr	Du	ω	Bi	γ	R	M	I_θ	I_ϕ
4	0.2	0.1	0.1	0.2	0.1	0.2	0.3	$\frac{\pi}{3}$	1	0.4	0.5	0.1	[–4.5, 150]	[-150, 150]
4.4													[-4.2, 150]	[-150, 150]
5													[-4.1, 150]	[-150, 150]
	0.6												[-4.2, 150]	[-150, 150]
	0.7												[-4.1, 150]	[-150, 150]
		0.2											[-0.9, 150]	[-150, 150]
		0.5											[-9.8, 150]	[-25, 150]
			0.2										[-10.5, 150]	[-20, 150]
			0.3										[-9.8, 25]	[-22, 150]
				0.4									[-12.5, 40]	[-15, 150]
				0.6									[-15.4, 41]	[-12, 150]
					0.2								[-8.9, 44]	[-15, 150]
					0.3								[-10.2 45]	[-15, 150]
						0.4							[-15, 150]	[-150, 150]
						0.6							[-15, 150]	[-150, 150]
							0.4						[-16, 150]	[-150, 150]
							0.5						[-16, 150]	[-150, 140]
								$\frac{\pi}{4}$					[16.5, 150]	[-150, 140]
								$\frac{\pi}{5}$					[-16.4, 150]	[-150, 140]
									1.2				[-13.2, 150]	[-150, 150]
									1.4				[-11.3, 110]	[-150, 110]
										0.6			[-11.2, 110]	[-150, 65]
										0.8			[-11.4, 30]	[-60, 23]
											1.4		[-10.2, 70]	[-50, 35]
											1.9		[-11.1, 80]	[-100, 50]
												0.3	[-11.1, 70]	[-100, 45]
												0.9	[-11.1, 80]	[-80, 35]

TABLE 4.3: The intervals for the initial guesses for the initial missing conditions when $A = 0.2$, $n = 0.2$, $S = 1$.

Table 4.3 portray the intervals I_θ and I_ϕ where from the missing initial conditions $\theta'(0)$ and $\phi'(0)$ respectively can be chosen. It is noteworthy that the intervals mentioned offer a considerable flexibility for the choice of initial guesses.

Impact of Casson Fluid Parameter β

Figure 4.2 depicts the impact of β on velocity profile. The graph reveals that velocity profile decreases by enhancing the values of β. Generally, the fluid viscosity is enhanced gradually by increasing the numerical values of β due to which high

resistance is induced in the fluid as a result, a decline in velocity profile of the fluid is observed. Figure 4.3 shows the effect of β on dimensionless temperature distribution $\theta(\xi)$. The plot shows a deceleration in temperature distribution for accelerating values of β. This decelerating behavior comes from the fact that the uprising values of β depresses the velocity of the fluid by depressing yield stress. Figure 4.4 shows the impact of different values of β on concentration distribution, the rising values of β decreases the concentration profile gradually. Actually, increasing values of β accelerates the flow velocity and as a result the viscous domination decrease the concentration profile.

Impact of Magnetic Parameter M

Figure 4.5 is drawn to analyze the influence of different values of M on velocity distribution of the nanofluid. The graph reveals that the velocity profile of the fluid is declined by small variation in M. Physically, the parameter M induces a resistive force in the conduction fluid. This induced resistive force declines the fluid velocity, that is why a decline in velocity is observed. Figure 4.6 analyzes the influence of M on the dimensional temperature distribution. Due to small increment in the magnetic parameter the temperature distribution is enhanced. Physically a resistive force is generated in the flow direction of the fluid which becomes the cause in the enhancement of temperature. Figure 4.7 investigates the influence of M on dimensionless concentration distribution $\phi(\xi)$. It is visible from the curve that the mounting values of M results an increase in the concentration distribution. Generally, fluid concentration and its corresponding boundary thickness are uprised by boosting values of M.

Impact of Prandtl Number Pr

Figure 4.8 shows the relationship between Pr and temperature profile. Since Pr can be written as a ratio of density to thermal diffusivity, when we increases the values of Pr it means that we are increasing the density of the fluid and decreasing

the thermal diffusivity, which causes a decrease in the temperature. Figure 4.9 illustrates the outcome of Pr on concentration distribution, which clearly shows an increment in the concentration profile of the nanofluid by enhancing values of Pr.

Impact of Brownian Motion Parameter Nb

Figure 4.10 illustrates a relationship between Nb and temperature profile. The temperature profile decreases by gradually enhancing the values of Nb. Generally the enhancement of Nb significantly increases the movement of fluid particles, which enhances the kinetic energy of the fluid particle as a result the temperature distribution also increases. Figure 4.11 illustrates the influence of Nb on the concentration distribution. The concentration distribution increases due to the growing values of Nb.

Impact of Inclination Angle ω

Figure4.13 reflects the influence of inclination angle ω on the velocity field. It is noticed that, as we increase the inclination angle ω the velocity profile also increases. Generally, an increment in inclination angle means we are reducing the resistance against the flow direction of the fluid as due to which the fluid velocity increases. Figure 4.14 shows the relationship between ω and temperature distribution of the fluid. As reflected from the plot that the temperature profile decreases by increasing ω. Physically, the enhancing values of ω reduce the friction force due to which the temperature distribution decreases. Figure 4.14 shows the relationship between inclination angle and concentration profile. The concentration profile decelerates due to increasing values of inclination angle.

Impact of Eckert number Ec

Figure 4.15 illustrates the impact of Ec on the temperature distribution. It is noticed that by growing values of Ec the temperature distribution increases. Actually, the dissipation increases by growing values of Ec due to this increase in dissipation the fluid internal energy also increases. This modification in internal energy also increases the temperature distribution of the fluid. Figure 4.16 is sketched to analyze the effect of Ec on the concentration distribution. It is obvious that the concentration distribution increases due to an increase in Ec, this is because of the growing values of Ec becomes a cause in increase of the thermal energy of the fluid.

Impact of Dufour Number Du

Figure 4.17 shows the influence of Du on temperature distribution. From the graph it is clear that the temperature profile is an increasing function of Du. Physically, the growing values of Du reflects an uprising in the thermal diffusibility which correspondingly increases the heat transfer. Figure 4.18 shows the relationship between Du on concentration distribution. Higher values of Du increase the concentration profile of the fluid. Generally, an increase in Du means increase in mass transfer, therefore, the concentration increases.

Impact of Chemical Reaction Parameter γ

Figures 4.19-4.20 illustrate the impact of γ on temperature and concentration profile, respectively. As can be seen from the graph that the increasing values of γ accelerate the temperature distribution while the concentration profile declines with boosting values of γ. Physically, the growing values of γ causes a decrement in the molecular diffusion as a result the concentration decreases and the corresponding boundary layer thickness reduces.

Impact of Velocity Ratio Parameter A

Figure 4.21 analyzes the impact of A on dimensional velocity distribution. The plot depicts that for boosting values of A the velocity profile accelerate. physically, when the stretching velocity is less than the free stream velocity then if we divide the free stream velocity by the stretching velocity then the ratio obtained will be greater than 1. then as a result the retarding force decreased and the flow velocity increased.

Impact of Radiation Parameter R

Figure 4.22 illustrates the impact of R on temperature distribution. From the curve we observe that the temperature profile increases with boosting values of R. Generally, more heat is transfer to the fluid due to increasing values of R, which in response increases both the temperature distribution as well the thermal boundary layer thickness.

Impact of Thermophoresis Parameter Nt

Figure4.23 shows the relation between Nt and temperature distribution of the fluid. It is shown that the temperature profile increases by the boosting numerical values of Nt. Physically, the increasing values of Nt drawn the nanoparticles from hotter to less hotter region as a result the overall temperature profile of the nanofluid increases.

Impact of Schmidt Number Sc

Figure 4.25 shows the relationship between Sc on concentration distribution, for expanding values of Sc the graph of dimensionless concentration distribution is decreased. Physically, it describes an inverse relation between the mass diffusivity

and Sc. The large numerical values of Sc produce less mass diffusion therefore, the nonoparticle concentration is dropped.

Impact of Soret Number Sr

The impact of Sr on the temperature distribution, is portraited in Figure 4.26. It is seen that when we enhance Sr the temperature profile accelerates. Figure 4.27 reflects the effect of Sr on concentration profile, of the nanofluid. The concentration distribution of the nanofluid is observed to be increasing for higher values of Sr. Physically, an increse in Sr represents the mass transfer from low to high regions which is caused by the temperature difference.

Impact of Suction Parameter S

Figure 4.28 illustrates the influence of S on dimensionless velocity, we observe that for boosting values of S the velocity distribution decreases. Actually, the higher values of S increase a density difference in the flow region. The density has a large values on the top region and small values on the bottom region. This change in density causes a decrease in the flow of fluid between the top and bottom region and hence a decline in velocity of the fluid is observed.

Impact of Nonlinear Stretching Parameter n

Figure 4.29 depicts the influence of n on dimensionless velocity distribution. It is seen from the curve that velocity distribution decreases for boosting values of n. Actually, the mounting values of n induces more pressure on the flow as a result, the dimensional velocity distribution reduces.

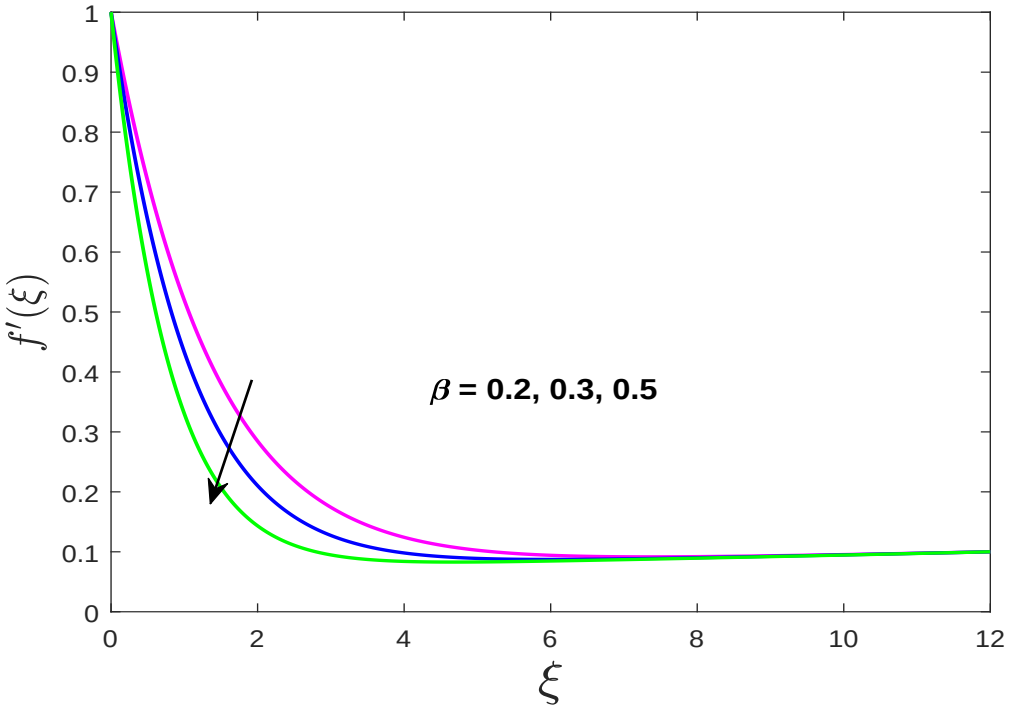

FIGURE 4.2: Effect of β on $f'(\xi)$.

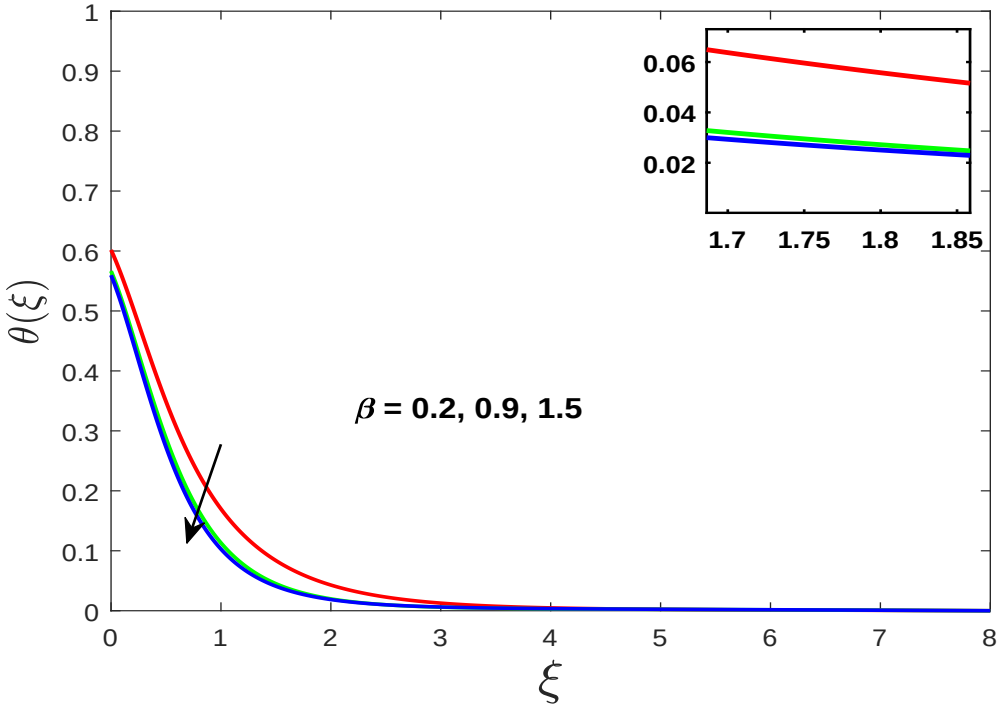

FIGURE 4.3: Effect of β on $\theta(\xi)$.

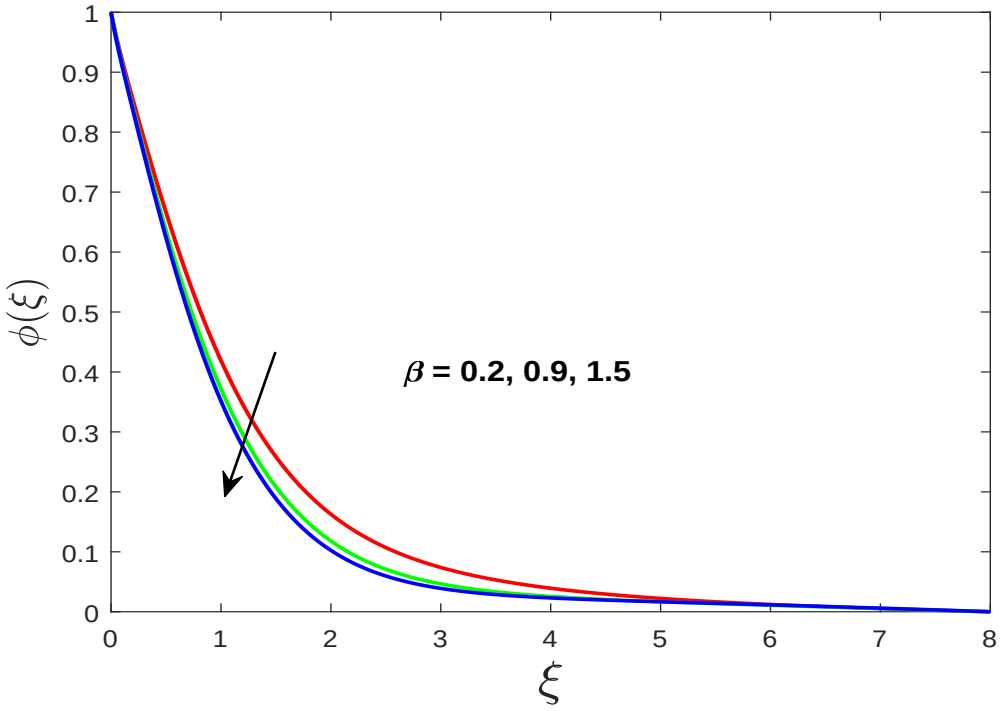

FIGURE 4.4: Effect of β on $\phi(\xi)$.

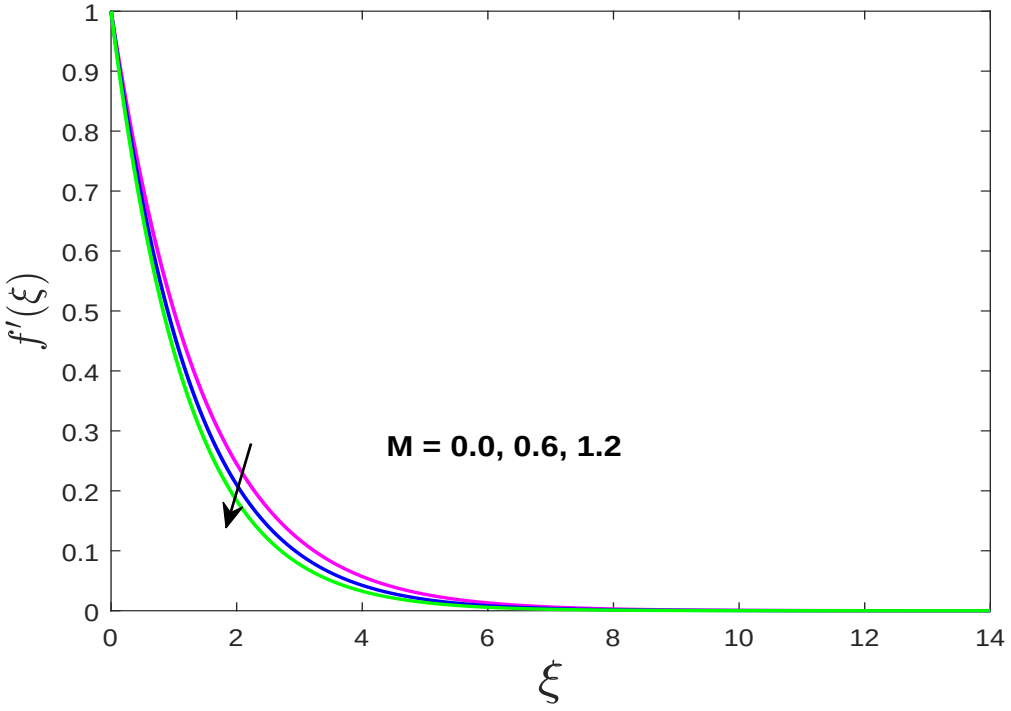

FIGURE 4.5: Effect of M on $f'(\xi)$.

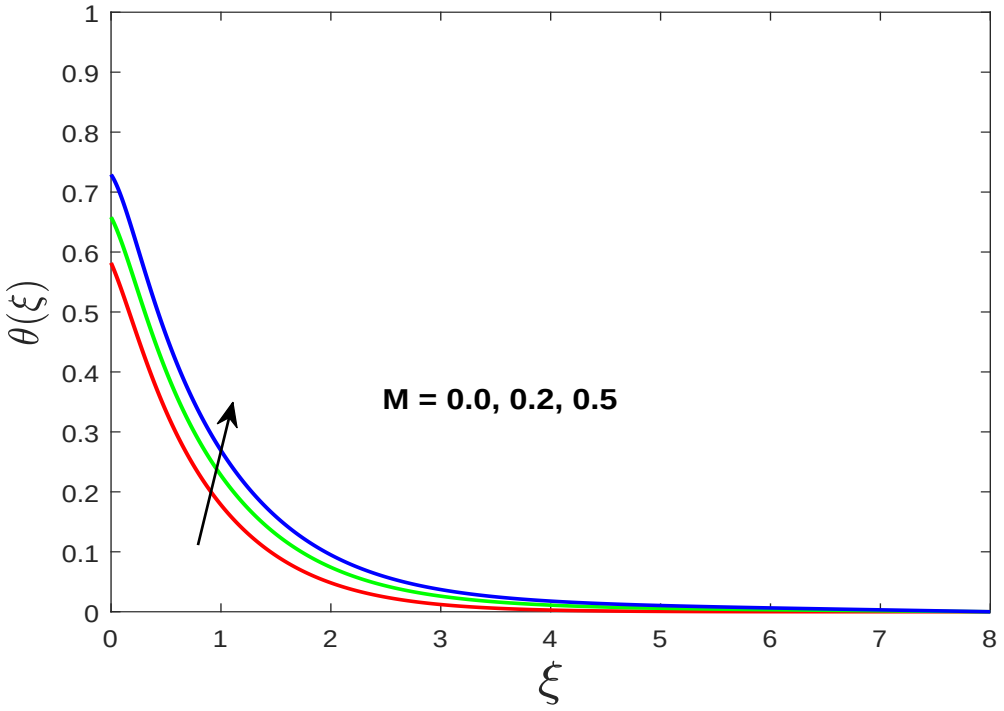

FIGURE 4.6: Effect of M on $\theta(\xi)$.

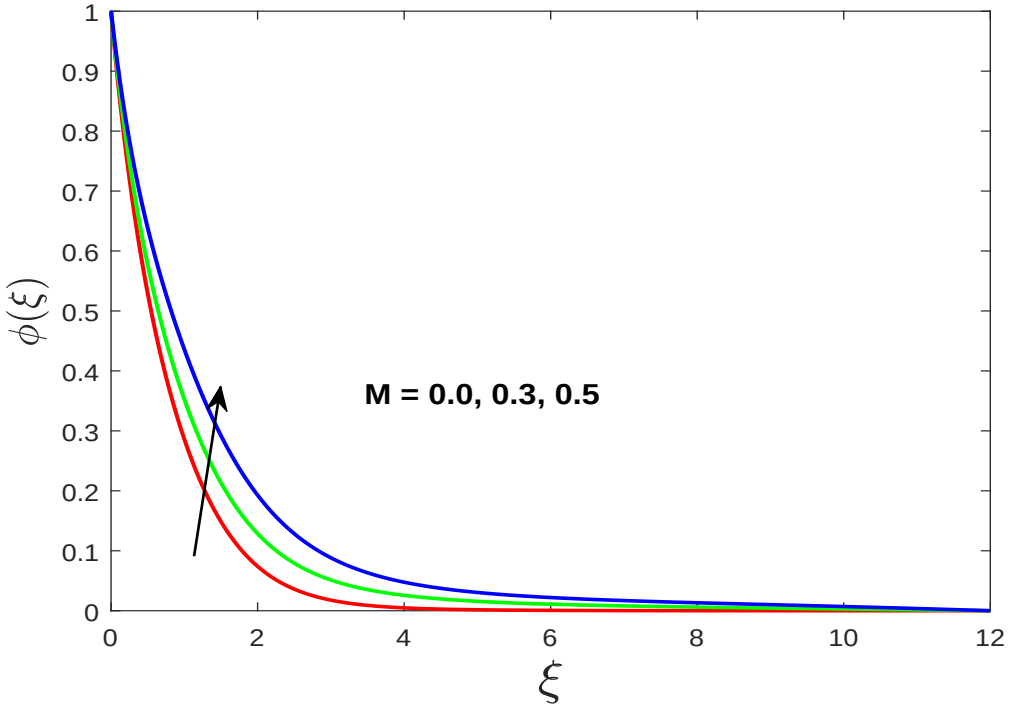

FIGURE 4.7: Effect of M on $\phi(\xi)$.

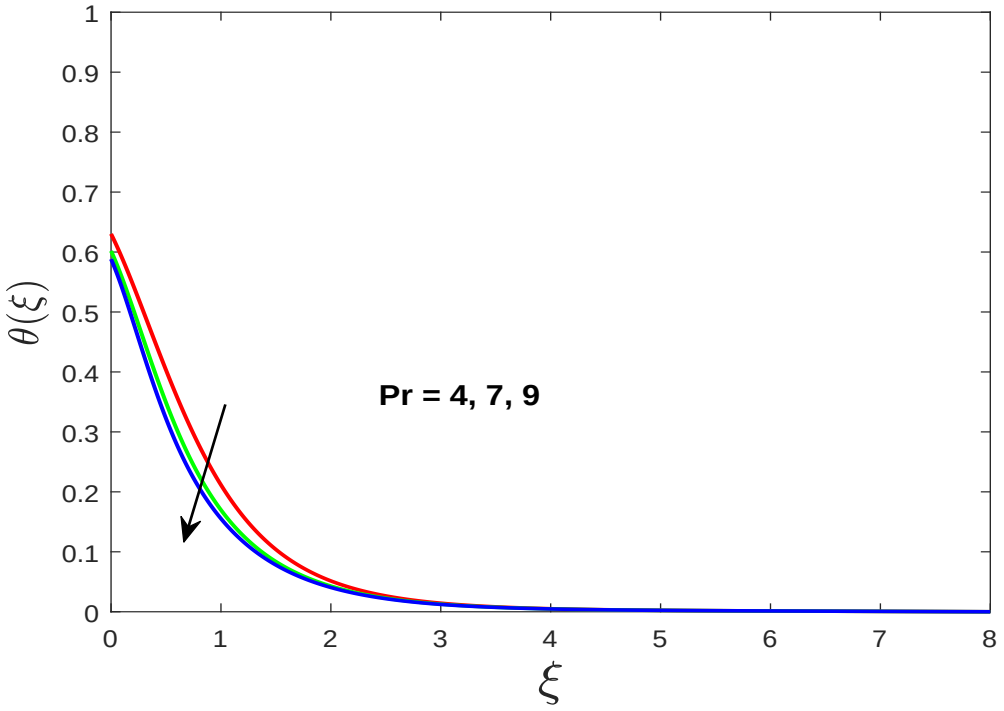

FIGURE 4.8: Effect of Pr on $\theta(\xi)$.

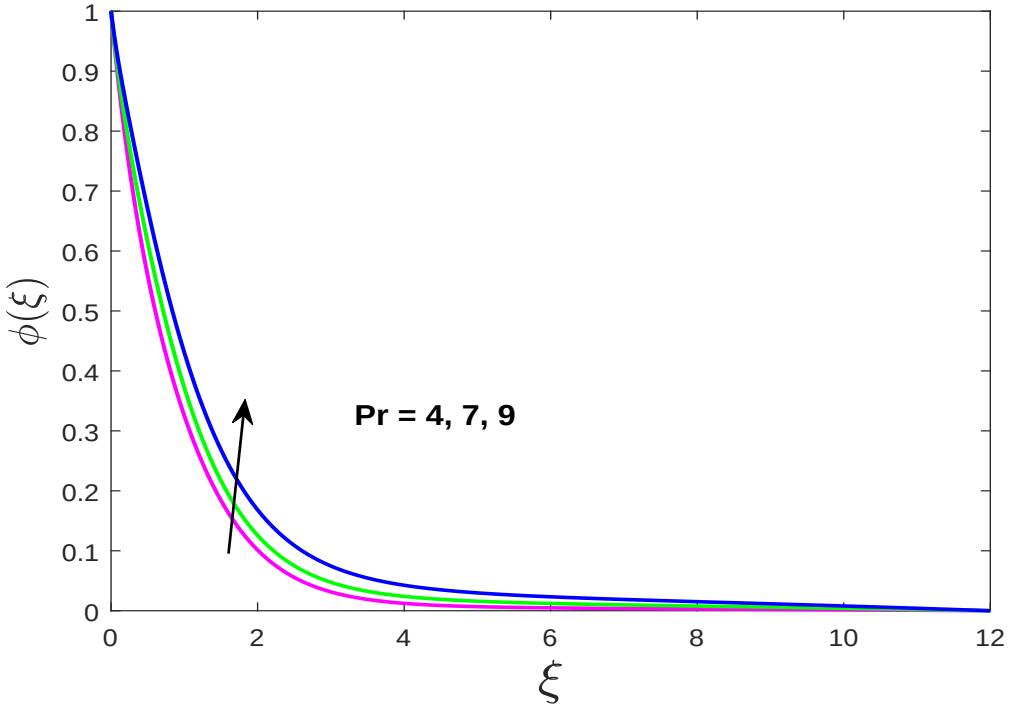

FIGURE 4.9: Effect of Pr on $\phi(\xi)$.

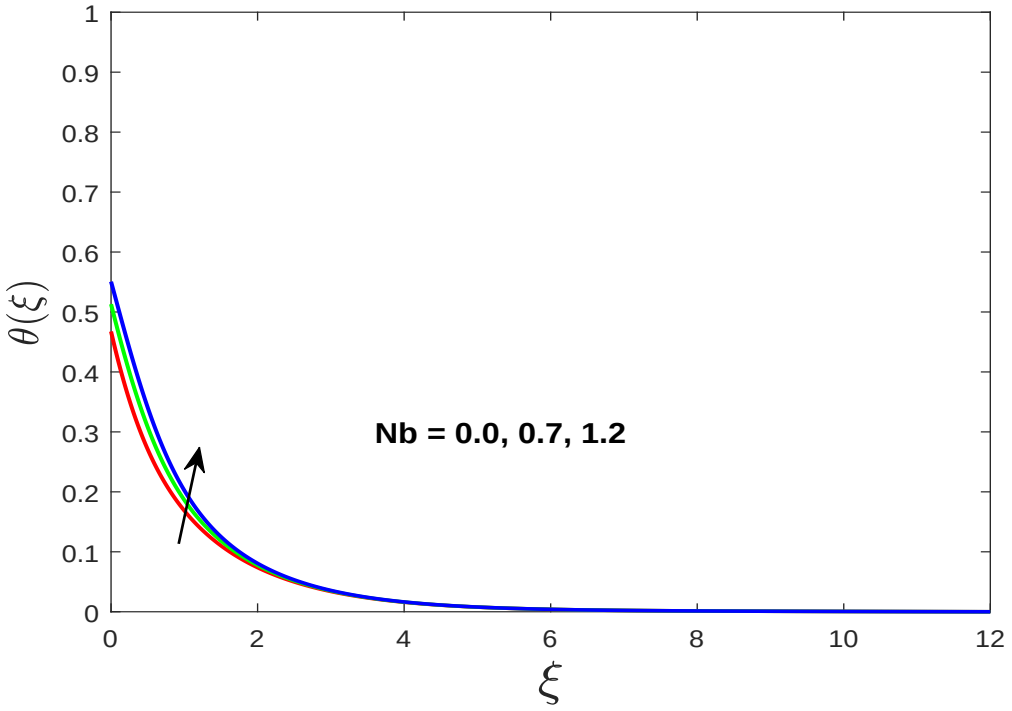

FIGURE 4.10: Effect of Nb on $\theta(\xi)$.

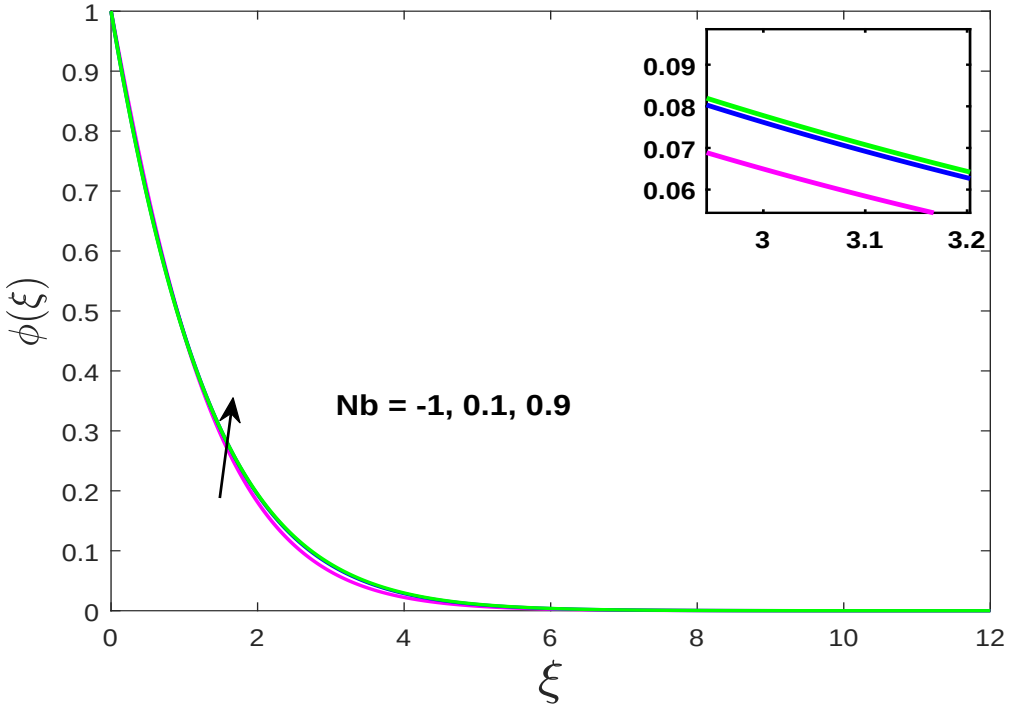

FIGURE 4.11: Effect of Nb on $\phi(\xi)$.

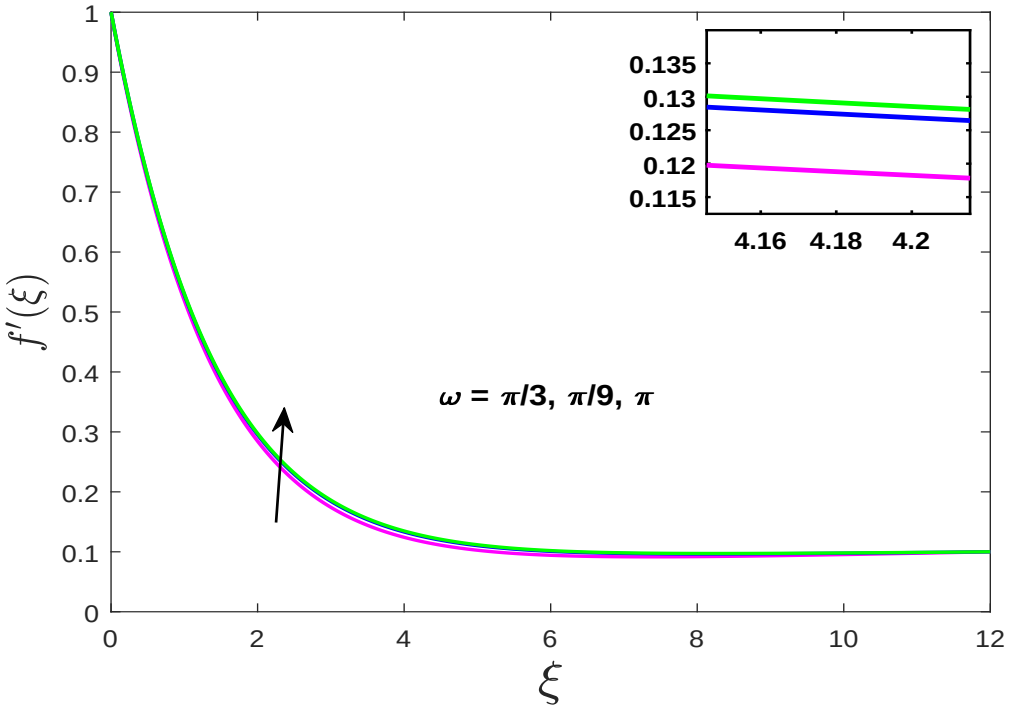

FIGURE 4.12: Effect of ω on $f'(\xi)$.

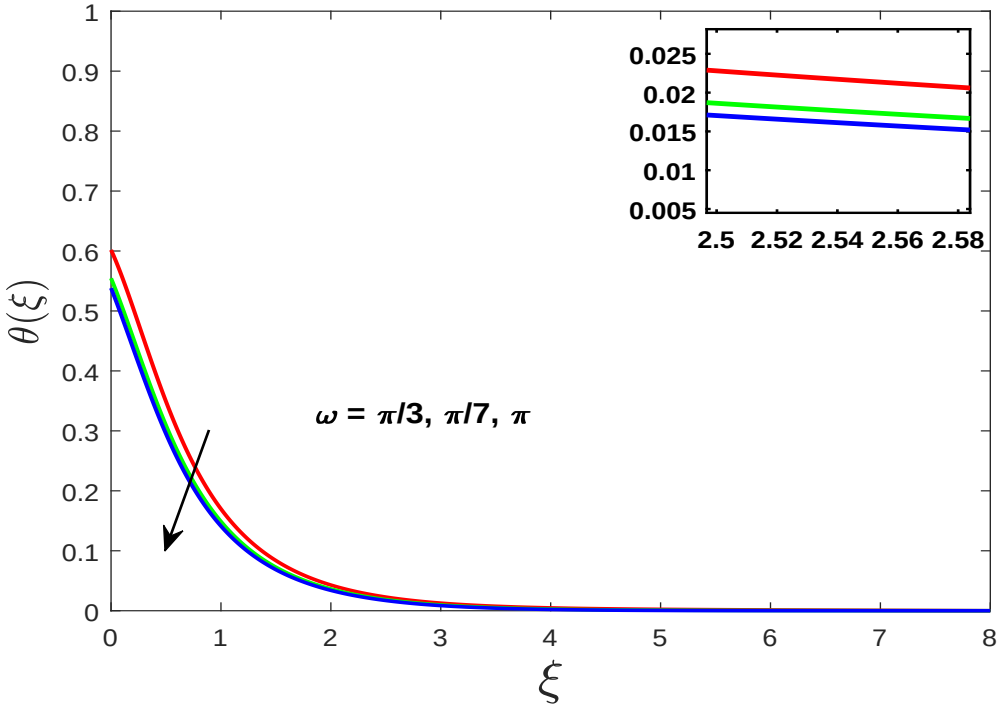

FIGURE 4.13: Effect of ω on $\theta(\xi)$.

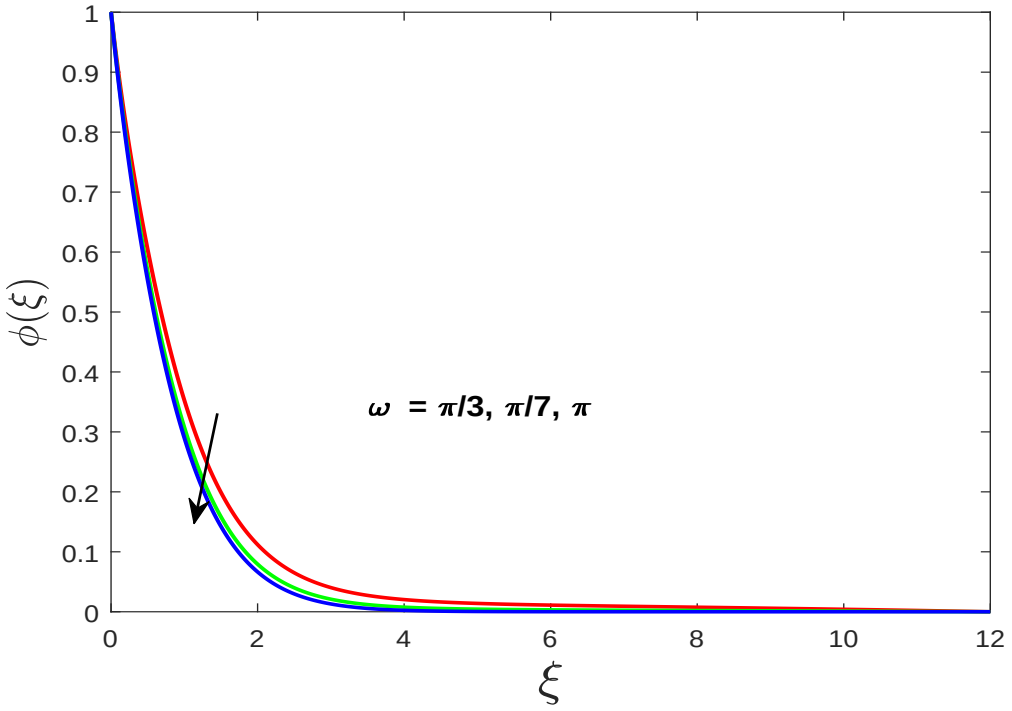

FIGURE 4.14: Effect of ω on $\phi(\xi)$.

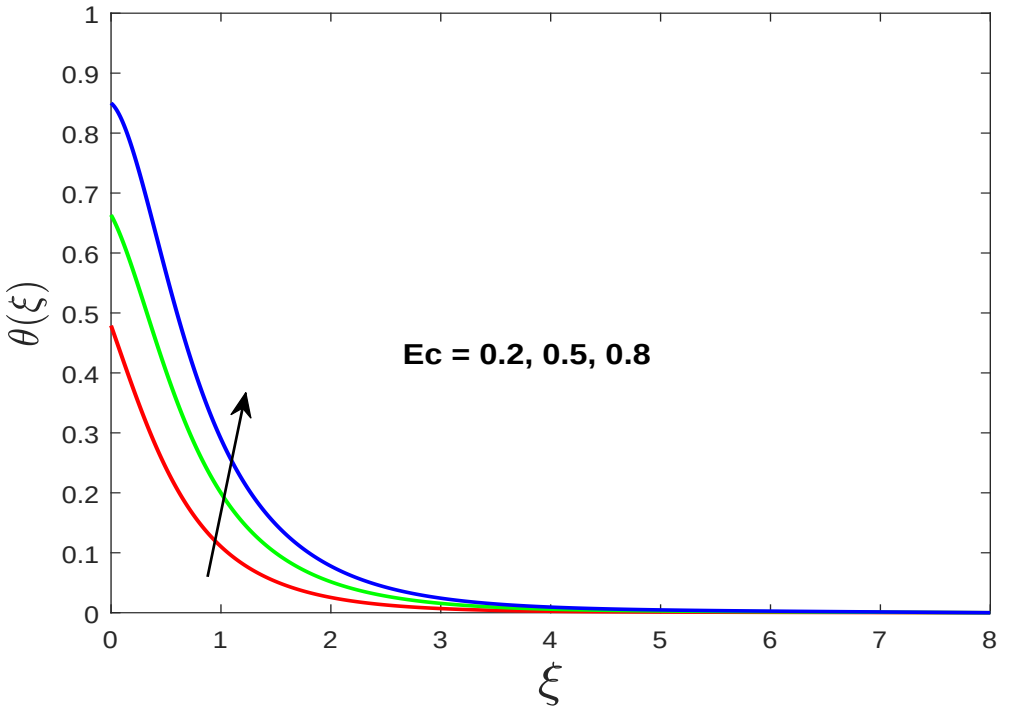

FIGURE 4.15: Effect of Ec on $\theta(\xi)$.

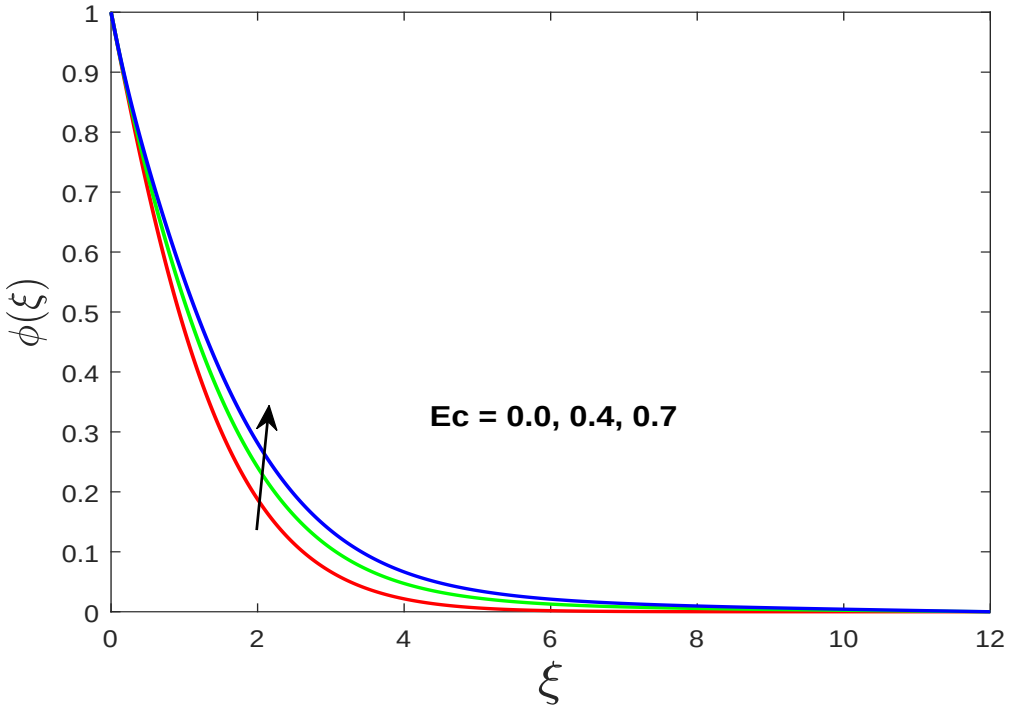

FIGURE 4.16: Effect of Ec on $\phi(\xi)$.

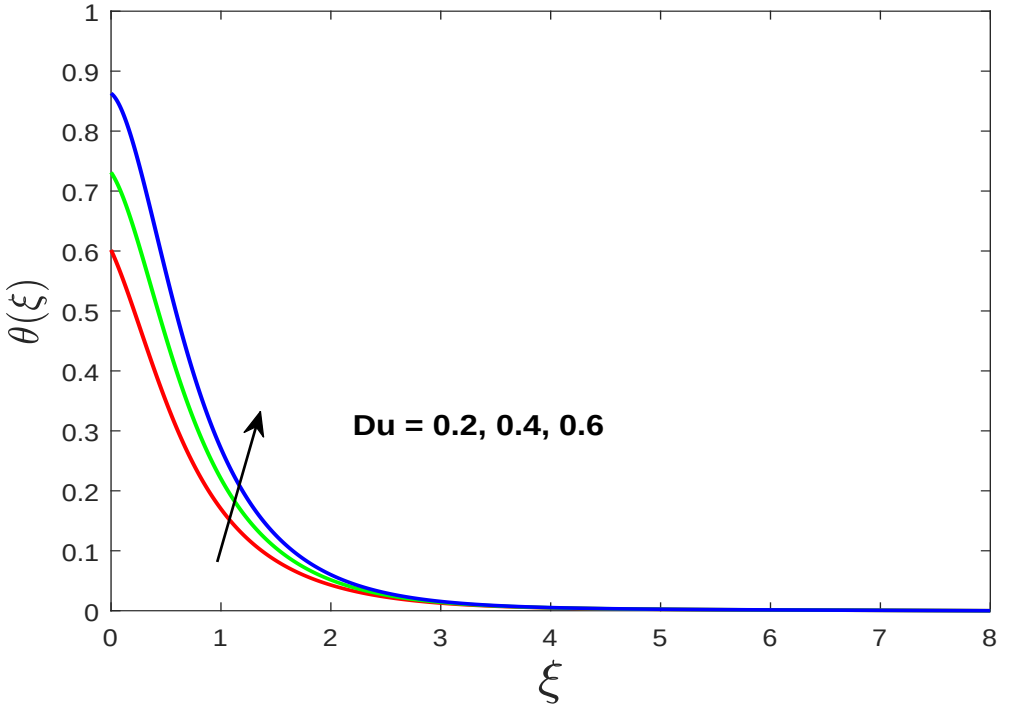

FIGURE 4.17: Effect of Du on $\theta(\xi)$.

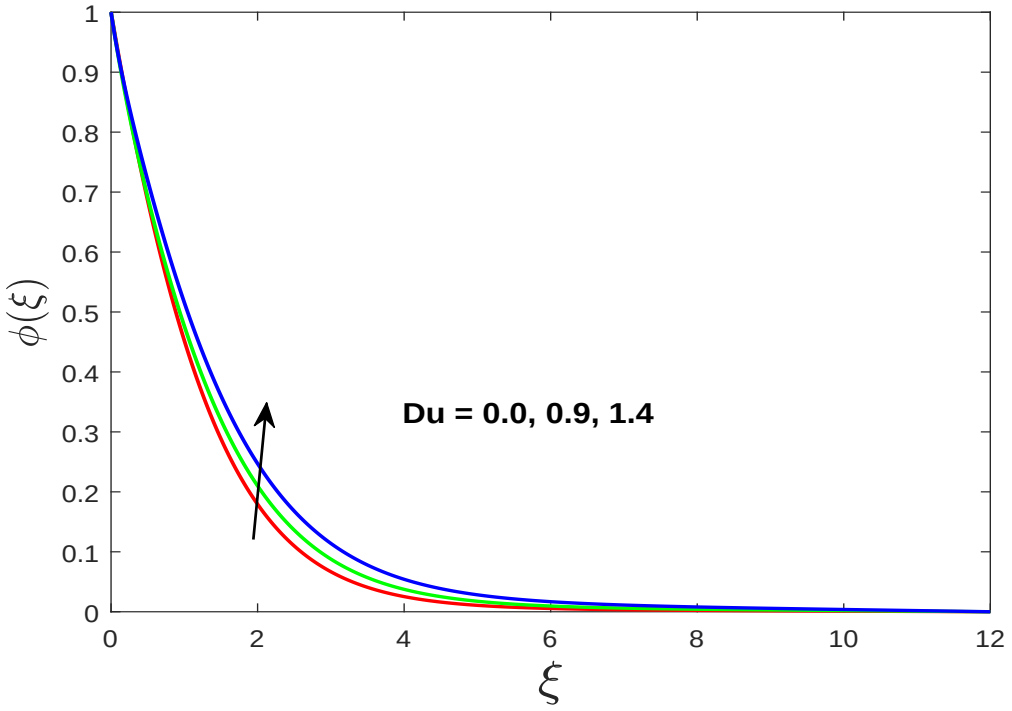

FIGURE 4.18: Effect of Du on $\phi(\xi)$.

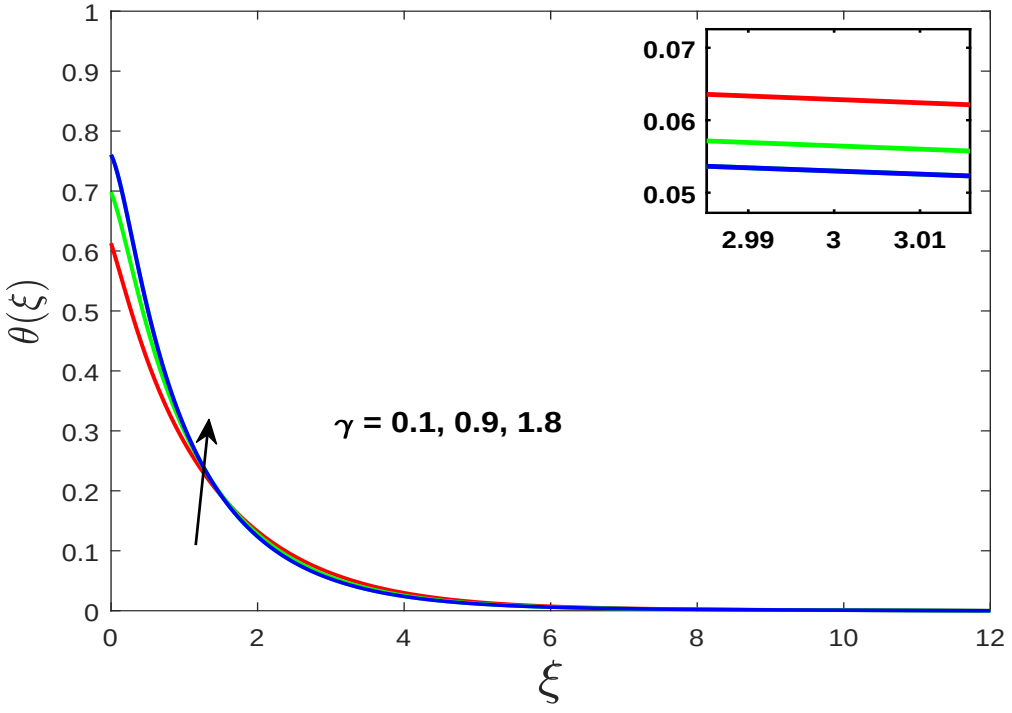

FIGURE 4.19: Effect of γ on $\theta(\xi)$.

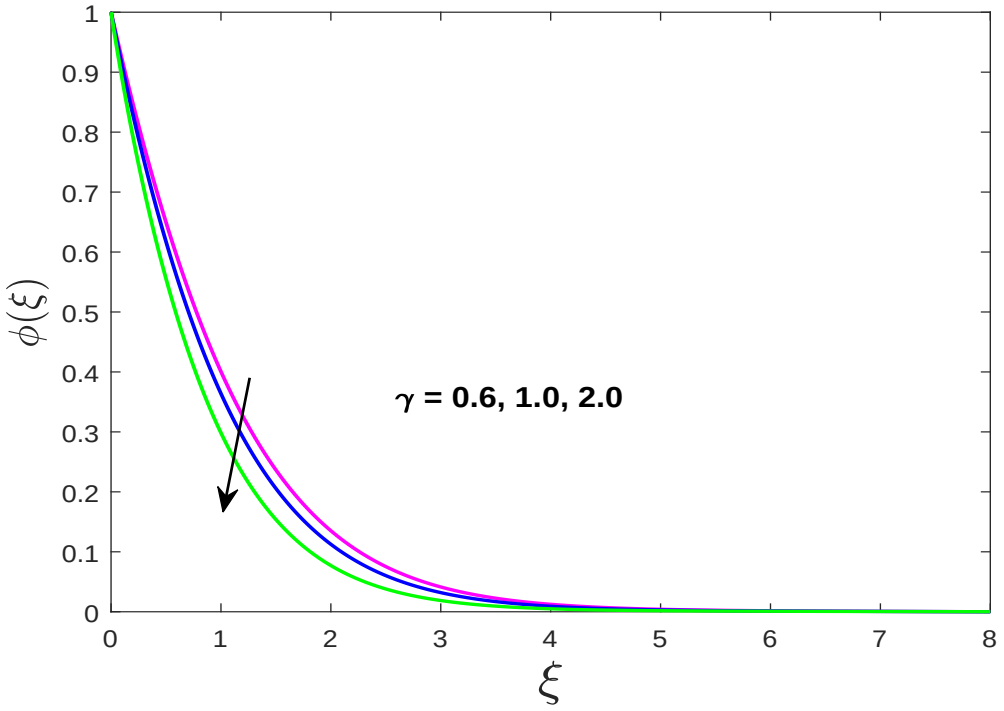

FIGURE 4.20: Effect of γ on $\phi(\xi)$.

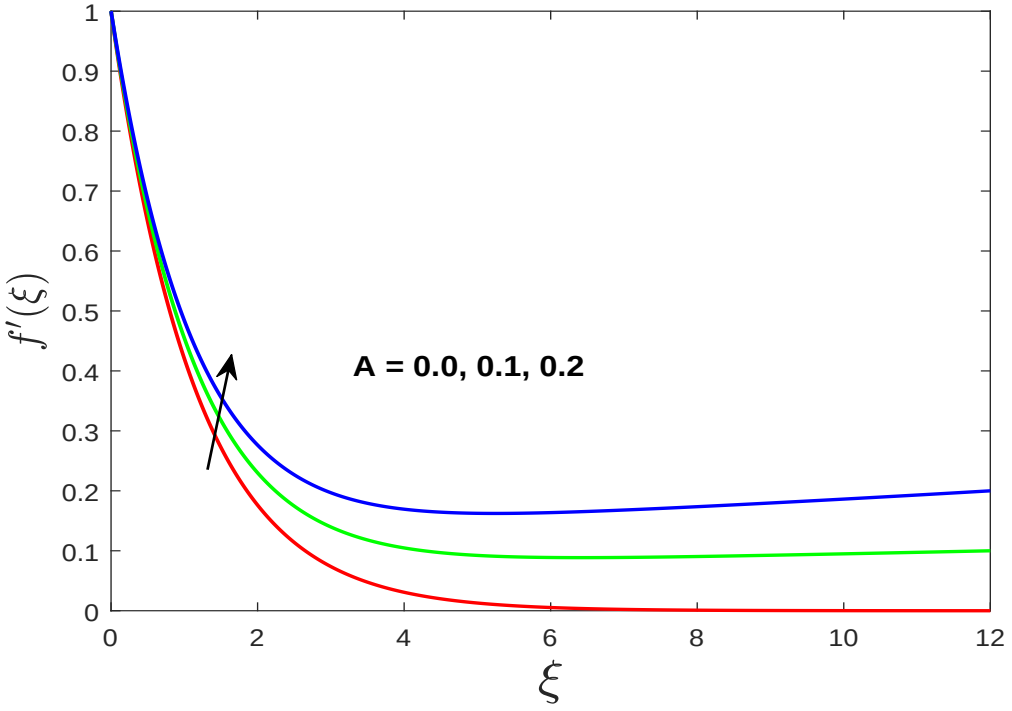

FIGURE 4.21: Effect of A on $f'(\xi)$.

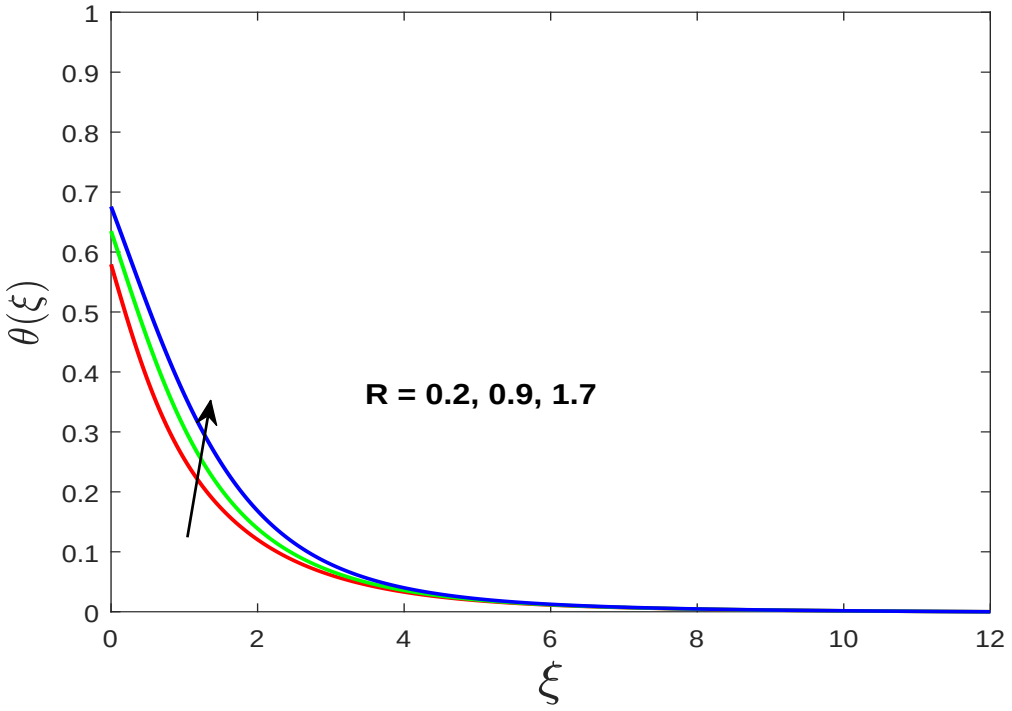

FIGURE 4.22: Effect of R on $\theta(\xi)$.

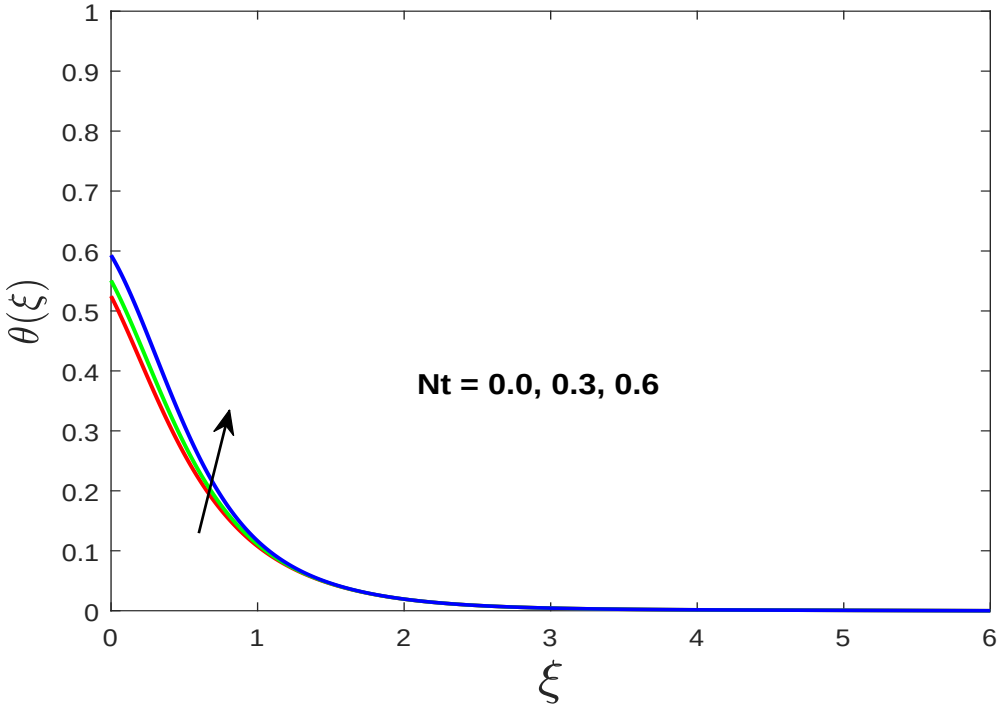

FIGURE 4.23: Effect of Nt on $\theta(\xi)$.

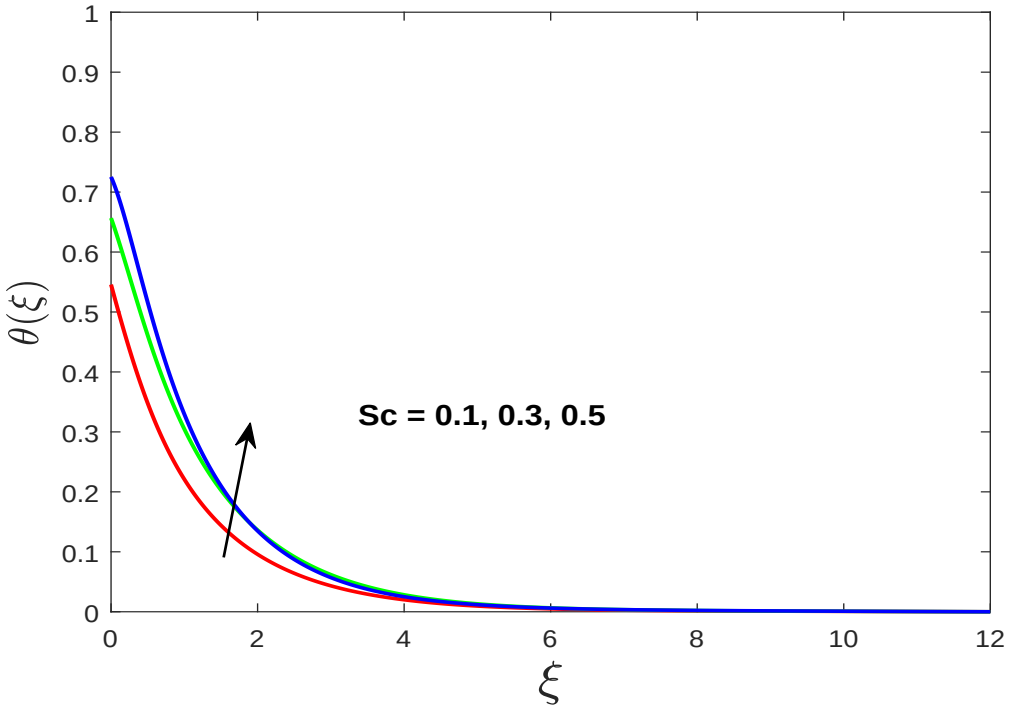

FIGURE 4.24: Effect of Sc on $\theta(\xi)$.

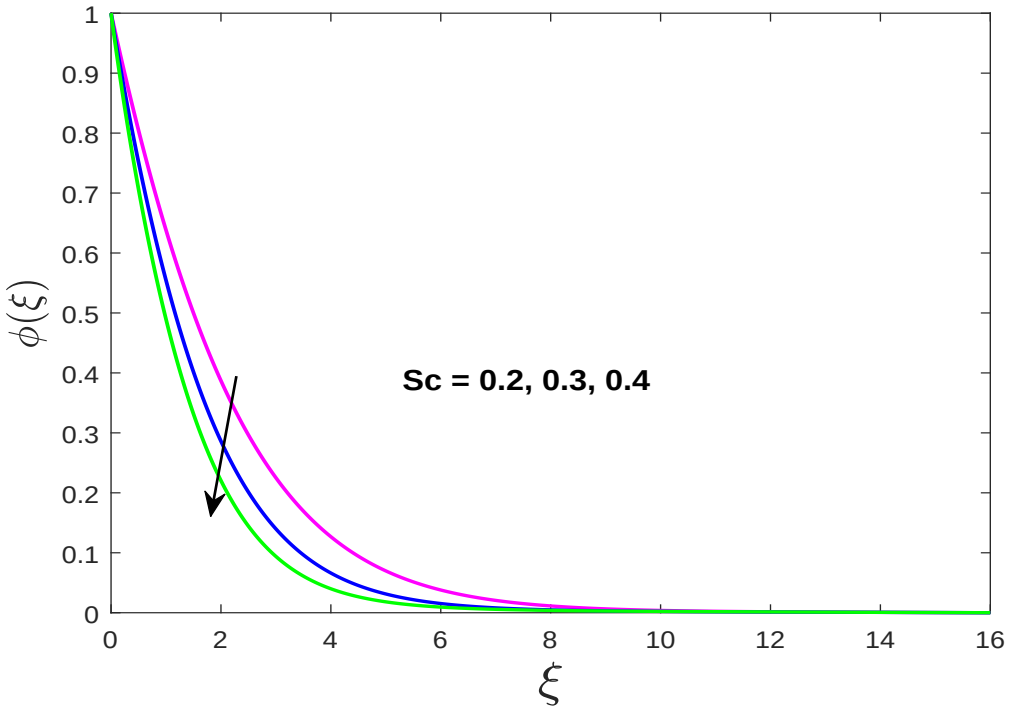

FIGURE 4.25: Effect of Sc on $\phi(\xi)$.

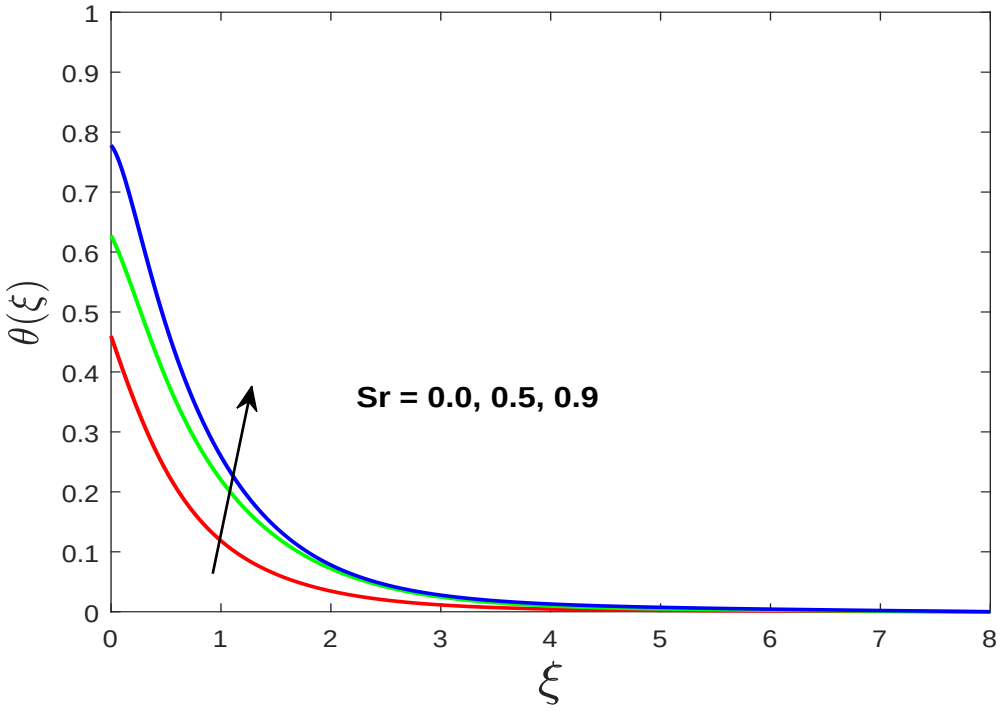

FIGURE 4.26: Effect of Sr on $\theta(\xi)$.

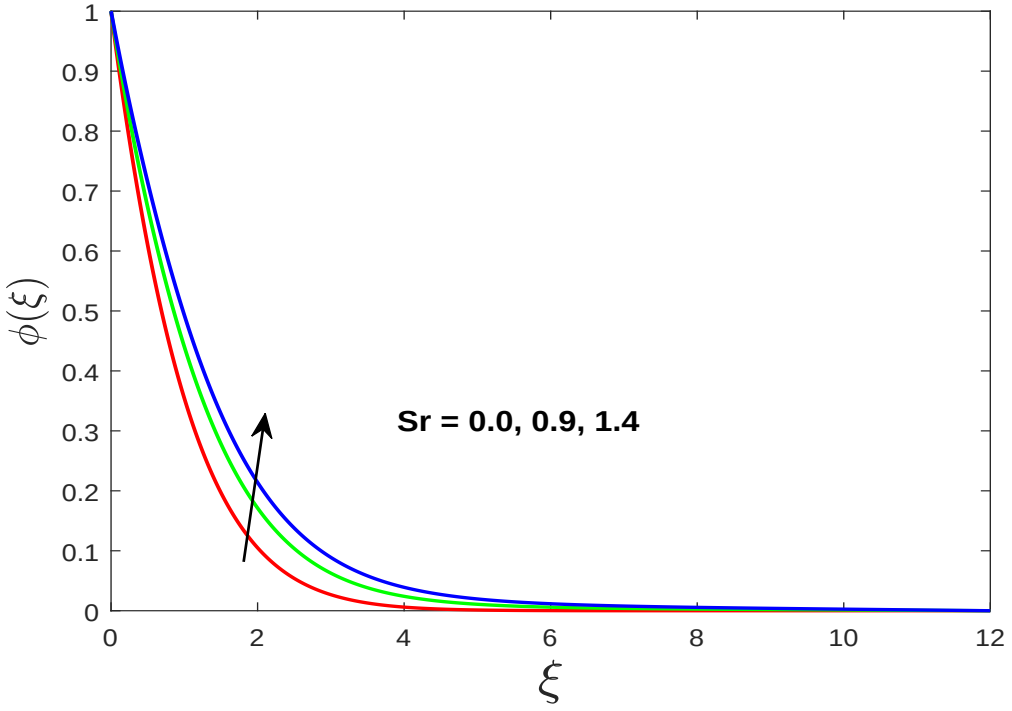

FIGURE 4.27: Effect of Sr on $\phi(\xi)$.

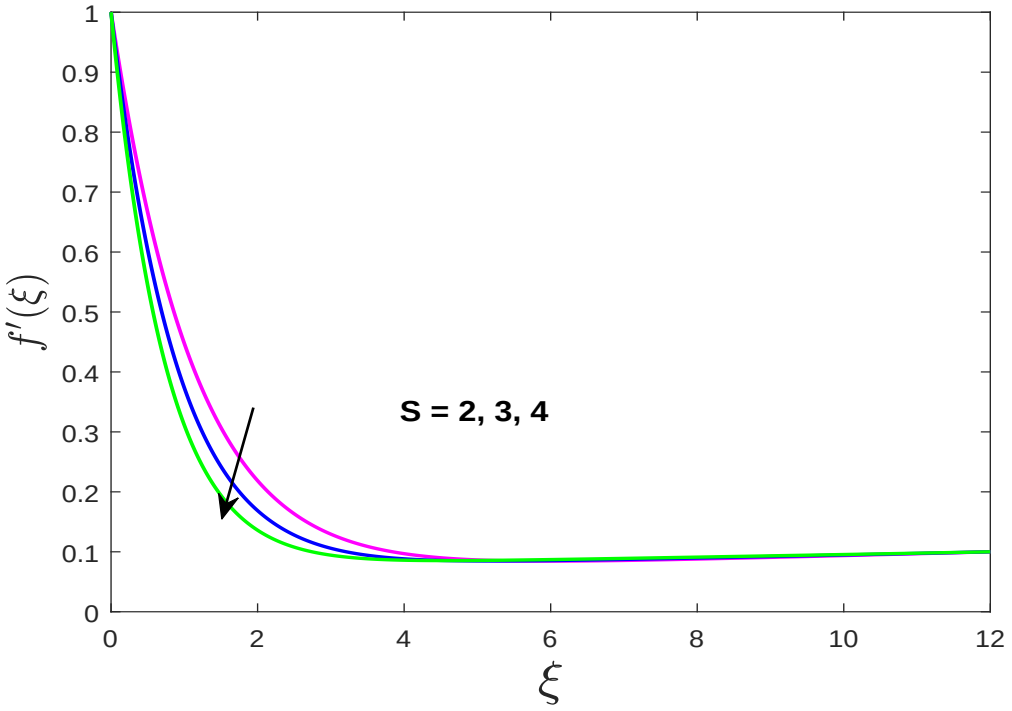

FIGURE 4.28: Effect of S on $f'(\xi)$.

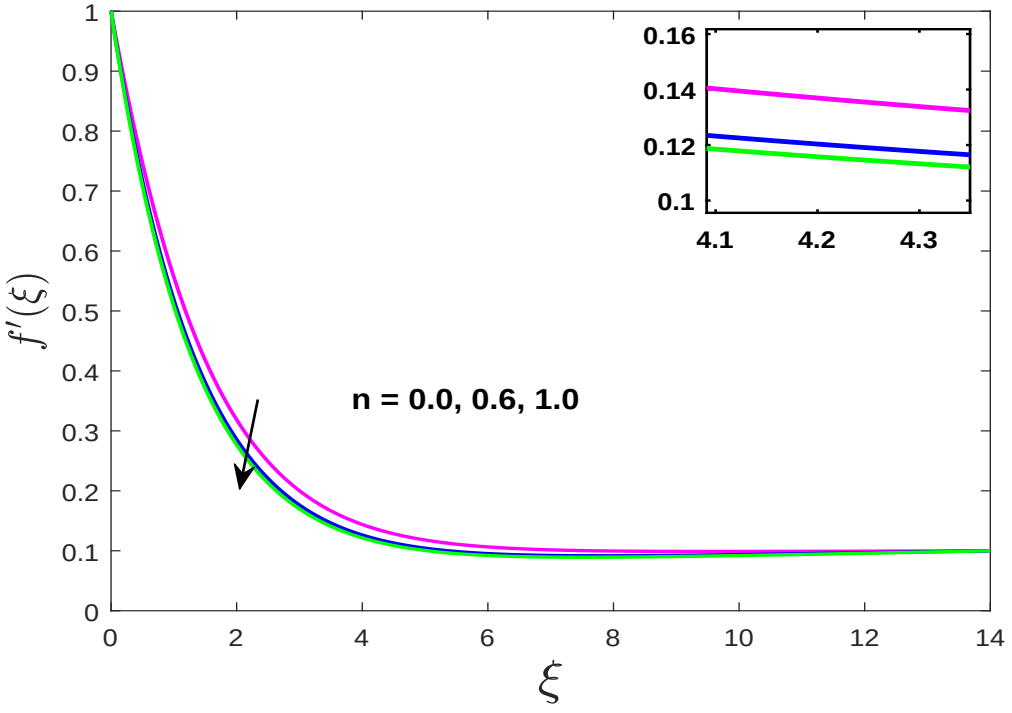

FIGURE 4.29: Effect of n on $f'(\xi)$.

Chapter 5

Conclusion

In this thesis, we have examined the numerical investigation of the MHD stagnation point flow of Casson nanofluid by including additional effect of Soret, Dufour and inclined magnetic field. The 2D Casson nanofluid has been investigated for different physical parameter i.e., magnetic field, Eckert number, Casson fluid parameter, Soret number, Dufour and inclined magnetic field. We get a set of ODEs by converting nonlinear PDEs of concentration, momentum and temperature by utilizing the similarity transformation. The Shooting technique has been used for calculation of numerical results in the presence model together with RK4. The impact of different suitable physical parameters on the velocity, energy and concentration distribution has been discussed in detail by using graphs and tables.

Conclusion Remarks

The overall conclusion drawn from the present work is summarized below.

- Decreasing behavior due to increasing the Casson fluid parameter and same behavior is noticed in the velocity distribution enhancing the numerical value of suction parameter.

- For the large value of magnetic parameter the velocity field reduce but opposite trend is observed in the graph of temperature and concentration distribution.
- The temperature distribution decelerate and the concentration distribution accelerate due to boosting value of Prandtl number.
- Temperature profile rises by increasing radiation parameter and same behavior is observed in the temperature field due to the effect of thermophoresis parameter.
- For uprising values of inclined magnetic field, velocity profile increased while temperature and concentration distribution decreases.
- Uprising of temperature field is observed for the increasing value of Eckert number.
- By increasing the Soret number both temperature and concentration profile accelerate.
- By uprising value of Dufour number both the temperature and concentration profile increases.
- Enlarging the velocity ratio parameter the velocity distribution is observed to be increase.

Future Work

The problem can also be extended by considering the different fluid models like Williamson, Burger, Jeffery and Tangent hyperbolic nanofluid. The problem can be analyzed by including various other effect like *nth*-order chemical reaction, inclination magnetic field, viscous dissipation, by taking dust particles. We can also solve the given problem by using different geometries like wedge, channel, cone and cylinder etc.

Bibliography

[1] Y. A. Cengel and J. M. Cimbala, *Fluid mechanics: fundamentals and applications*. McGraw-Hill, 1st edition, 2004.

[2] B. Xia and D. W. Sun, "Applications of computational fluid dynamics (CFD) in the food industry: a review," *Computers and electronics in agriculture*, vol. 34, no. 1-3, pp. 5–24, 2002.

[3] R. Banerjee, X. Bai, D. Pugh, K. Isaac, D. Klein, J. Edson, W. Breig, and L. Oliver, "CFD simulations of critical components in fuel filling systems," SAE technical paper, Tech. Rep., 2002.

[4] s. U. S. Choi, "Nanofluid technology: current status and future research," Argonne national lab.(ANL), Argonne, IL (United States), Tech. Rep., 1998.

[5] J. Buongiorno, "Convective transport in nanofluids," *Journal of heat transfer*, vol. 128, no. 3, pp. 240–250, 2006.

[6] F. Shahzad, M. Sagheer, and S. Hussain, "MHD tangent hyperbolic nanofluid with chemical reaction, viscous dissipation and Joule heating effects," *AIP advances*, vol. 9, no. 2, p. 025007, 2019.

[7] S. Naramgari and C. Sulochana, "MHD flow over a permeable stretching/shrinking sheet of a nanofluid with suction/injection," *Alexandria engineering journal*, vol. 55, no. 2, pp. 819–827, 2016.

[8] M. H. Abolbashari, N. Freidoonimehr, F. Nazari, and M. M. Rashidi, "Analytical modeling of entropy generation for Casson nano-fluid flow induced by

a stretching surface," *Advanced powder technology*, vol. 26, no. 2, pp. 542–552, 2015.

[9] S. Ghadikolaei, K. Hosseinzadeh, D. Ganji, and B. Jafari, "Nonlinear thermal radiation effect on magneto Casson nanofluid flow with Joule heating effect over an inclined porous stretching sheet," *Case studies in thermal engineering*, vol. 12, pp. 176–187, 2018.

[10] K. Das, P. R. Duari, and P. K. Kundu, "Nanofluid flow over an unsteady stretching surface in presence of thermal radiation," *Alexandria engineering journal*, vol. 53, no. 3, pp. 737–745, 2014.

[11] W. Ibrahim and B. Shankar, "MHD boundary layer flow and heat transfer of a nanofluid past a permeable stretching sheet with velocity, thermal and solutal slip boundary conditions," *Computers & fluids*, vol. 75, pp. 1–10, 2013.

[12] M. Krishnamurthy, B. Prasannakumara, B. Gireesha, and R. S. R. Gorla, "Effect of chemical reaction on MHD boundary layer flow and melting heat transfer of Williamson nanofluid in porous medium," *Engineering Science and technology, an International journal*, vol. 19, no. 1, pp. 53–61, 2016.

[13] H. M. Shawky, N. T. Eldabe, K. A. Kamel, and E. A. Abd-Aziz, "MHD flow with heat and mass transfer of Williamson nanofluid over stretching sheet through porous medium," *Microsystem technologies*, vol. 25, no. 4, pp. 1155–1169, 2019.

[14] D. Chauhan and R. Agrawal, "MHD flow and heat transfer in a channel bounded by a shrinking sheet and a plate with a porous substrate," *Journal of engineering physics and thermophysics*, vol. 84, no. 5, pp. 1034–1046, 2011.

[15] L. Zheng, J. Niu, X. Zhang, and Y. Gao, "MHD flow and heat transfer over a porous shrinking surface with velocity slip and temperature jump," *Mathematical and computer modelling*, vol. 56, no. 5-6, pp. 133–144, 2012.

[16] H. A. Attia, "Unsteady MHD Couette flow and heat transfer of dusty fluid with variable physical properties," *Applied mathematics and computation*, vol. 177, no. 1, pp. 308–318, 2006.

[17] H. M. Shawky, N. T. Eldabe, K. A. Kamel, and E. A. Abd-Aziz, "MHD flow with heat and mass transfer of Williamson nanofluid over stretching sheet through porous medium," *Microsystem technologies*, vol. 25, no. 4, pp. 1155–1169, 2019.

[18] T. Hayat, Z. Abbas, and M. Sajid, "MHD stagnation-point flow of an upper-convected Maxwell fluid over a stretching surface," *Chaos, solitons & fractals*, vol. 39, no. 2, pp. 840–848, 2009.

[19] N. S. Khashiie, N. M. Arifin, M. M. Rashidi, E. H. Hafidzuddin, and N. Wahi, "Magnetohydrodynamics (MHD) stagnation point flow past a shrinking/stretching surface with double stratification effect in a porous medium," *Journal of thermal analysis and calorimetry*, pp. 1–14.

[20] M. E. Yazdi, A. Moradi, and S. Dinarvand, "MHD mixed convection stagnation-point flow over a stretching vertical plate in porous medium filled with a nanofluid in the presence of thermal radiation," *Arabian journal for science and engineering*, vol. 39, no. 3, pp. 2251–2261, 2014.

[21] K. A. Kumar, V. Sugunamma, N. Sandeep, and J. R. Reddy, "MHD stagnation point flow of Williamson and Casson fluids past an extended cylinder: a new heat flux model," *SN applied sciences*, vol. 1, no. 7, p. 705, 2019.

[22] F. Aman, A. Ishak, and I. Pop, "Magnetohydrodynamic stagnation-point flow towards a stretching/shrinking sheet with slip effects," *International communications in heat and mass transfer*, vol. 47, pp. 68–72, 2013.

[23] H. Alfvén, "Existence of electromagnetic-hydrodynamic waves," *Nature*, vol. 150, no. 3805, p. 405, 1942.

[24] K. Hiemenz, "The boundary layer on a straight circular cylinder immersed in the uniform liquid flow," *J.Dinglers polytech*, vol. 326, pp. 321–324, 1911.

[25] E. Eckert, "The calculation of the heat transfer in the laminar boundary layer around the body," *VDI research issue*, vol. 416, pp. 1–24, 1942.

[26] A. Ishak, R. Nazar, and I. Pop, "Mixed convection boundary layers in the stagnation-point flow toward a stretching vertical sheet," *Meccanica*, vol. 41, no. 5, pp. 509–518, 2006.

[27] T. R. Mahapatra and A. Gupta, "Heat transfer in stagnation-point flow towards a stretching sheet," *Heat and mass transfer*, vol. 38, no. 6, pp. 517–521, 2002.

[28] T. Hayat, M. Mustafa, S. Shehzad, and S. Obaidat, "Melting heat transfer in the stagnation-point flow of an upper-convected Maxwell (UCM) fluid past a stretching sheet," *International journal for numerical methods in fluids*, vol. 68, no. 2, pp. 233–243, 2012.

[29] K. Jafar, A. Ishak, and R. Nazar, "MHD stagnation-point flow over a nonlinearly stretching/shrinking sheet," *Journal of aerospace engineering*, vol. 26, no. 4, pp. 829–834, 2011.

[30] M. Ashraf and M. A. Kamal, "Numerical simulation of MHD stagnation point flow towards a heated axisymmetric surface," *The anziam journal*, vol. 52, no. 3, pp. 301–308, 2011.

[31] M. K. A. Mohamed, M. Z. Salleh, R. Nazar, and A. Ishak, "Numerical investigation of stagnation point flow over a stretching sheet with convective boundary conditions," *Boundary value problems*, vol. 2013, no. 1, p. 4, 2013.

[32] G. S. Seth, R. Sharma, B. Kumbhakar, and R. Tripathi, "MHD stagnation point flow over exponentially stretching sheet with exponentially moving free-stream, viscous dissipation, thermal radiation and non-uniform heat source/sink," in *diffusion foundations*, vol. 11, Trans tech publ. Springer, 2017, pp. 182–190.

[33] R. U. Haq, S. Nadeem, Z. H. Khan, and N. S. Akbar, "Thermal radiation and slip effects on MHD stagnation point flow of nanofluid over a stretching

sheet," *Physica low-dimensional systems and nanostructures*, vol. 65, pp. 17–23, 2015.

[34] W. Ibrahim, "Nonlinear radiative heat transfer in magnetohydrodynamic (MHD) stagnation point flow of nanofluid past a stretching sheet with convective boundary condition," *Propulsion and power research*, vol. 4, no. 4, pp. 230–239, 2015.

[35] Z. Iqbal, M. Qasim, M. Awais, T. Hayat, and S. Asghar, "Stagnation-point flow by an exponentially stretching sheet in the presence of viscous dissipation and thermal radiation," *Journal of aerospace engineering*, vol. 29, no. 2, p. 04015046, 2015.

[36] R. Dash, K. Mehta, and G. Jayaraman, "Casson fluid flow in a pipe filled with a homogeneous porous medium," *International journal of engineering science*, vol. 34, no. 10, pp. 1145–1156, 1996.

[37] T. Hayat, M. Awais, and M. Sajid, "Mass transfer effects on the unsteady flow of UCM fluid over a stretching sheet," *International journal of modern physics*, vol. 25, no. 21, pp. 2863–2878, 2011.

[38] A. Jasmine Benazir, R. Sivaraj, and O. D. Makinde, "Unsteady magnetohydrodynamic Casson fluid flow over a vertical cone and flat plate with non-uniform heat source/sink," in *international journal of engineering research in africa*, vol. 21, Trans tech publ. Elsevier, 2016, pp. 69–83.

[39] I. Animasaun, E. Adebile, and A. Fagbade, "Casson fluid flow with variable thermo-physical property along exponentially stretching sheet with suction and exponentially decaying internal heat generation using the homotopy analysis method," *Journal of the nigerian mathematical society*, vol. 35, no. 1, pp. 1–17, 2016.

[40] M. Afikuzzaman, M. Ferdows, and M. M. Alam, "Unsteady MHD Casson fluid flow through a parallel plate with hall current," *Procedia engineering*, vol. 105, pp. 287–293, 2015.

[41] S. Ghadikolaei, K. Hosseinzadeh, D. Ganji, and B. Jafari, "Nonlinear thermal radiation effect on magneto Casson nanofluid flow with Joule heating effect over an inclined porous stretching sheet," *Case studies in thermal engineering*, vol. 12, pp. 176–187, 2018.

[42] M. Mustafa, "MHD nanofluid flow over a rotating disk with partial slip effects: buongiorno model," *International journal of heat and mass transfer*, vol. 108, pp. 1910–1916, 2017.

[43] M. Mustafa and J. A. Khan, "Model for flow of Casson nanofluid past a non-linearly stretching sheet considering magnetic field effects," *AIP advances*, vol. 5, no. 7, p. 077148, 2015.

[44] S. Pramanik, "Casson fluid flow and heat transfer past an exponentially porous stretching surface in presence of thermal radiation," *Ain shams engineering journal*, vol. 5, no. 1, pp. 205–212, 2014.

[45] C. Soret, *On the state of equilibrium which takes from the point of view of its concentration a originally homogeneous saline dissolution of which two parts are brought to different temperatures*. Academic press, 1880.

[46] E. Eckert and R. Drake, "Analysis of," *Heat and mass transfer*, p. 7511, 1972.

[47] Z. Dursunkaya and W. M. Worek, "Diffusion-thermo and thermal-diffusion effects in transient and steady natural convection from a vertical surface," *International journal of heat and mass transfer*, vol. 35, no. 8, pp. 2060–2065, 1992.

[48] N. Kafoussias and E. Williams, "Thermal-diffusion and diffusion-thermo effects on mixed free-forced convective and mass transfer boundary layer flow with temperature dependent viscosity," *International journal of engineering science*, vol. 33, no. 9, pp. 1369–1384, 1995.

[49] C. Abreu, M. Alfradique, and A. S. Telles, "Boundary layer flows with dufour and soret effects forced and natural convection," *Chemical engineering science*, vol. 61, no. 13, pp. 4282–4289, 2006.

[50] A. Postelnicu, "Influence of a magnetic field on heat and mass transfer by natural convection from vertical surfaces in porous media considering soret and dufour effects," *International journal of heat and mass transfer*, vol. 47, no. 6-7, pp. 1467–1472, 2004.

[51] M. Alam and M. Rahman, "Dufour and Soret effects on mixed convection flow past a vertical porous flat plate with variable suction," *Nonlinear analysis modelling and control*, vol. 11, no. 1, pp. 3–12, 2006.

[52] P. L. Narayana, "Soret and Dufour effects on free convection heat and mass transfer in a doubly stratified darcy porous medium," *Journal of porous media*, vol. 10, no. 6, 2007.

[53] S. Ibrahim, P. Kumar, G. Lorenzini, E. Lorenzini, and F. Mabood, "Numerical study of the onset of chemical reaction and heat source on dissipative MHD stagnation point flow of Casson nanofluid over a nonlinear stretching sheet with velocity slip and convective boundary conditions," *Journal of engineering thermophysics*, vol. 26, no. 2, pp. 256–271, 2017.

[54] R. K. Bansal, *A textbook of fluid mechanics and hydraulic machines 9th revised edition SI units(Chp. 1-11).* Laxmi publications, 9th revised edition, 2010.

[55] D. J. Tritton, *Physical fluid dynamics.* Springer Science & Business Media, 2012.

[56] S. Molokov, R. Moreau, and H. K. Moffatt, *Magnetohydrodynamics historical evolution and trends.* Springer, fourth edition, 2007.

[57] N. A. Shah, *Ideal fluid dynamics.* A-one publisher, 2015.

[58] F. M. White, *Fluid mechanics.* McGraw-Hill series in mechanical engineering, 2010, vol. 7th edition.

[59] J. H. Ferziger and M. peric, *Computational methods for fluid dynamics.* Springer, 2002, vol. 3rd edition.

[60] R. W. Lewis, P. Nithiarasu, and K. N. Seetharamu, *Fundamental of the finite element method for heat and fluid flow.* Wiley-AIChE.2005, 2005.

[61] D. F. Young, B. R. Munson, T. H. Okiishi, and W. W. Huebsch, *A brief introduction to fluid mechanics fifth edition.* Wiley-AlchE, 2010.

[62] T. C. Papanastasiou, G. C. Georgios, and H. A. N. Alexandrou, *Viscous fluid flow.* CRC press, 1999.

[63] J. Kunes, *Dimensionless physical quantities in science and engineering first edition.* Burlington, MA : Elsevier, 2012.

[64] T. Y. Na, *Computational methods in engineering bundary value problems.* Academic press, 1979.